Turn-up/turn-down of throughput in membrane bioreactors

Chua, Hwee Chuan

Award date:
2005

Awarding institution:
University of Bath

TURN-UP/TURN-DOWN OF THROUGHPUT IN MEMBRANE BIOREACTORS

submitted by Hwee Chuan Chua

for the degree of PhD

of the University of Bath

2004

ProQuest LLC
789 East Eisenhower Parkway
P.O. Box 1346
Ann Arbor, MI 48106-1346

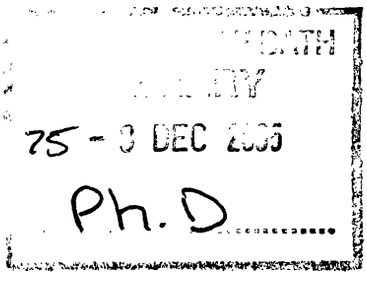
75 - 3 DEC
Ph.D

Contents

Figures

Tables

Nomenclature

		Dimension	Units
BOD	Biological Oxygen Demand	$M.L^{-3}$	$mg.l^{-1}$
CASP	Conventional Activated Sludge Process	-	-
CFV	Crossflow Velocity	$L.T^{-1}$	$m.s^{-1}$
COD	Chemical Oxygen Demand	$M.L^{-3}$	$mg.l^{-1}$
DOC	Dissolved Organic Carbon	$M.L^{-3}$	$mg.l^{-1}$
DOTM	Direct Observation Through the Membrane	-	-
DWF	Average Flow in Dry Weather	$M^3.T^{-1}$	$l.s^{-1}$
EPS	Extracellular Polymeric Substances	-	$mg.g^{-1}$
F/M	Food to Microorganism	T^{-1}	$g.g^{-1}.d^{-1}$
HRT	Hydraulic Retention Time	T	hours (h)
MBR	Membrane Bioreactor	-	-
MLSS	Mixed Liquor Suspended Solids	$M.L^{-3}$	$g.l^{-1}$
MLVSS	Mixed Liquor Volatile Suspended Solids	$M.L^{-3}$	$g.l^{-1}$
MWCO	Molecular Weight Cut-Off	M	Da
SMP	Soluble Microbial Products	-	$mg.g^{-1}$
SRT	Solid Retention Time	T	days (d)
SS	Suspended Solids	$M.L^{-3}$	$g.l^{-1}$
TKN	Total Kjeldahl Nitrogen	$M.L^{-3}$	$mg.l^{-1}$
TMP	Transmembrane Pressure	$M.L^{-1}.T^{-2}$	Pa
TN	Total Nitrogen	$M.L^{-3}$	$mg.l^{-1}$
TOC	Total Organic Carbon	$M.L^{-3}$	$mg.l^{-1}$
u_g	superficial gas velocity	$L.T^{-3}$	$mm.s^{-1}$

Abstract

Membrane bioreactors (MBRs) have been used increasingly for municipal wastewater treatment. The current wastewater treatment plants are designed to treat three times the average flow in dry weather (DWF) which covers the expected range of incoming flow rates. If throughput in MBRs can be changed readily by changing the energy input into the system, a smaller plant can be designed. This will result in substantial cost savings. Under varying throughput operation, a high aeration rate is required to generate a high crossflow to minimise fouling during high flow rates. At low flow rates, a low aeration rate is used to minimise energy consumption.

The aim of this work is to explore the feasibility of designing smaller membrane plants by varying the throughput. This requires the control of membrane fouling, so that chemical cleaning is not compromised. The permeate flux and aeration rate are important hydrodynamic parameters that must be controlled to avoid excessive membrane fouling. The maximum dynamic critical flux achievable by increasing the superficial gas velocity (u_g) for the system was found to be 22 $l.m^{-2}.h^{-1}$ at a mixed liquor volatile suspended solids (MLVSS) concentration of 17.15 $g.l^{-1}$, beyond which further flux increase becomes difficult. Intermittent permeation while retaining aeration was found to be an effective technique for long-term sustainability of high fluxes. An optimum MLVSS concentration of 14.53 $g.l^{-1}$ or food to microorganism (F/M) ratio 0.07 $gBOD.gMLVSS^{-1}.d^{-1}$ was found to give the highest dynamic critical flux of 22 $l.m^{-2}.h^{-1}$ at a u_g of 83 $mm.s^{-1}$. Using a

combination of suitable hydrodynamic conditions and intermittent permeation, membrane fouling can be controlled during short periods of high flows. Fouling can be removed during subsequent periods of low flows. The turn-up/turn-down design of MBRs is possible.

1 Introduction

Submerged membrane bioreactors (MBRs) have been increasingly used for wastewater treatment. The advantages of MBR include good effluent quality, complete removal of solids from effluent, small footprint, high loading rate, disinfection of effluent and low sludge production. The energy consumption of submerged MBRs is lower than that of sidestream MBRs due to the absence of the recirculation pump. Cote el al. [1] reported energy consumption rates of 2-10 kWh m^{-3} and 0.2-0.4 kWh m^{-3} for sidestream and submerged MBRs respectively. Aeration accounted for more than 90 % of the total power consumption of submerged systems [2]. Examples of commercial-scale submerged MBRs include Kubota, Zenon Env Inc and Mitsubishi Rayon. Kubota uses flat sheet membranes while Zenon and Mitsubishi use hollow fibre membranes.

Wastewater treatment plants are currently designed at 3 times the average flow in dry weather (DWF) to cope with the variable incoming flow rates, resulting in wastewater treatment plants operating at far below the maximum treatment capacity most of the time. Howell [3] showed that if it is possible to operate MBRs with a variable throughput by changing the energy input into the system, a smaller plant can be designed and substantial savings made in the treatment cost.

This work describes some of the effects of changing operational parameters in a dynamic fashion during the operation of a single stage submerged MBR.

Intermittent permeation is an in-situ membrane cleaning technique where permeation is suspended periodically. Particles deposited on the membrane will be removed by the crossflow when the transmembrane pressure (TMP) that held the particles is removed during the suspension of permeation. This technique allows long-term sustainability even when a plant is operated above the critical flux. The effectiveness of intermittent permeation was studied.

Operating MBRs with a variable throughput requires membrane fouling to be controlled, so that excessive chemical cleaning is not required. The aeration rate, which is the major cost factor, has to be optimised. This will make MBRs more economically viable in municipal wastewater treatment. This work explores the feasibility of operating MBRs with a variable throughput. This requires an understanding of the effects of the hydrodynamic parameters of permeate flux and aeration rate on membrane fouling. The behaviour of MBRs under variable throughput was then observed.

The effects of biomass concentration and food to microorganisms (F/M) ratio on the permeate flux were also investigated. This work is aimed towards a better understanding of fouling in MBRs and how the various parameters can be used to control fouling. This will help move towards optimised design on operation of submerged MBRs.

2 Membrane Bioreactors for Domestic Wastewater Treatment

2.1 Introduction

The membrane bioreactor (MBR) is a new development for the treatment of wastewater, which combines biological treatment with membrane separation. MBRs have been increasingly used for wastewater treatment. There are currently more than 2000 MBR plants worldwide, of which approximately 700 are Kubota plants (including small scale) [4]. The largest Kubota plant at Swanage, UK, has a 13000 $m^3.d^{-1}$ flow to treatment.

There are three modes of using a membrane in a MBR – removing treated water through the membrane [5], delivering oxygen or air through a membrane [6], and delivering organic material to the bioreactor via a membrane [7]. It is possible to use all three simultaneously if the conditions require it. Removing treated effluent can be via a submerged [8] or sidestream [5] membrane module. The bioreactor may be aerobic [5] or anaerobic [9]. The delivery of organics to the membrane may be through a dense (e.g. silicone) membrane [7], or through a porous membrane system where a solvent intermediate extraction system has been interposed [10]. Suspension MBR shall be used for the effluent removal membrane and biofilm MBR for the organics, oxygen or air delivery membrane as they result in a biofilm forming on the membrane and doing most of the work.

The suspension MBR replaces the gravitational sedimentation process in conventional biological processes such as the activated sludge process with membranes. After biological treatment, ultrafiltration or microfiltration membrane retains microorganisms and solids, while allowing solutes and water to pass through. The biofilm MBR for oxygen or air delivery uses gas-permeable hollow fibre membranes for bubbleless mass transfer of pure oxygen. Wastewater is fed to the biofilm formed on the outer surface of the membrane, while oxygen is transferred from the fibre lumen. The biofilm MBR for organics delivery can use silicone tubes to selectively extract organics from toxic industrial wastewater, or can extract organics via 2 hollow fibre membrane contactors and an intervening solvent phase. The extracted organics are then degraded without the microbes being affected by the toxicity of the inorganics [7]. It is also easier to control organics ingress where they are inhibitory in high concentrations. The suspension MBR and recently, the biofilm MBR for organics delivery have been commercialised.

2.2 Suspension Membrane Bioreactors

The use of membranes for the solid-liquid separation of activated sludge was first reported in the late 1960s [5]. Conventional activated sludge process (CASP) has a maximum sludge concentration limit of 5-8 $g.l^{-1}$ due to the need for a secondary settling process, hence limiting the volumetric load. High investment costs are necessary for the huge plants. Using membranes for solid-liquid separation eliminates the secondary settling stage and retains

microorganisms. MBR allows high sludge concentration, hence reducing the plant size. Mixed liquor suspended solids (MLSS) as high as 36 $g.l^{-1}$ have been reported to be feasible [8], although high MLSS gives rise to problems of membrane fouling and oxygen mass transfer. The usual operating MLSS for the MBR is between 10-20 $g.l^{-1}$. The advantages of MBR include good effluent quality, complete removal of solids from effluent, small footprint, high loading rate, disinfection of effluent and low sludge production. In addition, the MBR has been shown to be able to cope with varying influent concentration and flow rate due to the high MLSS.

Suspension MBR can be classified into 2 different types: sidestream and submerged. Sidestream MBR has its membrane module outside the bioreactor, and a recirculation pump drives the mixed liquor into the membrane module. Submerged MBR has its membrane module submerged inside the bioreactor, and permeate is removed either by gravity or a suction pump. Aeration serves to provide oxygen as well as scouring and cleaning the membrane surface. Examples of commercial-scale suspension MBRs include Kubota, Zenon Env Inc and Mitsubishi Rayon, all of which are submerged systems. Kubota uses flat sheet membranes while Zenon and Mitsubishi use hollow fibre membranes.

2.3 Commercial Membrane Bioreactors

2.3.1 Kubota Submerged Membrane Bioreactor

2.3.1.1 Background

The Kubota process originated from Kubota Corporation Environmental Plan Division in Japan. In Japan, where the cost of land is high, there is an increasing market for low footprint effluent treatment process, resulting in the rapid development of the Kubota process. The first commercial treatment plant started operating in 1990, and there are now over 700 Kubota plants worldwide (including small scale), the largest plant with a treatment capacity of 13000 $m^3.d^{-1}$ at Swanage, UK [4]. The Kubota process is used to treat a variety of effluents including sewage, pharmaceutical, photographic, cardboard manufacture, grey water recycling and shipboard wastewater.

2.3.1.2 Technology

The Kubota system is a high MLSS activated sludge process with flat sheet membranes submerged in an activated sludge tank. Air is introduced via a coarse bubble diffuser (1 cm pore size) situated at the bottom of the tank. Each membrane panel measures 1 m in height and 0.4 m in width, giving a total membrane area of 0.8 m^2. The nominal pore size is 0.4 μm. A standard

Kubota unit consists of 24-140 membrane panels arranged parallel in the vertical direction, separated by a 7 mm gap between panels. This allows an upward crossflow of approximately 0.5 $m.s^{-1}$ to be generated by the rising bubbles, thereby cleaning the membrane and allows low pressure filtration. Effluent flow is controlled either by a low pressure suction pump or gravity head of 1–1.5 m. Preliminary and final settlement is not necessary to produce a high quality effluent.

2.3.1.3 Domestic Wastewater Treatment with the Kubota Process

The Kubota process has been shown to treat domestic effluent to a high standard. This is summarized in Table 2-1. Denitrification takes place in an anoxic tank upstream of the aerated tank. The sludge production was reported to be 0.48 $kgMLSS.kgBOD^{-1}$ at a SRT of 40–70 days [11], about 50 % of CASP, or 0.35-0.53 $kgMLSS.kgCOD^{-1}$ at a shorter SRT of 20-30 days [12] [13], similar to CASP. Current energy consumption is estimated at less than 1 $kWh.m^{-3}$ of treated water.

Table 2-1 Effluent quality of the Kubota process

Parameter	PermeateConcentration/mg.l^{-1} (Removal Rate/%)	References
BOD	1-4 (98-99)	[14] [15] [16] [17]
TOC	5 (93)	[17] [14]
COD	7-25 (90-95)	[12] [13] [11] [17]
SS	0 (100)	[17] [12] [13] [14] [15]
NH_4-N	5 (95)	[16] [15]
TN	(60-80)	[14] [12] [13] [17]
NO_x	2	[11]
TP	(74)	[14]
Coliform Bacteria	6 log	[11] [14]

The Kubota process has been shown to be a stable process requiring little maintenance. Chemical cleaning of membrane was not required for more than a year [14]. The operating flux was stable at 0.4 m.d^{-1} (16.7 l.m^{-2}.h^{-1}), with a cycle of 8 hours filtration followed by 4 hours rest. The Kubota process can also handle the demands of treating domestic wastewater, which is characterised by diurnal flow fluctuations. Short-term operation at a flux rate of 30 l.m^{-2}.h^{-1} to cope with a variable load resulted in slight membrane fouling, but chemical cleaning was not necessary for 4 months [12] [13]. Large and expensive balancing tanks are not necessary as the Kubota process can cope

with a short-term increase of inflow [14] [18]. The operating conditions of the Kubota process are summarised in Table 2-2.

Table 2-2 Operating conditions of the Kubota process

Parameter	Unit	Range	Remarks
HRT	hours	4.5–14.2	
Flux	$l.m^{-2}.h^{-1}$	15–21.7	up to 35 for short periods
Filtration cycle		8 min on, 2 min off	
		8 h on, 4 h off	
		continuous	
Volumetric load	$kgBOD.m^{-3}.d^{-1}$	0.22-0.63	
Mass load	$kgCOD.kgMLSS^{-1}.d^{-1}$	0.03-0.1	
MLSS	$g.l^{-1}$	10-23	greater than 18, increase sludge viscosity
Sludge age	days	20-75	
TMP	kPa		up to 65 for short periods
			increase to 15 or 35, chemical cleaning
Air-flow	$l.min^{-1}.panel^{-1}$	11.8-13.3	
Coarse bubbles	mm	5	
Upward sludge crossflow	$m.s^{-1}$	0.5	

2.3.2 Zenon

2.3.2.1 Technology

The ZeeWeed membrane is a hollow fibre microfiltration membrane with a nominal pore size of 0.1 μm and an outer diameter of 1.9 mm. A module consists of hollow fibres mounted vertically with outside-in filtration and permeate is extraction from both ends by a combination of hydrostatic pressure and suction pump. The ZW-500 cassette has dimensions of 2, 1.8 and 0.7 m for height, length and width respectively with a total surface area of 368 m^2. Coarse bubble aerators are used to clean the ZeeWeed membranes and fine bubble aerators to provide the remaining oxygen requirement. Permeate backwash is used to control fouling between chemical cleaning.

The high effluent quality Zenon process is summarized in Table 2-3. The sludge production was reported to be 0.2 $kgMLSS.kgCOD^{-1}$ (0.46 $kgMLSS.kgBOD^{-1}$) at a SRT of 50 days, 30-50 % less than CASP [1] [19]. Rosenberger et al. [20] reported sludge stabilization at a F/M ratio of 0.07 $kgCOD.kgMLSS^{-1}.d^{-1}$ without sludge wastage. Energy consumption is currently estimated at 0.4-0.9 $kWh.m^{-3}$ [21]. The operating conditions of the Zenon process are summarized in Table 2-4.

Table 2-3 Effluent quality of the Zenon process

Parameter	Permeate Concentration/mg.l^{-1} (Removal Rate/%)	References
BOD	5 (97)	[22] [1] [19]
COD	10-35 (95-98)	[22] [1] [19] [20]
SS	0 (100)	[22] [1] [19]
NH_4-N	0-0.4 (99-100)	[20] [22]
TN	11-13 (80-82)	[22] [1] [19] [20]
TKN	2-3 (94-97)	[22] [1] [19]
Coliform Bacteria	6 log	[22] [1] [19]
Bacteriophages	4 log	[22] [1]

Table 2-4 Operating conditions of the Zenon process

Parameter	Unit	Range
HRT	hours	2–15.6
SRT	days	5-50
Flux	l.m^{-2}.h^{-1}	16–35
TMP	kPa	20-30
Volumetric load	kgCOD.m^{-3}.d^{-1}	1.1-1.7
Mass load	kgCOD.kgMLSS^{-1}.d^{-1}	0.07-0.08
MLSS	g.l^{-1}	10-20

2.3.3 Mitsubishi

The Mitsubishi Rayon membrane is a microporous polyolefin hollow fibre membrane. Each element has a surface area of 1.5 m^2 and each module has 70 elements with a total surface are of 105 m^2. Each module is continuously aerated at 1200 $l.min^{-1}$ and intermittent permeation of 8-13 mins on and 2 mins off is employed. Chemical cleaning takes place approximately every 2-3 months when the TMP increases by 20 kPa. There are about 500 Mitsubishi MBRs worldwide with a total capacity of 50000 $m^3.d^{-1}$. Good effluent quality has been reported and summarized in Table 2-5 [23] [24].

Table 2-5 Effluent quality of the Mitsubishi MBR

Parameter	**Permeate Concentration/mg.l^{-1} (Removal Rate/%)**
BOD	1 (99)
COD	5 (93)
TOC	3.5 (92)
SS	0 (100)
NH_4-N	0-0.4 (99-100)
TN	5.1 (83)
TP	1.1 (70)

2.4 Operating Conditions

In the conventional activated sludge process (CASP), the mass loading rate or food to microorganism (F/M) ratio is a very important design parameter and is generally from 0.2-0.4 $kgCOD.kgMLSS^{-1}.d^{-1}$. A very high or low mass loading rate results in poor effluent quality. The mass loading rate of MBR ranges from 0.03-0.1 $kgCOD.kgMLSS^{-1}.d^{-1}$, lower than the CASP. This is due to the MBR being operated at higher MLSS concentrations, typically 10-15 $g.l^{-1}$ MLSS [25]. Hence, the volumetric loading rate of 1.1-1.7 $kgCOD.m^{-3}.d^{-1}$ for the MBR is higher than the 0.4-0.8 $kgCOD.m^{-3}.d^{-1}$ for the CASP. This allows a smaller footprint for the MBR and hydraulic retention time (HRT) to be lower for the same feed concentration and treatment level. The HRT and solid retention time (SRT) of full scale MBRs range from 1.5-5.5 hours and 50-200 days respectively [25]. The operating conditions of MBR are summarized in Table 2-6.

Table 2-6 Summary table of operating conditions of MBRs

Parameter	Range
HRT (h)	1.5-5.5
SRT (d)	50-200
MLSS ($g.l^{-1}$)	10-15
Volumetric load ($kgCOD.m^{-3}.d^{-1}$)	1.1-1.7
Mass load ($kgCOD.kgMLSS^{-1}.d^{-1}$)	0.03-0.1

Laboratory scale MBRs have also been operated outside these ranges. A high volumetric loading rate of 6-13 kgCOD.m^{-3}.d^{-1} was reported to achieve an effluent COD of less than 30 mg.l^{-1}, representing a removal rate of greater than 95 % [26]. Xing et al. [27] showed that the MBR could cope with a varying load without any significant deterioration of the effluent quality. The effluent COD for a MBR was only 21 mg.l^{-1} and 10 mg.l^{-1} at the maximum volumetric loading rate of 10.7 kgCOD.m^{-3}.d^{-1} (13-27 times the CASP) and mass loading rate of 2 kgCOD.kgMLVSS^{-1}.d^{-1} (5-20 times of the CASP) respectively. The average effluent COD was 9.4 mg.l^{-1}, representing a removal rate of 97 %. This suggests that unlike the CASP, organic loading rate is not crucial to the MBR. This is probably due to the retention of organic compounds by a gel layer on the membrane surface. Much higher supernatant TOC or COD than that of the effluent demonstrates the retention effect of the membrane or degradation in a biofilm. Chaize and Huyard [28] reported effluent and supernatant TOC being 15 mg.l^{-1} and up to 500 mg.l^{-1} respectively. Huang et al. [29] obtained 7 mg.l^{-1} and up to 90 mg.l^{-1} for the effluent and supernatant TOC respectively. Cicek et al. [30] reported 3 mg.l^{-1} and 898 mg.l^{-1} for the effluent and supernatant COD respectively.

MBRs are operated at long SRT of 50-200 days [25]. It is not possible to operate the CASP at long SRTs because activated sludges do not settle well at high concentrations and suspended solids (SS) are present in the effluent, resulting in bad effluent quality. Effluent quality of MBRs is not dependent on good settling properties of the sludges, hence operation at long SRT and high MLSS concentrations is possible. Besides a small footprint and capital

cost reduction, long SRTs allow the development of slow growing microorganisms that improve the removal of nitrogen compounds (greater than 5 days for nitrifiers) and refractory organic matter. Long SRTs also lead to lower sludge production in MBRs. From activated sludge modelling:

$$Y_{obs} = \frac{Y_T}{1 + \frac{K_d}{\mu}}$$

where Y_{obs} = observed yield coefficient, Y_T = true growth yield,

K_d = microbial decay coefficient, $time^{-1}$ and μ = specific growth rate, $time^{-1}$.

Since 1/SRT = μ, Y_{obs} has an inverse relationship with SRT. Cell yield decreases as SRT increases. Huang et al. [31] reported a decrease in sludge yield from 0.37 $gVSS.gCOD^{-1}$ at a SRT of 5 days to 0.28 $gVSS.gCOD^{-1}$ at a SRT of 80 days.

In the CASP, a very high or low mass loading rate results in poor effluent quality due to increased soluble microbial products (SMP) production. SMP refer to "the pool of organic compounds that are released into solution from substrate metabolism (usually with biomass growth) and biomass decay", excluding volatile fatty acids for anaerobic systems [32]. SMP comprise a huge variety of compounds such as humic and fulvic acids, polysaccharides, proteins, nucleic acids, organic acids, amino acids, antibiotics, steroids, enzymes, structural components of cells, and products of energy metabolism. SMP make up the majority of soluble organic matter in the effluents from

biological treatment systems [33]. Hence, SMP are important for achieving good effluent quality in terms of BOD, COD or TOC. Barker and Stuckey [32] reviewed SMP in wastewater treatment systems and SMP production increases with influent concentration. The optimal solid retention times (SRTs) that minimize SMP production are 2-15 days and 25 days for aerobic and anaerobic systems respectively. The optimal organic loads are 0.3-1.2 $kgCOD.kgMLSS^{-1}.d^{-1}$. Overloading results in the sludge not able to remove all the organic substances from solution. Underfeeding results in the sludge decomposing and releasing organic matter into solution. In this work, extracellular polymeric substances (EPS) and SMP will be used to differentiate extractable and soluble EPS respectively.

While effluent quality is expected to deteriorate at longer SRT or higher MLSS concentration due to higher SMP concentration from cell lysis, this has not been observed in MBRs. Good effluent quality (9.4-17 $mg.l^{-1}$ COD and 90-97 % removal rate) independent of SRT from 5-40 days and MLSS concentration up to 23 $g.l^{-1}$ has been observed [31] [27] [34] [35] [26]. COD removal greater than 90 % was observed when the MLSS concentration increased to 40-50 $g.l^{-1}$ [34]. MBRs were also operated at infinite SRT [8] [17], with COD removal rates between 95 % [36] [20] and 85 % [37]. Only Yamamoto et al. [8] observed a sudden increase of effluent COD when the MLSS increased to a very high concentration of 47 $g.l^{-1}$. The reasons for the effluent quality being independent of SRT or MLSS concentration in the MBR are likely to be due to the retentive effect of the membrane, degradation in a biofilm or lower SMP concentration at longer SRT or higher MLSS contrary

to the CASP. Brookes et al. [38] reported lower SMP concentration at longer SRT in MBRs, and Lee et al. [39] suggested that this is due to the more active uptake of SMP from cell lysis by the higher biomass concentration.

2.5 Biological Performances

Good effluent quality is due to the complete mineralisation of organics by the high biomass concentration and the retention of high molecular-weight compounds by the membrane. The high conversion efficiency of the MBR decreases the need for effluent post treatment. COD removal efficiency greater than 95 % has been reported [1] [26] [22] [19] [27] [40] [41] [30] [42] [34] [36] [20] [43] [44] [45]. BOD and total organic carbon (TOC) removal efficiency greater than 98 % and 94 % respectively were also reported [1] [22] [19] [29].

The MBR promotes the growth of slow growth rate bacteria such as nitrifying bacteria. The retention of microorganisms by the membrane and operation at long SRT allow efficient nitrification in MBRs. Total Kjeldahl nitrogen (TKN) removal efficiency greater than 95 % has been reported [1] [22] [19] [41] [30] [43] [44] [45]. Denitrification occurs in the Kubota plants by having effectively a two-tank system with the first anoxic tank (receiving raw feed and a recycle sludge) unaerated. Total nitrogen (TN) removal efficiency greater than 80 % has been reported [1] [22] [19] [41] [36]. Alternatively, Chiemchaisri et al. [37] reported TN removal efficiency up to 80 % by

intermittent aeration of 5 minutes every 10 minutes. Yamamoto et al. [8] reported denitrification efficiency up to 60 % by intermittent aeration of 3 minutes every 10 minutes. However, it was difficult to optimise the intermittent aeration cycle to achieve both high nitrification and denitrification.

2.6 Sludge Yield

Sludge disposal accounts for a significant portion of the operating cost of conventional systems, and the MBR can have a low sludge production when operating at long SRT or low F/M ratio. At very low F/M ratio that are possible with MBRs, more carbon is used for maintenance purposes and less for growth. Several workers have operated MBRs with no sludge wastage [8] [46] [20]. Yamamoto et al. [8] reported the complete oxidation of influent biodegradable materials for a MBR treating synthetic wastewater. Sludge stabilization was observed at a mass loading of 0.1 $kgCOD.kgMLSS^{-1}.d^{-1}$. Sludge stabilization was also reported by Rosenberger et al. [20] and Muller et al. [46] for MBRs treating municipal wastewater, at mass loadings of 0.07 and 0.021 $kgCOD.kgMLSS^{-1}.d^{-1}$ respectively. The difference may be due different microbial populations or feed composition.

Sludge production in the MBR was reported to be approximately 0.2-0.44 $kgMLSS.kgCOD^{-1}$ at SRT of 25-55 days [11] [1] [19] [30] [43] [44] [45] [12]

[13] [47]. This is illustrated in Figure 2-1. Lower sludge production is observed at longer SRT.

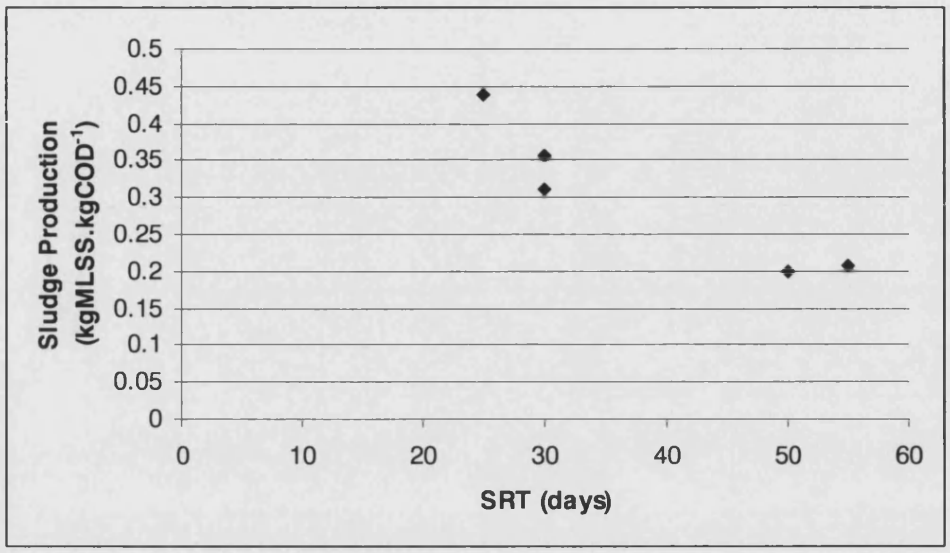

Figure 2-1 Sludge production at various SRT in the MBR

2.7 Membrane Performances

The permeate flux at which a MBR operates depends on factors such as transmembrane pressure (TMP), aeration rate or crossflow velocity (CFV) for submerged and sidestream MBRs respectively, membrane and biomass characteristics. These factors are inter-related in a complex way that is currently not well understood. The duration and frequency of membrane cleaning techniques such as backwashing, backpulsing and intermittent permeation, as well as the chemical cleaning of membrane determine the operating permeate flux of the MBR. Sidestream MBRs have been reported to

operate at a sustainable flux level of 78.8 $l.m^{-2}.h^{-1}$, with a chemical cleaning every 7 days [30] [43] [44] [45]. Submerged MBRs were reported to operate at lower flux levels of less than 35 $l.m^{-2}.h^{-1}$. At this flux level and backwashing (4 times 30 seconds backwash every hour, 15 minutes backwash every week), chemical cleaning was necessary only after 5 months of operation [22]. At a lower flux level of 25 $l.m^{-2}.h^{-1}$ and backwashing (12 times 15 seconds backwash every hour, 15 minutes chlorinated permeate backwash every week), the MBR was operated for 1 year without chemical cleaning [1] [22] [19].

Pathogens are also removed by the membrane, reducing the cost of disinfection for water intended for potable reuse. Complete retention of suspended solids (SS), bacteria and viruses in MBRs have been reported [1] [22] [19] [48] [23] [27] [40] [41] [30] [49] [35] [36] [43] [44] [45] [50] [51].

Table 2-7 Summary table of membrane performances of MBRs

Parameter	Submerged	Sidestream	References
Flux ($l.m^{-2}.h^{-1}$)	4.6-35	78.8	[24] [22] [43] [30] [44] [45]
TMP (kPa)	13-42	30-500	[8] [41] [43] [30] [44] [45] [51]
Chemical cleaning	140 h-1 yr	7-40 d	[42] [22] [19] [1] [43] [30] [44] [45] [51]

2.8 Power Consumption

The sidestream MBR is not cost effective due to the high power consumption by the recirculation pump. High power consumption is required to maintain a high CFV (usually 2-4 $m.s^{-1}$) to maintain a reasonable flux rate by reducing fouling and the need for chemical cleaning. The ratio of the volume of circulation feed to filtrate is approximately 10-20:1. In addition, the high shear stress can damage the bacterial cells in the circulating feed, hence reducing the bacterial activity.

Yamamoto et al. [8] first reported the submerged MBR, where a hollow fibre microfiltration membrane was submerged in activated sludge. This represents a significant step towards the application of MBR for wastewater treatment. The absence of the recirculation pump makes the submerged MBR a potential system for replacing the CASP. The submerged MBR uses either hollow fibre or flat sheet membranes, with pore sizes ranging from 0.1-0.45 μm, and is operated at a low TMP. Gander et al. [2] estimated that the power consumption of submerged MBR to be 2 orders of magnitude lower than sidestream MBR. Aeration accounted for more than 90 % and approximately only 20 % of the total power consumption of submerged and sidestream systems respectively. The main energy cost for the sidestream MBR is the recycling of the retentate, which accounts between 60-80 % of the total cost.

Published data for power consumption varies depending on system. Ueda et al. [23] reported an average power consumption of 2.0 $kWh.m^{-3}$ of treated

water for a submerged hollow fibre system treating domestic wastewater. Cote et al. [22] reported a much lower power consumption of 0.3 $kWh.m^{-3}$ for a submerged hollow fibre MBR treating municipal wastewater, of which aeration and the centrifugal pump for permeate extraction accounted for 0.28 $kWh.m^{-3}$ and 0.02 $kWh.m^{-3}$ respectively. The BIOSEP process, which uses submerged hollow fibre or flat sheet membranes, reported a power consumption of 0.4–1 $kWh.m^{-3}$. X-Flow's AirFlush process, which uses air-driven liquid circulation similar to submerged MBRs, has a similar power consumption of 0.5–1.0 $kWh.m^{-3}$. For other submerged systems, Gunder and Krauth [13] estimated the energy consumptions for submerged flat sheet (Kubota) at 1.5 $kWh.m^{-3}$. Ueda et al. [14] reported a higher average power consumption of 2.4 $kWh.m^{-3}$ for the Kubota system, compared to 3–4 $kWh.m^{-3}$ for sidestream MBRs. Cote el al. [1] reported energy consumption rates of 2-10 $kWh.m^{-3}$ and 0.2-0.4 $kWh.m^{-3}$ for sidestream and submerged MBRs respectively.

For sidestream MBRs, van Dijk et al. [52] reported a power consumption of 6-8 $kWh.m^{-3}$ for tubular membrane. Thomas et al. [53] reported a much lower power consumption of 1.75 $kWh.m^{-3}$ for a tubular sidestream MBR operated at a CFV of 2.3 $m.s^{-1}$. At a slightly lower CFV of 2 $m.s^{-1}$, Gunder and Krauth [13] estimated an energy consumption of 3.0 $kWh.m^{-3}$ for a tubular MBR.

Although the reported values for power consumption of MBRs varies, it is clear that submerged MBRs have lower power requirements than sidestream systems. The energy consumptions for submerged flat sheet and hollow fibre

systems are comparable, 0.4-2.4 and 0.3-2 $kWh.m^{-3}$ respectively. For sidestream tubular systems, the energy consumption is higher at 1.75-8 $kWh.m^{-3}$. Recent estimates of energy requirements for sidestream and submerged systems are 1-3 $kWh.m^{-3}$ and 0.4-0.9 $kWh.m^{-3}$ respectively [21], which correspond with the lower end of the ranges.

Table 2-8 Summary table of energy consumption of MBRs

System	Energy Consumption ($kWh.m^{-3}$)	References
Submerged flat sheet	0.4-2.4	[14]
Submerged hollow fibre	0.3-2	[22] [23]
Sidestream tubular	1.75-8	[53] [52]

2.9 Cost

The treatment cost of domestic wastewater by the MBR has decreased from 107 $\$.m^{-3}$ in 1992 to 0.11 $\$.m^{-3}$ in 2001 [4]. This is primarily due to a decrease in membrane cost from more than 400 $\$.m^{-2}$ in 1992 to the current estimate of 50 $\$.m^{-2}$. Membrane cost, membrane replacement frequency and power used to be the main contributions to the overall cost of the MBR, and power consumption is mainly attributed to pumping influent, recycling retentate, permeate suction and aeration [54]. Currently, power consumption is the major cost component, followed by sludge disposal and then membrane

replacement [4]. While the treatment cost has a major influence on the applications of the MBR, other factors such as footprint, aesthetics, disinfection and retrofit expansion may favor the use of MBR technology.

2.10 Summary

MBR technology for domestic wastewater treatment has been reviewed. Suspension MBR has been defined for effluent removal membrane and biofilm MBR for the organics, oxygen or air delivery membrane. The operating conditions of MBR have been discussed. The volumetric and mass loadings of MBRs treating domestic wastewater are usually 1.1-1.7 $kgCOD.m^{-3}.d^{-1}$ and 0.03-0.1 $kgCOD.kgMLSS^{-1}.d^{-1}$ respectively, with the HRT from 1.5-5.5 hours. The SRT ranges from 50-200 days, giving MLSS of 10-15 $g.l^{-1}$. Due to longer SRT, hence higher MLSS in the MBR compared to CASP, the MBR has a smaller footprint and lower sludge production. Sludge production is approximately 0.2-0.44 $kgMLSS.kgCOD^{-1}$ at SRT of 25-55 days. Effluent quality is high, with COD, BOD, TOC, TKN and TN removal rates greater than 95 %, 98 %, 94 %, 95% and 80 % respectively. SS are completely retained. Sidestream MBRs have higher fluxes but also greater energy consumptions of 1.75-8 $kWh.m^{-3}$, compared to 0.3-2.4 $kWh.m^{-3}$ for submerged systems. Long-term operation of submerged MBR without chemical cleaning for more than a year is possible. The cost of treatment for domestic wastewater is estimated at 12 and 6 $p.m^{-3}$ for maximum throughputs of 22.5 and 1.4 $Ml.d^{-1}$, and is competitive with the CASP up to 22.5 $Ml.d^{-1}$.

An industrial system, the Kubota process, has been discussed and shown to be a stable process for treating domestic wastewater. Membrane fouling by activated sludge and variable throughput operation of MBRs will be reviewed in the next chapter.

3 Turn-Up/Turn-Down of Throughput in MBRs

3.1 Introduction

Flow rates to wastewater treatment plants vary due to usage and weather. Wastewater treatment plants are currently designed at 3 times DWF to cope with this variability, with the high flow rates occurring for only a small fraction of the time. Hence, wastewater treatment plants are operated below their maximal design capacity most of the time. Howell [3] showed that if a smaller wastewater treatment plant could be designed to cope with the variable incoming flow rates, substantial cost savings could be achieved. This is possible if throughput can be controlled by changing the energy input into the system to control membrane fouling, so that chemical cleaning is not compromised.

3.2 Variations in Wastewater Flow Rates

Wastewater flow rates to treatment plants follow a diurnal pattern. Minimum flows occur during the early morning hours and peak flows occur in the late morning and early evening. Seasonal variations also occur due to seasonal activities, such as at resort areas and rainfall.

3.3 Traditional and Turn-Up/Turn-Down Design

Wastewater treatment plants are currently designed to treat a maximum flow rate equal to 3 times DWF to cope with the variations in wastewater flow rates. However, the average influent flow rate is approximately 1.4 times DWF. This implies that wastewater treatment plants would be operating at far below the maximum treatment capacity most of the time. Reducing the maximum treatment capacity from 3 times DWF would result in a reduction in the treatment cost. Davies et al. [16] estimated a 25 % reduction in the treatment cost for MBR plants if the maximum treatment capacity is reduced to 2 times DWF. This is competitive with conventional activated sludge plants up to a treatment capacity of 22 $Ml.d^{-1}$, as compared to 12 $Ml.d^{-1}$ for 3 times DWF. However, wastewater treatment plants designed at 2 times DWF are expected to be adequate only 88 % of the time, assuming that throughput cannot be increased by simply increasing the energy input into the system.

Owen et al. [54] reported that for wastewater treatment, the major cost components are annualised capital, recirculation power and membrane replacement costs. Cost optimisation will involve a trade-off between these components. The optimum crossflow velocities were not that which gave maximum fluxes for such cost optimisation. The optimisation assumed that flow would be a constant 3 times DWF. Designing smaller wastewater treatment plants can reduce annualised capital and membrane replacement costs.

If increasing the crossflow velocity can increase flux, smaller wastewater treatment plants can be designed to cope with the maximum flow rate. This is the turn-up/turn-down design. At high flow rates, the energy consumption would be high, but at low flow rates, the energy consumption would be low. Howell [3] showed that the overall energy consumption for the optimised turn-up/turn-down design is similar to the traditional design, but the plant size is smaller and thus the cost of treatment is lower. The turn-up/turn-down design requires membrane fouling to be controlled, so that chemical cleaning of the membrane is not compromised. How this can be achieved and the feasibility of the turn-up/turn-down design remains to explored, and is the objective of this work.

3.4 Membrane Fundamentals

3.4.1 Introduction

Membranes are filters that reject at least one component of a mixture and allowing the other components to pass through (Figure 3-1). Membranes can be porous or non-porous, and can separate particle diameters of less than 5 nm. Membrane separation processes can be used for desalination of seawater or brackish water, recovering paint from electro-dip-coating of car bodies and household appliances, dehydration of ethanol and many other applications. Membrane separation is based on a physical mechanism and the components

are not subjected to chemical, biological or thermal change. A direct reuse of components is also possible.

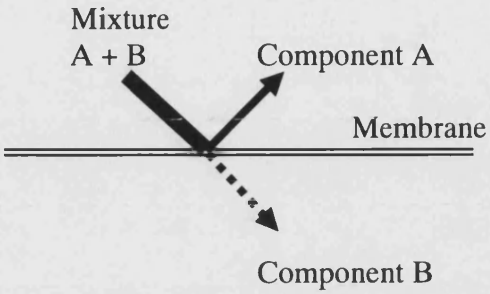

Figure 3-1 Basic principle of membrane processes

3.4.2 Membrane Classification

Membranes are classified according to the size range of materials that are separated and the driving force used in separation. This is shown in Table 3-1. Reverse osmosis, nanofiltration and electrodialysis can separate ions from water. Reverse osmosis and electrodialysis are used for the desalination of brackish water. Ultrafiltration membranes can reject particles and dissolved macromolecules between 5-100 nm and this is defined by the molecular weight cut-off (MWCO) in Daltons of the rejected solute. Ultrafiltration is used for paint recovery in the car industry. Microfiltration can only remove suspended materials down to approximately 0.1 μm and is used in wastewater treatment for the retention of biomass.

Table 3-1 Classification of membrane processes

Process	Separation Size Range	Driving Force
Microfiltration	0.1-10 μm	Pressure Gradient
Ultrafiltration	5-100 nm	Pressure Gradient
Nanofiltration	< 5 nm	Pressure Gradient
Reverse Osmosis	< 5 nm	Pressure Gradient
Electrodialysis	< 5 nm	Electric Field Gradient

3.4.3 Crossflow Microfiltration

Microfiltration is a pressure driven process with a separation size range of 10-0.1 μm, and is typically used for concentration of suspensions. Examples of materials separated include microbial cells, large colloids and small particles. The transmembrane pressure (TMP) difference in microfiltration is usually less than 3 bars, and separation is based on particle size, although other factors such as interactions between the membrane and the rejected or transmitted components and shape of particles also affect separation. Microfiltration membranes are usually symmetric with a thickness of 10 to over 150 μm. Sieving is the basic mechanism of microfiltration, where molecules greater than the pore size of the membrane are rejected.

There are 2 modes of operation in microfiltration: dead end and crossflow. The concept of crossflow microfiltration is illustrated in Figure 3-2. The feed stream is the solution at the start of the membrane process and is pumped parallel to the surface of the membrane. The retentate stream is the rejected solution or suspension by the membrane, and also contains components that would but have not pass through the membrane. The solution that has passed through the membrane is the permeate stream. The crossflow limits cake deposition and concentration at the membrane surface, hence flux increases.

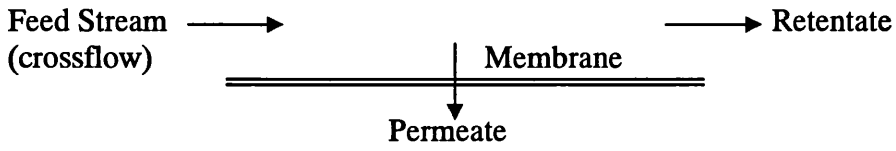

Figure 3-2 Concept of crossflow microfiltration

In dead end microfiltration, the feed flow is directly towards the membrane (Figure 3-3). Particles are rejected by the membrane and a cake layer builds up on the membrane surface. The thickness of the cake layer increases with time and the permeate flux decreases.

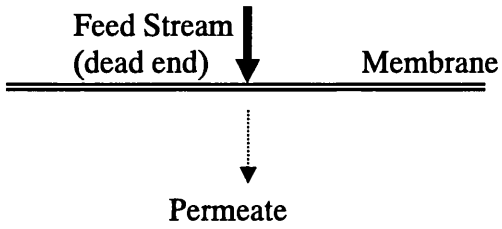

Figure 3-3 Concept of dead end microfiltration

3.4.4 Concentration Polarisation and Fouling

The driving force for microfiltration and ultrafiltration is a pressure gradient. The factors that oppose the driving force include concentration of rejected solute, gel layer formation, cake layer formation and foulant accumulation on or inside the pores of the membrane. Concentration polarization is the reversible build-up of solute at the membrane-solution interface due to a balance between the convective flow towards the membrane and back diffusion away from the membrane. Based on the classical concentration polarization model, this build-up occurs exponentially with increasing flux for Brownian diffusion.

$$J = \frac{D_B}{\delta} \ln\left(\frac{C^*}{C}\right)$$

where D_B is the Brownian diffusion coefficient ($m^2.s^{-1}$), C* and C are the concentrations at the membrane surface and in the bulk solution respectively, δ is a constant boundary layer thickness and the ratio D_B / δ is the mass transfer coefficient k ($m.s^{-1}$).

Solute and particle deposition on or inside the pores of the membrane occur when the permeation flux is higher than the various back-transport mechanisms. Together with macromolecular adsorption, this is known as membrane fouling. Membrane fouling is the irreversible deposition or adsorption of particles or solutes onto the surface or into the pores of the

membrane. This results in a flux decline or higher TMP when operating under constant TMP or constant flux respectively. The retention properties of the membrane are modified. Hermia [55] described 4 blocking mechanisms for dead-end filtration: complete pore blocking, partial pore blocking, cake filtration and internal pore blocking for dead-end filtration. Field [56] extended this to crossflow filtration. This is illustrated in Figure 3-4.

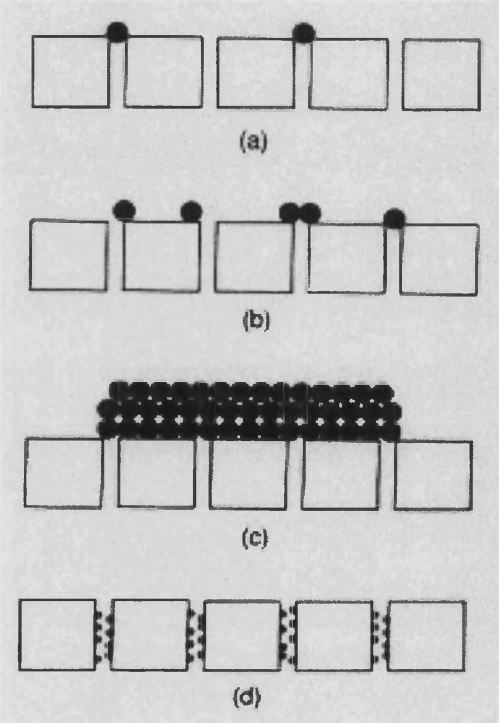

Figure 3-4 Membrane blocking mechanisms: (a) complete pore blocking, (b) partial pore blocking, (c) cake filtration, and (d) internal pore blocking (from Field [56])

3.4.5 Mechanism and Theory of Microfiltration

The flux through the membrane is generally described on Darcy's law as a function of TMP:

$$J = P \cdot (p_F - p_p) = P \cdot \Delta p$$

where P is the permeability constant. P is a function of the viscosity of permeate, pore size distribution and porosity of the membrane. P can be described by the Carmen-Kozeny equation when the membrane can be compared to an arrangement of spherical particles:

$$J = \frac{\varepsilon^3}{K\eta S^2.(1-\varepsilon)^2} \cdot \frac{\Delta p}{l_{pore}}$$

When straight capillaries can be assumed in the membrane, the Hagen-Poiseuille equation can be used:

$$J = \frac{\varepsilon . d_{pore}^2}{32\eta.\tau} \cdot \frac{\Delta p}{l_{pore}}$$

The physical membrane parameters such as porosity ε, pore diameter d_{pore}, pore length l_{pore} and tortuosity of pores τ are important parameters affecting the separation. The transmembrane pressure Δp is inversely proportional to the membrane thickness l_{pore}, hence thin membranes are desirable.

3.5 Fouling in the Microfiltration of Activated Sludge

Many workers have studied membrane fouling in the microfiltration of activated sludge. It is still not very well understood as activated sludge is a complex mixture, which makes it difficult to identify the fouling component. Parameters such as the different fractions of activated sludge, bacterial extracellular polymeric substances (EPS), MLSS and particle size have been studied and will be discussed. There is unlikely to be a single fouling component and the standard methods of characterising the fractions of the activated sludge do not help too much as they are all complex mixtures of different components themselves. None of the components described below are pure compounds and their composition will vary with the waste material being treated and the operating conditions of the plant. The discussion starts by describing the effects of the fouling factors reported in the literature. In particular, insights of the interactions between the fouling factors and operating hydrodynamic conditions have been incorporated. The effects of biological operating parameters such as SRT and loading rate on membrane will then be discussed.

3.5.1 Fractions of Activated Sludge

Defrance et al. [57] investigated the effect of the 3 fractions of activated sludge: suspended solids, colloids and solutes on membrane fouling. It was reported that the 3 fractions caused 65 %, 30 % and 5 % of the filtration

resistance respectively. The sum of the resistances of the 3 fractions was 50 % higher than the measured total resistance.

Two other groups [58] [59] did the same study and obtained different results. The results are summarised in Table 3-2 and appear inconclusive. Bouhabila et al. [59] used synthetic wastewater simulating dairy effluent. Defrance et al. [57] and Wisniewski et al. [58] used domestic wastewater. While the different feed solutions may be the reason for the different results, a careful examination shows that the different hydrodynamic conditions are more likely to be the cause.

Wisniewski et al. [58] did the filtration with backflushing. Suspended solids and colloids were more easily removed, resulting in a smaller cake resistance due to the two fractions. Solutes adsorption was difficult to remove and gave a larger fouling resistance. Defrance et al. [57] performed the experiments with a crossflow system under a constant TMP of 1 bar and a crossflow velocity of 3 $m.s^{-1}$. Deposition of biomass flocs was significant as suggested by the initial rapid flux decline and the high fouling resistance of 6.75×10^{12} m^{-1} for the filtration of the complete sludge. This resulted in the high fouling percentage for the suspended solids. In contrast, Bouhabila et al. [59] did the tests with a submerged MBR under constant flux operation. The results were reported in permeability and the actual flux and TMP were thus not known. However, the fouling resistance was only 1.06×10^{12} m^{-1} for the complete sludge, suggesting that the operating flux was probably below the critical flux of the biomass flocs. Fouling by the biomass flocs was thus not significant

and resulted in the high fouling percentage for the colloids. The colloids, being smaller, were preferentially deposited on the membrane under constant flux operation. This suggests that the mode of operation (constant flux or TMP), hydrodynamic conditions (aeration or crossflow velocity, flux or TMP) and cleaning techniques (backpulsing, air of liquid backflushing, intermittent permeation) closely affect how membrane fouling by a complex feed occurs.

Table 3-2 Contributions of different fractions to membrane fouling

Fraction	Bouhabila et al. [59] (%)	Defrance et al. [57] (%)	Wisniewski et al. [58] (%)
Suspended solids	26	65	23
Colloids	50	30	25
Solutes	24	5	52

3.5.2 Bacterial Extracellular Polymeric Substances and Soluble Microbial Products

Bacterial extracellular polymeric substances (EPS) have been reported to be an important parameter in membrane biofouling. Chang and Lee [60] studied the effect of the physiological state of activated sludge on membrane fouling. It was reported that for any physiological state, a higher amount of EPS in the activated sludge resulted in a faster flux decline. The EPS around the biomass

floc and not the cell contributed to the filtration resistance. Lee et al. [61] then suggested that the proportion of protein to carbohydrate was more important than the actual amount of EPS. A larger proportion of protein resulted in a higher filtration resistance for the microbial flocs. Both work suggested the importance of fouling by EPS. Batch filtrations were used in both cases to determine the resistances.

The hydrodynamic conditions can be controlled such that biomass flocs do not deposit on the membrane, that is, below the critical flux of the biomass flocs. Under such operating conditions, fouling by EPS can be expected to be less important than SMP. Rosenberger and Kraume [62] reported that SMP had the most effect on the filterability of activated sludge when compared with MLSS, viscosity and EPS. Tardieu et al. [63] suggested that the gradual TMP rise is due to the soluble and colloidal fractions, as the cake composition was found to be similar to the supernatant. SMP thus plays a very important role in the long-term fouling of MBRs, since long-term operation of MBRs involves low fluxes or pressures where deposition of biomass flocs is not significant.

3.5.3 Mixed Liquor Suspended Solids

Mixed liquor suspended solids (MLSS) is a standard and easily measured parameter in wastewater treatment. Several workers have studied its effect on membrane fouling. Shimizu et al. [64] [65] studied the microfiltration of

activated sludge using submerged hollow fibre membrane. It was reported that the steady-state filtration flux ($m.s^{-1}$)

$$J_{ss} = V_L = K' u^{*1.0} MLSS^{-0.5}$$

where V_L, K', u* and MLSS are the lift velocity ($m.s^{-1}$), filtration constant ($kg^{0.5}.m^{-1.5}$), air-liquid two-phase flow velocity ($m.s^{-1}$) and MLSS ($kg.m^{-3}$) respectively. Thomas et al. [53] reported that for 3 sidestream tubular membranes at MLSS from 2-15 $g.l^{-1}$,

$$Js = - a \ln (SS) + b$$

where Js is the specific flux ($l.m^{-2}.s^{-1}.bar^{-1}$), SS is the suspended solids ($mg.l^{-1}$), a and b are arbitrary constants.

Cicek et al. [30] determined the limiting flux for MLSS from 2.1-15.4 $g.l^{-1}$. It was reported that the limiting flux decreased with increasing MLSS, rapidly between 2–8 $g.l^{-1}$ and slower between 8-15 $g.l^{-1}$. These work showed that the permeate flux decreased non-linearly with increasing MLSS.

A linear decrease in flux with increasing MLSS has also been reported. Madaeni et al. [66] reported that critical flux decreased approximately linearly with increasing MLSS from 3-10 $g.l^{-1}$. In the case of an anaerobic MBR, Beaubien et al. [67] reported that

$J_{sta} = \alpha C_x + J^0sta$

where J_{sta} is the stabilised permeate flux ($\mu m.s^{-1}$), α the proportionality factor ($m^4.s.kg^{-1}$), C_x the MLSS ($kg.m^{-3}$) and J^0_{sta} ($\mu m.s^{-1}$) the extrapolated stabilised flux at negligible suspended solids concentration. The stabilized permeate flux decreased linearly with increasing MLSS at MLSS from 1.6-22 $g.l^{-1}$.

Contrary to the above results, a positive effect of MLSS on the permeate flux has also been observed. Yamamoto et al. [8] reported that the highest flux decline occurred at the highest MLSS of 19.2 $g.l^{-1}$. Under a constant TMP of 40 kPa, a slightly higher flux decline was observed at an MLSS of 5.2 $g.l^{-1}$ than at an MLSS of 10.8 $g.l^{-1}$. Under a constant TMP of 80 kPa, the flux decline became slightly higher at the MLSS of 10.8 $g.l^{-1}$ than 5.2 $g.l^{-1}$. This could be due to the formation of a dynamic cake layer protecting the membrane from fouling by small particles. Under the higher TMP of 80 kPa, the flux decline for the MLSS of 5.2 $g.l^{-1}$ and 10.8 $g.l^{-1}$ was higher. The normalised flux was approximately 0.6 after 2.5 hours. Particle deposition on the membrane was evident and the higher MLSS resulted in a higher flux decline. Under the lower TMP of 40 kPa, flux decline was slow and the normalised flux was higher than 0.9 after 6 hours. This implied that cake formation was not significant. Under such a condition, the flux decline was higher for the lower MLSS presumably due to fouling by small particles.

The permeate flux controls the convection of particles towards the membrane. Under constant flux operation, the flux can be controlled below the critical

flux and no particles deposit on the membrane. Defrance and Jaffrin [68] reported that the sludge from a classical wastewater treatment plant with a MLSS of 3.9 $g.l^{-1}$ resulted in a higher filtration resistance as compared to the sludge from an MBR with an MLSS of 10 $g.l^{-1}$. The floc sizes of the classical wastewater treatment plant were also larger than the MBR sludge, and were less likely to deposit on the membrane. The absence of a dynamic cake layer would have exposed the membrane to fouling by small particles, which were difficult to remove and less reversible than the MBR sludge. Lee et al. [42] operated at constant flux (25 $l.m^{-2}.h^{-1}$) and found that as MLSS increased, the operation time for the TMP to reach 26 kPa decreased when increasing MLSS from 0.1-5 $g.l^{-1}$. The MBR was operated at a constant flux of 25 $l.m^{-2}.h^{-1}$. An attached growth system had 2 $g.l^{-1}$ biomass attached on looped cord media and 0.1 $g.l^{-1}$ in the reactor. Compared to a suspended growth system of 3 $g.l^{-1}$ MLSS, the TMP took 140 hours and 20 hours to reach 26 kPa respectively. The supernatant TOC, protein and polysaccharide of both systems were similar. Scanning electron microscopy showed microbial flocs for suspended growth and a slime and gel layer for attached growth. Interestingly, the operation time for an attached growth system with 2 $g.l^{-1}$ MLSS in the reactor was similar to a suspended growth system of 2 $g.l^{-1}$ MLSS, 70 hours and 75 hours respectively. These results again suggest the formation of a dynamic cake layer by the MLSS, which prevents the adsorption of soluble organics onto the surface or inside the pores of the membrane.

It is interesting to note that all the work that reported a negative effect of MLSS on the permeate flux was under constant TMP operation. All these

work also reported significant flux decline, which is the usual case for constant TMP operation, implying significant particle deposition on the membrane. Under constant flux operation, the permeate flux is usually controlled below the critical flux and deposition of large particles on the membrane is not significant. The absence of a protective dynamic cake layer results in higher membrane fouling by small particles, which are difficult to remove. As viscosity increases with increasing MLSS, deposition of large particles, which are reversible becomes more significant. Small particles are then deposited on the dynamic cake layer and can be removed together with the dynamic cake layer. This is likely to occur near the critical flux of the large particles. When viscosity becomes too high with increasing MLSS and the critical flux of the large particles is exceeded, the permeate flux is expected to decrease with increasing MLSS concentration.

3.5.4 Particle Size

Particle size has been known to affect membrane fouling due to deposition on the membrane surface. A larger particle, having a higher critical flux, will result in a higher permeate flux. Besides being preferentially deposited, small particles result in a compact cake giving high filtration resistance. The high shear required to minimize fouling, especially in sidestream membrane systems, resulted in smaller particle sizes for the MBR compared to CASP. Wisniewski and Grasmick [69] observed biological floc destruction and particle size reduction with recirculation. For dead-end filtration, the presence

of small particles and polymers led to a decrease in filterability. Similarly, Kim et al. [47] studied the effect of pump shear on membrane performance. Only 4 % of the floc sizes were below 10 μm before recirculation. This increased to 23 % and 61 % for a centrifugal and rotary pump respectively. The flux decline was reported to coincide with the floc size decrease and was faster for the rotary pump. This was attributed to the fine colloids and EPS released due to floc breakup. For an anaerobic MBR treating alcohol-distillery wastewater, Choo and Lee [70] also observed that the floc size reduction resulted in an initial exponential flux decline.

The average particle diameter has been reported to be approximately 2-3.5 μm for sidestream MBRs. Choi et al. [71] showed that the floc size decreased after the start-up of a sidestream MBR and remained constant after 4 hours. The floc size had a narrow distribution near 2 μm. Bailey et al. [34] observed particle sizes of 2 μm and 103 μm for the MBR and CASP respectively. Muller et al. [46] observed that the biomass in an MBR consisted of free cells and small flocs of less than 50 μm. Floc fragments, protozoa and metazoa were absent. The particle sizes in the CASP were 100-1000 μm. The biomass contained flagellates, ciliates, and sometimes rotifers, nematodes and mosquito larvae were also present. In summary, the MBR contains smaller particles compared to the CASP. The reduction in particle size due to floc break-up resulted in a flux decline or higher specific resistance.

3.5.5 Viscosity

For sidestream MBRs, increased viscosity is important as this results in increased frictional loss during pumping. For submerged systems, increased viscosity results in a deceleration of the air-liquid two-phase flow velocity. In both cases, viscosity affects the flow regime at the membrane surface and influences membrane fouling. The relationship between viscosity and MLSS has been observed to increase rapidly above a certain MLSS concentration, which ranges widely from 8-40 $g.l^{-1}$. Shimizu et al. [64] reported that viscosity increased rapidly above 8 $g.l^{-1}$ MLSS. Churchouse [11] and Yamamoto [8] observed this rapid increase in sludge viscosity at MLSS of 18 $g.l^{-1}$ and 40 $g.l^{-1}$ respectively. The wide range of MLSS at which this rapid increase occurs suggests that other mixed liquor components such as SMP have important roles. Nagaoka et al. [72] suggested increased viscosity of mixed liquor being due to SMP. Ueda et al. [23] reported that increased sludge viscosity corresponded with increased dissolved organic carbon (DOC).

Several authors have reported empirical relationships between sludge viscosity and concentration. Xing et al. [40] reported a linear relationship between sludge viscosity and concentration up to a MLSS of 17 $g.l^{-1}$:

$\eta = 0.1488 \times MLSS + 1.036$

where η is the sludge viscosity in mPa.s and MLSS the mixed liquor suspended solids in $g.l^{-1}$.

Liu et al. [73] reported an exponential relationship:

$$\mu = 1.61\, e^{0.07 \times MLSS}$$

where μ is the sludge viscosity in mPa.s and MLSS the mixed liquor suspended solids in $g.l^{-1}$.

3.6 Effects of SRT and Loading Rate on Membrane Fouling

As discussed above, factors such as EPS, SMP, particle size, viscosity, MLSS and the different fractions of activated sludge have been known to affect membrane fouling. The effects of operating parameters such as SRT and loading rate on these factors will be discussed. This will provide important insights to designing and operating of MBRs.

MBRs have been operated with SRT ranging from 5 days to complete sludge retention [22] [8]. While a long SRT, hence high MLSS concentration has the advantages of a small footprint and low sludge production, cell viability decreases and EPS may increase due to cell lysis. Shin and Kang [74] reported that the active cells were 55 % and 32 % for SRTs of 15 days and 44

days respectively in a MBR treating synthetic wastewater. Chaize and Huyard [28] measured dehydrogenase activity and O_2 specific consumption as an indicator of the active biomass fraction. The specific activities decreased as the biomass aged. However, the decrease in the active biomass fraction did not affect carbon removal [46]. COD removal greater than 90 % was observed when the MLSS concentration increased to 40-50 $g.l^{-1}$ [34].

EPS has been reported to decrease with increasing SRT or independent of SRT. Chang et al. [75] reported that the EPS content of floc decreased with increasing SRT for SRTs of 3, 8 and 33 days. Membrane fouling increased with increasing EPS. Lee et al. [61] reported the EPS concentration to be independent of SRT for SRTs of 20, 40 and 60 days. The protein to carbohydrate ratio increased with increasing SRT, as did filtration resistance. Taken together, the results suggest decreasing EPS content of floc with increasing SRT up to 20 days after which the concentration is stable, but beyond 20 days, the protein to carbohydrate ratio increased.

SMP is expected to increase with increasing SRT due to cell lysis, which is proportional to the MLSS concentration. Nagaoka et al. [72] reported the accumulation of SMP causing an increase in viscosity and filtration resistance over 140 days. In contrast, Yamamoto et al. [8] reported that the supernatant COD and TOC did not increase with MLSS. Lysis products may not present a huge fouling problem in MBRs, possibly due to their degradation at long SRTs or high MLSS concentrations. The model of Lee et al. [39] suggested that SMP decreased with longer SRT due to the more active uptake of lysis

products at higher MLSS when the F/M ratio is less than 1.2. Lee et al. [61] reported that the filtration resistance of the supernatant was independent of SRT for 3 SRTs of 20, 40 and 60 days. Bouhabila et al. [59] observed that the specific resistance of the supernatant decreased after more than 30 days at a SRT of 30 days. Such a decrease was not observed for the SRTs of 10 and 20 days, suggesting the degradation of lysis products at long SRTs.

Various authors have observed the accumulation and subsequent degradation of organics in MBRs. Chaize and Huyard [28] reported the accumulation of supernatant TOC that was subsequently degraded after 160 days in an MBR treating domestic wastewater. Huang et al. [29] also observed this phenomenon of supernatant TOC accumulation and subsequent degradation after 5 months in an MBR treating synthetic wastewater. Shin and Kang [74] observed increasing dissolved organic carbon (DOC), which then decreased gradually after 100 days. This was due to the degradation of high molecular weight compounds.

The factors affecting the accumulation or non-accumulation, as well as the degradation of organics in MBRs are not clear. The accumulation and subsequent degradation of TOC has been observed at low SRT and MLSS of 20 days and 3-4 $g.l^{-1}$ respectively [29]. The synthetic wastewater contained glucose and starch. Yamamoto et al. [8] and Shin and Kang [74] used synthetic wastewater containing glucose. No TOC accumulation and DOC accumulation that was subsequently degraded were observed respectively. No

clear conclusions can be made. The different microorganisms in the sludges are probably important.

With regard to particle size, Huang et al. [31] reported mean particle sizes of 14.82, 48.24 and 30.61 μm for SRTs of 5, 20 and 40 days respectively in a submerged MBR treating domestic wastewater. A likely explanation for the smaller particle size at a lower SRT is the high shear resulting in the breakup of biomass flocs. The MLSS was 0.75-1 $g.l^{-1}$ and 7 $g.l^{-1}$ at SRTs of 5 and 40 days respectively. The viscosity of the mixed liquor increases with increasing MLSS and floc breakup is expected to be less significant. Lee et al. [61] reported that the floc size distribution was similar for SRTs of 20, 40 and 60 days in a submerged MBR treating synthetic wastewater. The mean floc size increased with increasing SRT, being 5.2, 6, and 6.6 μm for SRTs of 20, 40 and 60 days. The large difference in particle size between the 2 sludges is not clear, as both are submerged systems.

The effect of volumetric loading rate on membrane fouling has been investigated by Nagaoka et al. [76] [77]. A sudden increase in TMP after 40 days was observed for a high loading of 1.5 $gTOC.l^{-1}.d^{-1}$. This occurred after 120 days for a low loading of 0.5 $gTOC.l^{-1}.d^{-1}$. The MLSS increased from 6-25 $g.l^{-1}$ and 6-10 $g.l^{-1}$ respectively. The higher MLSS and presumably viscosity may be the reason for the difference.

In conclusion, it appears that there is an optimum SRT or F/M ratio. Short SRTs of 8 days or less have been reported to result in increased EPS content

of floc. Lysis products can be degraded by specialized microorganisms that can develop at long SRTs, resulting in lower SMP concentrations at longer SRTs. The work of Brookes et al. [38] showed that EPS and SMP concentrations decreased with increasing SRT from 4-80 days. The effect of high MLSS and viscosity is expected to become significant at long SRT or low F/M ratio, resulting in a lower permeate flux.

3.7 Fouling Control

Fouling can be controlled by using suitable hydrodynamic conditions. Fouling control using crossflow velocity, gas-liquid two-phase flow, the concept of critical flux and intermittent permeation will be discussed.

3.7.1 Crossflow Velocity

For sidestream MBRs, the crossflow velocity (CFV) is expected to be important for controlling particle deposition onto the membrane surface. Tardieu et al. [63] studied the effect of CFV on bioparticle deposition using a tubular MBR. It was reported that the deposition of floc particles on the membrane surface at a low CFV of 0.5 $m.s^{-1}$ resulted in a rapid increase of hydraulic resistance. At a high CFV of 4 $m.s^{-1}$, floc particle deposition was not observed and the TMP increased linearly with time even at high fluxes of 75-150 $l.m^{-2}.h^{-1}$. Cicek et al. [30] reported that flux increased with increasing

TMP, but reached a maximum as expected from the concept of limiting flux. There was a linear relationship between the maximum flux and CFV.

In contrast, Thomas et al. [53] reported a negative effect at high CFV for a sidestream tubular MBR. The fouling resistance decreased up to a CFV of 3.1 $m.s^{-1}$, then increased thereafter. This was suggested to be due to a more compact fouling layer and increased pore plugging caused by a higher TMP by the author. This could be the phenomenon of reduced deposition of large particles at the high CFV and thus deposition of the smaller and more fouling small particles as described by Howell [78] on the experiments of Tanaka.

3.7.2 Gas-Liquid Two-Phase Flow

In submerged MBRs, the movement of the rising bubbles, which generates a crossflow, retards fouling. Air sparging has been shown to enhance permeate flux, by bubble induced secondary flow and increased bulk fluid flow. Gas-liquid two-phase flow can be classified into bubble flow, slug flow, churn flow, annular flow and mist flow. Bubble flow occurs at low gas flow rates. Slug flow occurs at higher gas flow rates due to bubbles colliding and coalescing, and is favorable for permeate flux enhancement. In large diameter pipes, the injection factor

$$\varepsilon = \frac{U_{GS}}{(U_{GS} + U_{LS})}$$

where U_{GS} and U_{LS} are the superficial gas and liquid velocities respectively.

If $\varepsilon < 0.2$, bubble flow develops where there are dispersed bubbles in the liquid phase. If $0.2 < \varepsilon < 0.9$, slug flow occurs where there are alternating gas and liquid slugs. If $\varepsilon > 0.9$, annular flow is observed where there is a continuous gaseous phase in the center of the pipe and liquid flows on the wall. The values of ε studied ranged from 0-0.83 [79], which corresponded to bubble and slug flows. Flux enhancement up to 320 % was reported. The effects of gas flow rate, liquid flow rate, TMP and feed concentration on permeate flux enhancement by gas-liquid two-phase flow are discussed below.

The permeate flux increased with the injection of air. Flux enhancement up to 320 % was reported [79]. Using a light microscope, Chang and Fane [80] observed that air injection controlled particle deposition on the membrane and enhanced the permeate flux. Both the reversible and irreversible fouling were decreased and the permeate flux was important for controlling particle deposition. Laborie et al. [81] and Cabassud et al. [82] suggested that two-phase flow expanded the cake, resulting in a decrease in specific resistance and increase in porosity and thickness. The permeate flux increased with increasing gas flow rate. A maximum flux was observed, which could not be increased further with increasing gas flow rate [81] [82] [83] [84] [85]. Cui et al. [86] suggested that this is due to the size and strength of the primary wake being independent of the slug size above a critical length. Increasing the superficial gas velocity increased the slug size and frequency. The maximum flux enhancement occurred when the space between air slugs were entirely

occupied by primary wakes. Further increase in the superficial gas velocity then affected the primary wakes or resulted in bubble coalescing. Chang and Fane [84] suggested that deposition occurred in the liquid slugs at low gas or liquid superficial velocities. Increasing the gas or liquid superficial velocities reduced the deposition and resulted in flux enhancement. It was theoretically shown that the velocity of the falling film was insensitive to the total superficial velocity. At high gas or liquid superficial velocities, deposition occurred at the falling film and no further increase in flux was observed.

Permeate flux enhancement in gas-liquid two-phase flow increased and then decreased with increasing liquid flow rate. Cui and Wright [79] reported that flux enhancement increased with liquid Reynolds number up to a maximum, and the enhancement effect was not significant when the liquid flow was turbulent. Mercier et al. [83] reported that flux enhancement increased up to 220 % at a liquid flow rate of 0.2 $m^3.h^{-1}$ and decreased thereafter. Chang and Fane [84] reported that increasing the liquid velocity resulted in an initial increase and then decrease in flux. Flux enhancement was smaller for a higher liquid velocity. Cui and Wright [85] and Bellara et al. [87] reported that the liquid flow rate had little effect on the permeate flux for gas-sparged ultrafiltration of dextran solution, hence a higher flux enhancement at a lower liquid flow rate. Vera et al. [88] studied gas-sparged microfiltration of ferric hydroxide suspension and biologically treated wastewater with inorganic tubular membrane. The permeate flux enhancement was highest for a moderate liquid velocity of 0.5 $m.s^{-1}$ and decreased at higher liquid crossflow.

Cui and Wright [79] [85] studied gas-sparged ultrafiltration of dextran solution. Flux enhancement with air injection increased with increasing TMP, due to the disruption of a more severe concentration polarization. In contrast, Vera et al. [88] studied gas-sparged microfiltration of ferric hydroxide suspension and biologically treated wastewater with inorganic tubular membrane. Flux enhancement decreased with TMP for ferric hydroxide due to compression. For the wastewater, flux enhancement showed a minimum at a TMP of 2 bars. Another possible explanation could be that microfiltration membranes are more susceptible to pore clogging. Mercier et al. [83] reported that flux enhancements increased and decreased for ultrafiltration and microfiltration membranes respectively with increasing TMP. This was thought to be due to more severe pore clogging at higher TMP for microfiltration membrane. For a TMP of 0.55 bar, flux enhancement reached 150 % and 160 % for ultrafiltration and microfiltration membranes respectively. Flux enhancement increased to 290 % at a TMP of 2 bars for ultrafiltration, but decreased to 120 % at a TMP of 2.5 bars for microfiltration. Lee et al. [89] showed that air slugs increased the permeate flux for ultrafiltration and microfiltration of a bacterial suspension with hollow fibre and flat sheet membranes respectively. Air injection was approximately 50 % more effective on reducing filtration resistance for a 300 000 MWCO ultrafiltration membrane than a 0.2 μm microfiltration membrane for bacterial suspensions.

Similar to the effect of TMP, flux enhancement with air injection increased with increasing feed concentration due to the disruption of a more severe

concentration polarization for gas-sparged ultrafiltration of dextran solution [79] [87]. Mercier-Bonin et al. [90] studied the ultrafiltration and microfiltration of yeast suspension with ceramic flat sheet membrane. The permeate flux was always higher with air injection and decreased similarly with increasing concentration. As the final flux was smaller, flux enhancement was higher with increasing concentration, when particle deposition was more severe. Flux enhancement of 100 % (18 and 9 $l.m^{-2}.h^{-1}$ with and without air injection respectively) and 200 % (12 and 4 $l.m^{-2}.h^{-1}$ with and without air injection respectively) were observed for 5 and 20 $g.l^{-1}$ respectively. Mercier et al. [83] studied alcoholic fermentation with *Saccharomyces Cerevisiae* coupled with an ultrafiltration membrane. The permeate flux was always higher with air injection whatever the cell concentration. Flux enhancement was 60 % at 20 $g.l^{-1}$ and increased to 100 % at a higher concentration of 50 $g.l^{-1}$.

Ghosh and Cui [91] modelled gas-sparged ultrafiltration for slug flow in tubular membrane, considering the mass transfer in the 3 different zones near the gas slug. The trends were similar between the theoretical and experimental results for 167 kDa dextran, although the experimental values of the effects of gas flow rate and bubbling frequency on permeate flux were always higher than the theoretical values. The model predicted higher permeate flux for increasing gas flow rate, TMP, decreasing liquid flow rate and feed concentration.

Besides permeate flux enhancement, enhanced selectivity for the fractionation of proteins by gas-sparged ultrafiltration has also been reported [92] [93] [94].

For wastewater treatment, aeration has been reported to have a positive effect on permeate flux. Vera et al. [88] reported that the permeate flux increased with gas sparging for the microfiltration of biological treated wastewater. The resistance was reduced by half with gas sparging at a TMP of 1 bar and a liquid velocity of 3 $m.s^{-1}$, compared to 1.91×10^{9} m^{-1} for unsparged filtration. Ueda et al. [48] studied the effect of aeration on submerged hollow fibre membrane. The suction pressure decreased with increasing aeration rate up to a critical value where the pressure did not decrease further. The suspension of permeation for 7 days allowed a previously deposited cake layer to be removed, as the pressure was restored to that before the cake built-up. Davies et al. [16] reported a lower membrane throughput rate when the aeration rate was reduced for the Kubota system operated with gravity suction.

Table 3-3 Operating conditions and flux enhancement of gas-liquid two-phase flow

System	Operating Conditions	Flux Enhancement (%)	References
Ceramic flat sheet membrane, yeast suspension (5-20 $g.l^{-1}$)	u_l = 0.3–1.4 $m.s^{-1}$, u_g = 0-0.8 $m.s^{-1}$, ε = 0-0.73	up to 280	[90]
Hollow fibre membrane, clay suspension (0.9–5.2 $g.l^{-1}$) and river water	u_l = 0.5–0.9 $m.s^{-1}$, u_g = 0-1 $m.s^{-1}$, ε = 0-0.67	20-200 (clay suspensions)	[81] [82]
Hollow fibre membrane, yeast suspension (5 $g.l^{-1}$)	u_l = 0-0.42 $m.s^{-1}$, u_g = 0-0.68 $m.s^{-1}$	50-94	[80] [84]
Flat sheet membrane, proteins		7-50	[93]
Tubular membrane, dextran (1.9 $g.l^{-1}$)	u_l = 0-0.42 $m.s^{-1}$, u_g = 0.001-0.009 $m.s^{-1}$	30	[86]
Tubular mineral membrane, yeast suspension (20 $g.l^{-1}$)	u_l = 0-0.5 $m.s^{-1}$, u_g = 0-0.68 $m.s^{-1}$	300	[83]
Tubular membrane, BSA and dextran solutions		60 (dextran) 91 (BSA)	[85]
Tubular membrane, dextran solution (1-10 $g.l^{-1}$)	u_l = 0.141-0.778 $m.s^{-1}$, u_g = 0-0.68 $m.s^{-1}$, ε = 0-0.83	up to 320	[79]
Hollow fibre membrane, dextran and albumin solutions (10-40 and 2-20 $g.l^{-1}$ respectively)		20-50 (dextran) 10-60 (albumin)	[87]

System	Operating Conditions	Flux Enhancement (%)	References
Hollow fibre membrane, clay suspension (0.9-5.2 $g.l^{-1}$)	u_l = 0.5 $m.s^{-1}$, u_g = 0-1 $m.s^{-1}$, ε = 0-0.67	up to 110	[95]
Tubular membrane, MLSS (3.2 $g.l^{-1}$)	ε = 0-0.5	43	[96]

3.7.3 The Concept of Critical Flux

Field et al. [97] first proposed the concept of critical flux, that there is a flux on start-up below which the TMP does not increase with time. Below the critical flux, a flux increase or decrease will not result in hysteresis. Above the critical flux, fouling occurs and the TMP increases with time. A hysteresis is observed when flux is decreased. The critical flux is dependent on the crossflow velocity, particle size and other variables. There are 2 types of critical flux. The strong form is that the flux is the same as the clean water flux at the same TMP. The weak form is that the flux is lower than the clean water flux, but is linear with the TMP below the critical flux. Howell [78] has reviewed the concept of critical flux. Recent developments on the concept of critical flux are summarised below.

Chen et al. [98] studied the transition from concentration polarisation to cake formation using colloidal silica. It was reported that below critical flux, the TMP remained stable when flux was increased and then decreased in steps. Kwon et al. [99] studied the critical flux for kaolin clay suspension from 10–100 $mg.l^{-1}$. The critical flux decreased with increasing kaolin clay concentration. The addition of 0–4 $mg.l^{-1}$ of organic (fulvic acid) concentration had no effect on critical flux. Madaeni [100] studied the critical flux for colloidal latex suspensions of 1.0 μm, 0.1 μm and their mixture. The respective critical fluxes were determined to be 120, 105 and 88 $l.m^{-2}.h^{-1}$ by a stepwise increase of flux and monitoring the TMP. The strong form of critical

flux was observed for the 1.0 μm latex suspension. The critical flux was higher at higher crossflow and lower concentration. The critical flux was the lowest for the mixture. This was thought to be due to the higher packing density of the flowing cake layer. In a further study using electron microscopy [101], no deposition of latex beads was observed below the critical flux for the 1.0 μm and 0.1 μm latex suspensions. Although there was no deposition of latex beads after 2 hours for the mixture, deposition was observed after ten hours even below critical flux.

Kwon and Vigneswaran [102] studied the effects of particle size and surface charge on critical flux using latex particles. It was concluded that critical flux increased with particle size. The strong form of critical flux was observed. Wu et al. [103] filtered 2 colloidal silica suspensions, BSA solution and baker's yeast suspension using a polyethersulphone membrane. The colloidal silica suspension HT50 exhibited the weak form of critical flux, while the strong form of critical flux was observed with the X30 silica, BSA and baker's yeast. The TMP was very low below critical flux. Fradin and Field [104] determined the critical fluxes for magnesium hydroxide suspension at various crossflows and concentrations. It was observed that the critical flux increased with increasing crossflow and decreasing concentration. A critical concentration was reported above which the strong form of critical flux was not observed. Manttari and Nystrom [105] studied the critical fluxes for nanofiltration of effluents of the paper industry and high molar mass polysaccharides. The critical flux increased with decreasing concentration and linearly with increasing crossflow (2.7–3.6 $m.s^{-1}$). The weak form of critical

flux was observed. Both reversible and irreversible fouling decreased with increasing crossflow. Fouling was mostly reversible. Both the strong and weak form of critical flux were observed for the high molar mass polysaccharides. Metsamuuronen et al. [106] studied the critical fluxes for myoglobin solution and yeast suspension. The critical flux was observed to increase with increasing crossflow and decrease linearly with the logarithm of the solute concentration for myoglobin and the hydrophilic C30G membrane. No critical flux was observed for myoglobin and the hydrophobic GR51 membrane. Irreversible fouling occurred when the flux was decreased, as the pure water pressure (PWP) had a higher slope, even though the TMP was mostly restored. In summary, these work showed the existence of the strong and weak form of critical flux. No hysteresis occurred below critical flux. The critical flux increased with increasing crossflow, particle size and decreasing concentration.

Membrane pore size has been reported to have no significant effect on critical flux. Vyas et al. [107] reported that the critical fluxes were similar for membrane pore sizes of 0.2 μm and 1.0 μm for the microfiltration of lactalbumin suspension. Madaeni et al. [66] reported that the critical flux was higher for hydrophilic membrane, but was not dependent on membrane pore sizes from 0.22-0.65 μm. Kwon et al. [108] investigated the effect of membrane pore sizes from 0.1-0.65 μm and latex particles of 0.816 μm on critical flux. The membrane pore size did not have any significant effect on critical flux. Below critical flux, the TMP was lower for larger membrane pore sizes. Above critical flux, the rate of TMP increase was higher for larger

membrane pore sizes. In contrast, Chen [109] reported that the critical flux was observed to increase with increasing membrane pore sizes from 0.1-0.4 μm for BSA microfiltration. As rejection decreased with increasing pore size, concentration polarization was less severe, resulting in higher critical fluxes.

New developments on the concept of critical flux include the direct observation through the membrane (DOTM) technique and definition of critical flux based on material balance. The DOTM technique has been developed by Li et al. [110] and enable the visualization of the membrane surface. It was reported that there was no deposition of particles below critical flux when filtering latex beads. Above critical flux, particle layers were observed on the membrane surface. In a further work, Li et al. [111] investigated the critical fluxes at different crossflows for latex, yeast and algae particles of 3-12 μm. The critical flux increased with increasing crossflow, particle size and decreasing feed concentration.

Vigneswaran et al. [112] studied the concept of critical flux for microfiltration based on 3 different definitions:

1. material balance. The change of particle concentration in the fluid phase was determined by monitoring the suspension turbidity. The critical flux is the highest flux that no particles were deposited.
2. increase in the TMP. The critical flux is the highest flux that the TMP was constant.
3. direct observation through the membrane (DOTM). The critical flux is the minimum flux leading to the permanent deposition of particles.

For the monodispersed suspensions of polystyrene latex particles from 0.3-11.9 μm, the smaller particles were observed to have a higher tendency of deposition. The critical fluxes based on material balance and increase in the TMP increased with increasing particle size. The rate of increase of critical flux was higher based on the increase in the TMP than material balance. The critical flux based on DOTM was very low. For the polydispersed kaolin clay suspension, the critical flux based on material balance was found to be more realistic in field conditions. In a related work, Kwon et al. [108] investigated the effects of particle size, membrane pore size and concentration on critical flux. The critical flux based on the increase in the TMP was found to decrease with increasing particle size from 0.1-0.46 μm, and then increased with increasing particle size from 0.46-11.9 μm. The minimum critical flux corresponded to the particle size of 0.46 μm. The higher critical fluxes for the smaller particle sizes are due to higher Brownian diffusion. The effect of membrane pore size on critical flux was investigated for the membrane pore sizes from 0.1-0.65 μm and latex particles of 0.816 μm. The membrane pore size did not have any significant effect on critical flux. Below the critical flux, the TMP was lower for larger membrane pore sizes. Above the critical flux, the rate of TMP increase was higher for larger membrane pore sizes. The effect of concentration from 30-400 $mg.l^{-1}$ on critical flux showed that critical flux decreased slightly with increasing concentration. The rate of TMP increase was higher at lower concentrations. These developments clearly demonstrate the existence of critical flux, but the critical flux where no particle deposition occurs is probably lower than that observed for a stable TMP.

Several workers have investigated the concept of critical flux for wastewater treatment. Defrance and Jaffrin [113] compared constant flux and constant TMP filtrations of activated sludge using a ceramic membrane. A critical flux was reported and it increased linearly with CFV. In a further work [68], the reversibility of fouling was studied. It was reported that fouling was reversible below the critical flux. Above the critical flux, fouling was partially irreversible. Fouling was observed to be reversible below a TMP of 400 kPa. Fouling was also reversible when the CFV was decreased from 5 to 1 $m.s^{-1}$ and then increased. Madaeni et al. [66] investigated the factors affecting the critical flux in the filtration of activated sludge. It was reported that critical flux increased with higher CFV and lower MLSS. The critical flux was higher for hydrophilic membrane, but was not dependent on membrane pore size. Vera et al. [114] and Elmaleh et al. [115] microfiltered secondary treated wastewater using a 0.14 μm inorganic composite membrane. A critical flux of 100 $l.m^{-2}.h^{-1}$ at a TMP of 1 bar and a CFV of 3 $m.s^{-1}$ was reported.

While critical fluxes with stable TMPs are observed during short-term filtration, TMPs have been reported to rise slowly and then rapidly during long-term filtration even when under sub-critical conditions. Ahn and Song [50] reported a 'critical flux' of 20 $l.m^{-2}.h^{-1}$ for a submerged MBR. Operating with an intermittent permeation of 2 minutes suspension every 12 minutes, the TMP stabilised until the 50^{th} day. Chemical cleaning was required after 77 days of operation. Using a fouled membrane, the TMP was observed to decrease when operated at the 'critical flux'. Cho and Fane [116] suggested that the gradual rising of the TMP was due to the deposition of SMP on the

membrane. The plugging of membrane pores reduced the effective area for filtration. This caused the localised permeate flux to increase above the critical flux of the biomass flocs. The deposition of the dominant foulant on the membrane resulted in a rapid increase in the TMP. This phenomenon was termed the TMP jump.

3.7.4 Intermittent Permeation

Yamamoto et al. [8] first reported that intermittent permeation allowed long-term operation of MBR. Intermittent permeation is an in situ membrane cleaning technique where permeation is suspended periodically while maintaining the crossflow. Particles deposited on the membrane will be removed by the crossflow when the TMP that held the particles is removed during the suspension of permeation. Intermittent permeation is used for delicate membranes, which will rupture by backwashing. The advantages of intermittent permeation include its simplicity as no additional equipment is required and the independent control of the filtration and cleaning phases. Energy consumption for the crossflow may be optimised [117].

Several workers have studied intermittent permeation using yeast suspensions. Tanaka et al. [118] showed that flux recovery increased with higher crossflows when permeation was suspended. There was an optimal crossflow beyond which flux recovery could not be increased further. The flux after 3 hours filtration was 4 times higher with a 10 minutes on and 4 minutes off cycle. A

faster flux decline was observed with a 10 minutes on and 1 minute off cycle. The final and initial fluxes increased when the permeation time was decreased from 10 to 2.5 minutes, with 1 minute suspension. Kuruzovich and Piergiovanni [119] studied intermittent permeation cycles of 0.5-6 minutes on and 5-90 seconds off. It was observed that 10-15 seconds suspension was necessary for every 0.5-1 minute permeation to maintain a steady state flux. Longer suspension times were necessary for longer permeation times. The longer the total suspension time, the slower the flux declined.

Kuberkar and Davis [120] compared intermittent and continuous permeation using yeast suspension, BSA solution, and a mixture of yeast and BSA. It was observed that intermittent permeation was only partially effective for the removal of the external cake formed during yeast filtration. The flux was higher than that for continuous crossflow filtration, but declined gradually with time. Intermittent permeation was completely ineffective in removing the internal foulants during BSA filtration. During the filtration of yeast-BSA mixture, the flux was higher initially due to the complete or partial removal of the yeast cake. This exposed the membrane to internal fouling by BSA and the flux became similar to that for continuous crossflow filtration. Various suspension times of 0.2-10 seconds after 6 minutes permeation were investigated. The net permeate obtained after 4000 seconds increased with longer suspension times.

In summary, the permeation duration ranges from 0.5-10 minutes, followed by 0.2-240 seconds of suspension. The permeation: suspension ratio ranges from

1500:1 to 10:4. Intermittent permeation has some effect on cake fouling, but little effect on internal fouling by proteins.

In wastewater treatment, it has been reported that the TMP recovered after the suspension of permeation while maintaining the aeration. Ueda et al. [48] reported that the suspension of permeation for 7 days allowed a previously deposited cake layer to be removed, as the pressure was restored to that before the cake built-up using a submerged hollow fibre membrane.

Many workers operated MBRs using intermittent permeation cycles from 1-9 minutes to 30-2 minutes on-off [8] [50]. Ueda and Hata [14] used a 8-4 hours on-off intermittent permeation cycle. The most common intermittent permeation cycles are 8-13 minutes permeation followed by 2 minutes suspension [48] [23] [36] [31]. The Kubota system uses a 8-2 minutes on-off intermittent permeation cycle [11] [12] [15].

There are few comparisons of different intermittent permeation cycles. Ahn and Song [50] studied intermittent permeation cycles of 10–2, 10–0.5 and 30–2 minutes on–off. The longest operation time before chemical cleaning was required was observed for the intermittent permeation cycle of 10 minutes on and 2 minutes off. This is expected since the permeation: suspension ratio is the lowest, hence the longest total suspension time. This result is similar to the work of Kuruzovich and Piergiovanni [119] on yeast suspension described earlier. Similar operation times were observed for the other 2 intermittent permeation cycles. It should be noted that the permeation: suspension ratio for

the 10–0.5 and 30–2 minutes on–off are similar, which may explain why the operation times were similar.

3.8 Behaviour of Variable Flux Operation

Several authors have reported the behaviour of operating MBRs under varying flux conditions. Ishida et al. [18] increased the TMP for 5 hours, and the flux was observed to decrease gradually under a constant TMP, implying gradual membrane fouling. Decreasing the flux subsequently restored the TMP to approximately its original value. This implied that although fouling was removed, a little residual fouling had occurred. Similarly, Ueda et al. [14] doubled the flux from 15.8 to 31.7 $l.m^{-2}.h^{-1}$ for 22 days. Both the TMP and filtration resistance were observed to increase gradually under a constant flux. Returning the flux back to 15.8 $l.m^{-2}.h^{-1}$ did not restore the TMP and filtration resistance to its original value. Gunder et al. [12] simulated a diurnal pattern flowrate, resulting in the flux varying between 10 and 35 $l.m^{-2}.h^{-1}$. The permeability decreased from more than 200 to 110 $l.m^{-2}.h^{-1}.bar^{-1}$ in the initial 20 days, then increased slightly to 130 $l.m^{-2}.h^{-1}.bar^{-1}$ in the following 25 days to achieve a stable operation. All these work suggest that increasing the flux would result in residual fouling. In contrast, Cote et al. [22] simulated a diurnal flow with a peak to average ratio of 2.5 for several months, and reported that the pressure and flux profiles were reproducible, indicating the absence of residual fouling.

3.9 Summary

The idea of operating MBRs with a varying throughput is introduced. Membrane filtration and fouling are described. The fouling components or factors such as the different fractions of activated sludge, EPS, SMP, MLSS, particle size and viscosity in the microfiltration of activated sludge have been discussed. The interactions between these components or factors and the hydrodynamic conditions are discussed. It is believed that these interactions are important in determining the fouling propensity of the different components or factors, and resolve the contradicting results in the literature. The effects of operating parameters such as SRT and loading rate on membrane fouling have been reviewed and suggest an optimal SRT or F/M ratio. Fouling control by gas-liquid two-phase flow, the concept of critical flux and intermittent permeation is also discussed.

3.10 Project Objectives

The main project objective is to investigate the feasibility of operating MBRs with a variable throughput. To achieve this, the effects of important hydrodynamic parameters such as aeration and permeate flux on membrane fouling will be determined. The behaviour of MBRs under varying flux operation will be investigated.

Long-term operation of MBRs will also be studied. This involves understanding membrane cleaning techniques such as intermittent permeation and the concept of critical flux applied to activated sludge. The effects of MLVSS or F/M ratio on membrane fouling will be investigated.

3.10.1 Varying Throughput Operation of MBRs

The 3 times DWF design of MBRs results in MBRs being operated below their maximum treatment capacity most of the time. Power consumption due to aeration, which is significant in submerged systems, could be reduced when MBRs are not operating at their maximum treatment capacity. Such an optimization requires a relationship between membrane fouling, permeate flux and aeration that is currently not available. The behaviour of MBRs under varying throughput operation with simultaneous changes in aeration has also not been reported. Hence, the feasibility of varying throughput operation of MBRs will be investigated.

3.10.2 Intermittent Permeation

Membrane cleaning techniques such as permeate or air backwash and intermittent permeation are necessary for the long-term operation of MBRs. All 3 techniques have been used for hollow fibre or tubular membranes, while only intermittent permeation has been reported for flat sheet systems. The Kubota system uses intermittent permeation. The more aggressive techniques

such as permeate and air backwash are likely to decrease the lifetime of the membranes. Hence, intermittent permeation will be studied, as there are few comparisons of different intermittent permeation cycles in the literature.

3.10.3 Concept of Critical Flux

While critical fluxes for activated sludge have been reported for short-term experiments, the concept of critical flux for long-term operation of MBRs is not clear. Hence, the concept of critical flux will be studied.

3.10.4 MLVSS or F/M Ratio

MLVSS or F/M ratio are easily determined parameters in the field of wastewater treatment and are useful design parameters. While EPS, particle size and viscosity have been known to affect membrane fouling, these factors cannot be used for designing purposes. Membrane fouling due to these factors is also dependent on the complex interactions between the biological and hydrodynamic conditions. The scope of this work will be limited to the effects of MLVSS or F/M ratio on membrane fouling.

4 Materials and Methods

4.1 Design of Laboratory Scale MBR

The laboratory scale MBR was designed as a scaled down version of the actual Kubota system. A single laboratory scale Kubota membrane (pore size 0.4 μm), with dimensions of 0.3 m x 0.2 m giving a total membrane area of 0.12 m^2, was used for the MBR, instead of the 24–140 membrane panels (measuring 1 m x 0.4 m) that a standard Kubota unit consists (Figure 4-1). Hence the laboratory scale MBR represented a scaled down portion of a standard Kubota unit, consisting of a single membrane panel with a channel on both sides of the membrane. A standard Kubota unit is submerged at a height of 1 m above the bottom of the activated sludge tank. The membrane was situated 0.3 m above the bottom of the laboratory scale MBR, since the laboratory scale membrane was only 0.3 m in height, instead of 1 m for a standard panel. The flow of the Kubota system is based on the airlift reactor, with uprisers and downcomers. This is illustrated in Figure 4-2.

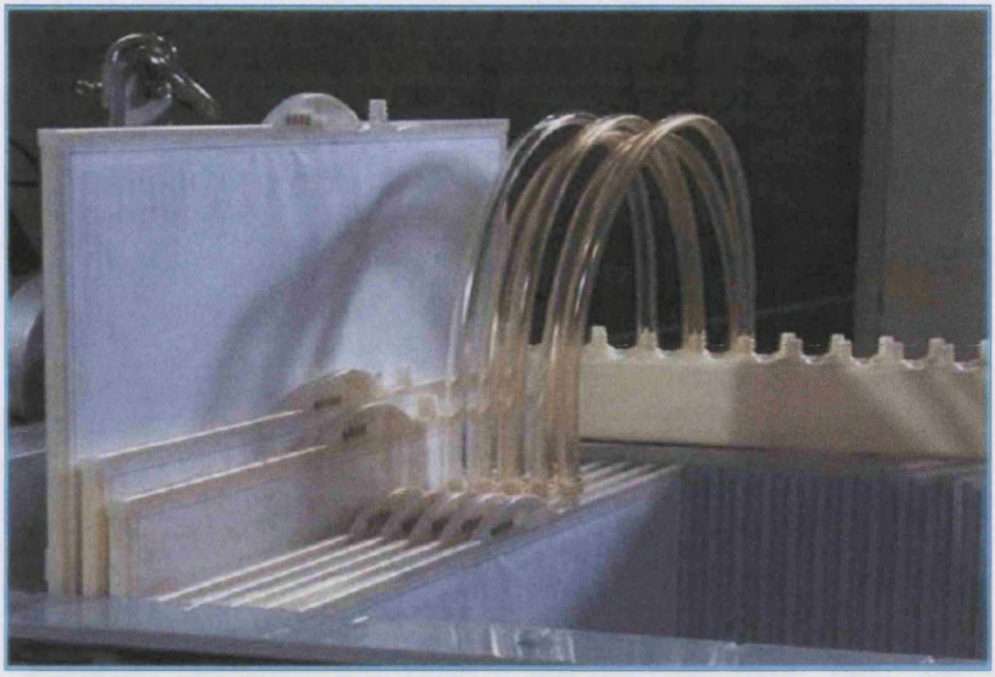

Figure 4-1 A standard Kubota unit of flat sheet membranes

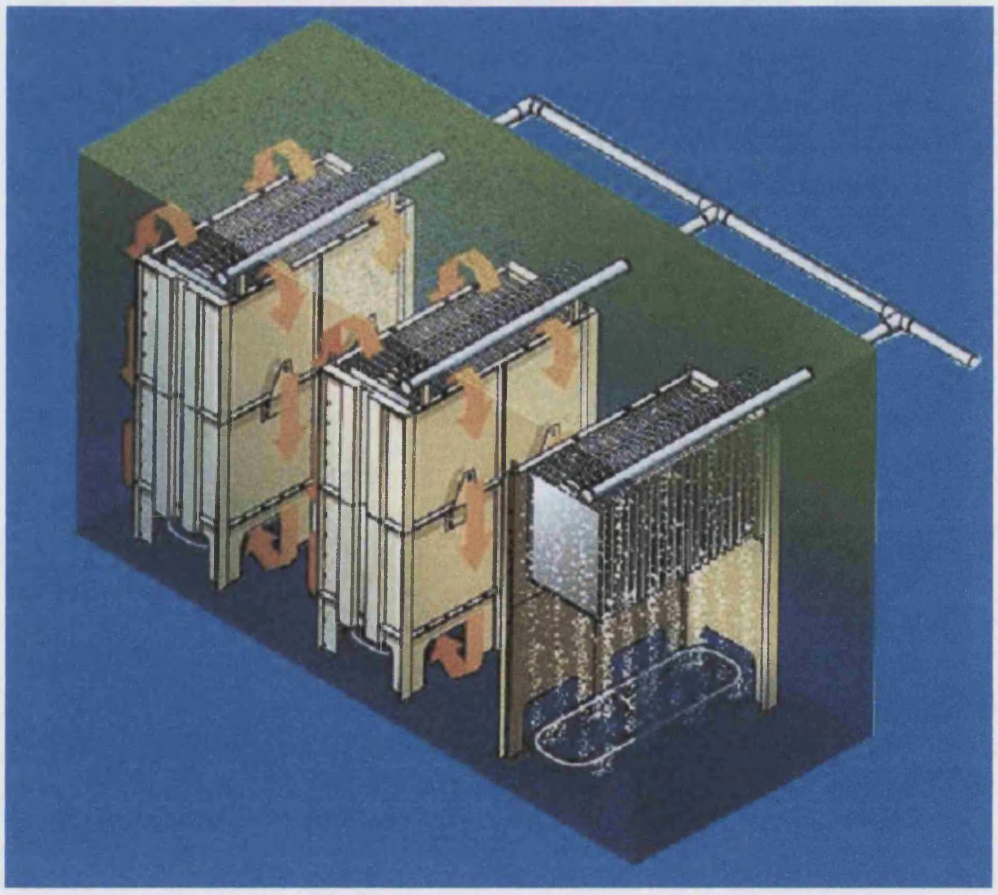

Figure 4-2 The Kubota process

The flow of the laboratory scale MBR was kept consistent with an upriser and a downcomer. However the downcomer was situated behind the membrane instead of on both sides of the membrane. Figure 4-3 shows the side view of the laboratory scale MBR. The cross-sectional areas of the upriser (excluding the thickness of the membrane) and downcomer were equal. The top of the MBR opened up with twice the cross sectional area to facilitate gas disengagement from the liquid. Temperature was kept constant at 20 ^{o}C using a water jacket at the front and back of the MBR.

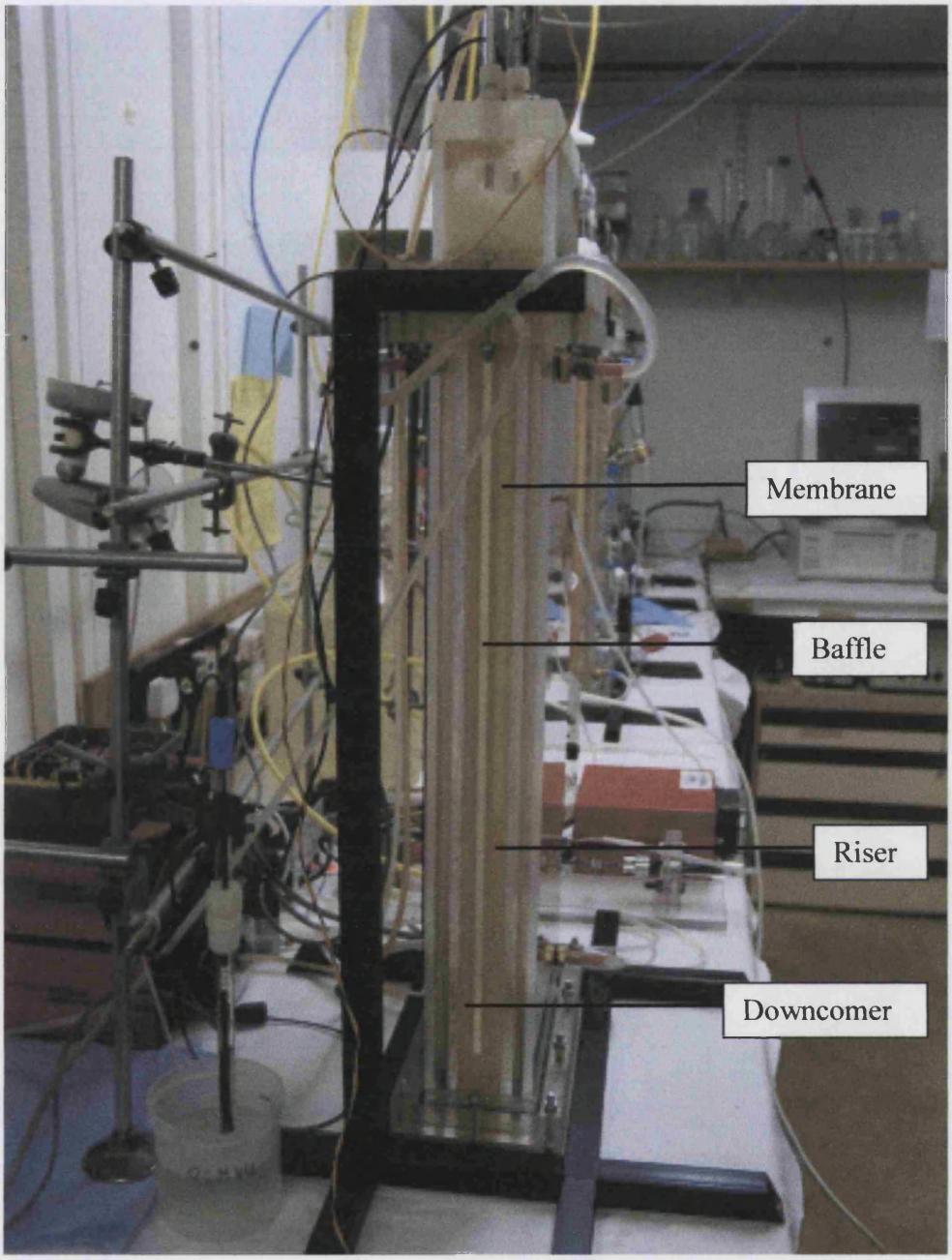

Figure 4-3 Side view of MBR, illustrating Kubota membrane, baffle, riser and downcomer

The MBR was constructed with Perspex (Acrylic), with a working volume of approximately 3.5 l. The volume was kept constant using a level sensor. The high and low sensors were situated approximately 10 mm above and below the designed activated sludge level at a height of approximately 617 mm respectively. As there was excess membrane area relative to the volume of the MBR, permeate was recycled back into the MBR when the volume in the MBR dropped below the low sensor. As the volume in the MBR rose to the high sensor, permeate recycling stopped until the volume in the MBR dropped below the low sensor and the cycle was repeated. Air was introduced via a Perspex tube with 4 holes of 1.5 mm at the bottom of the riser. The dissolved oxygen probe, pH probe, temperature sensor, level sensor, feed pipe, permeate pipe, sludge wastage pipe and gas outlet were situated at the top of the MBR. Figure 4-4 shows the front view of the MBR.

Figure 4-5 shows the dimensions of the MBR used. The width, height and breadth measured 32 mm, 592 mm and 222 mm respectively, above which was the gas disengagement section. The size of the gas disengagement section was 64 mm, 104 mm and 222 mm for the width, height and breadth respectively. The activated sludge level in the MBR fluctuated approximately between 607-627 mm. The width of the membrane module itself was 6 mm and the thickness of both the upflow (excluding the thickness of the membrane) and downflow channels were 10 mm. The clearances below and above the membrane unit itself were 247 mm and 55 mm respectively.

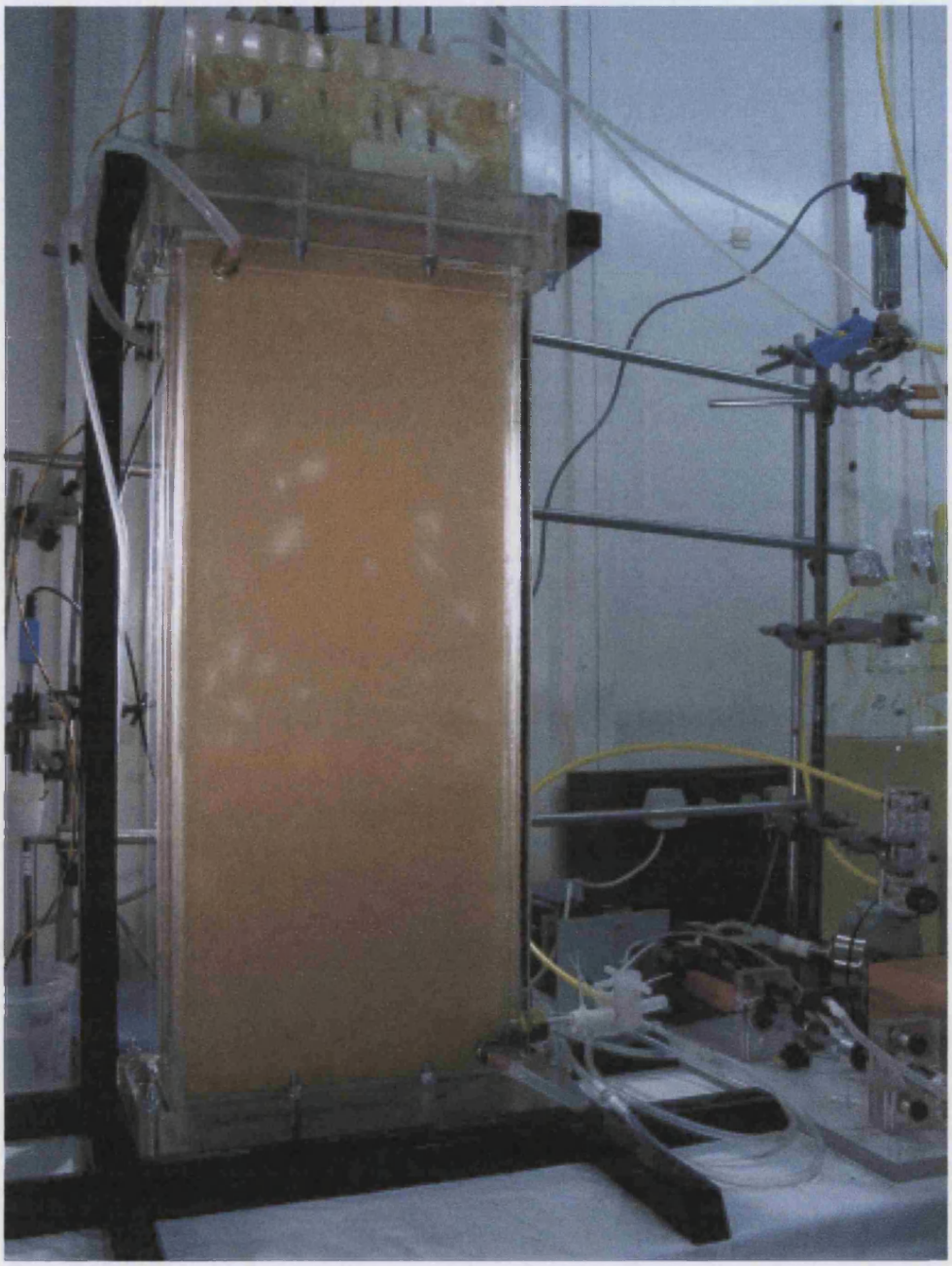

Figure 4-4 Front view of MBR with a submerged Kubota membrane

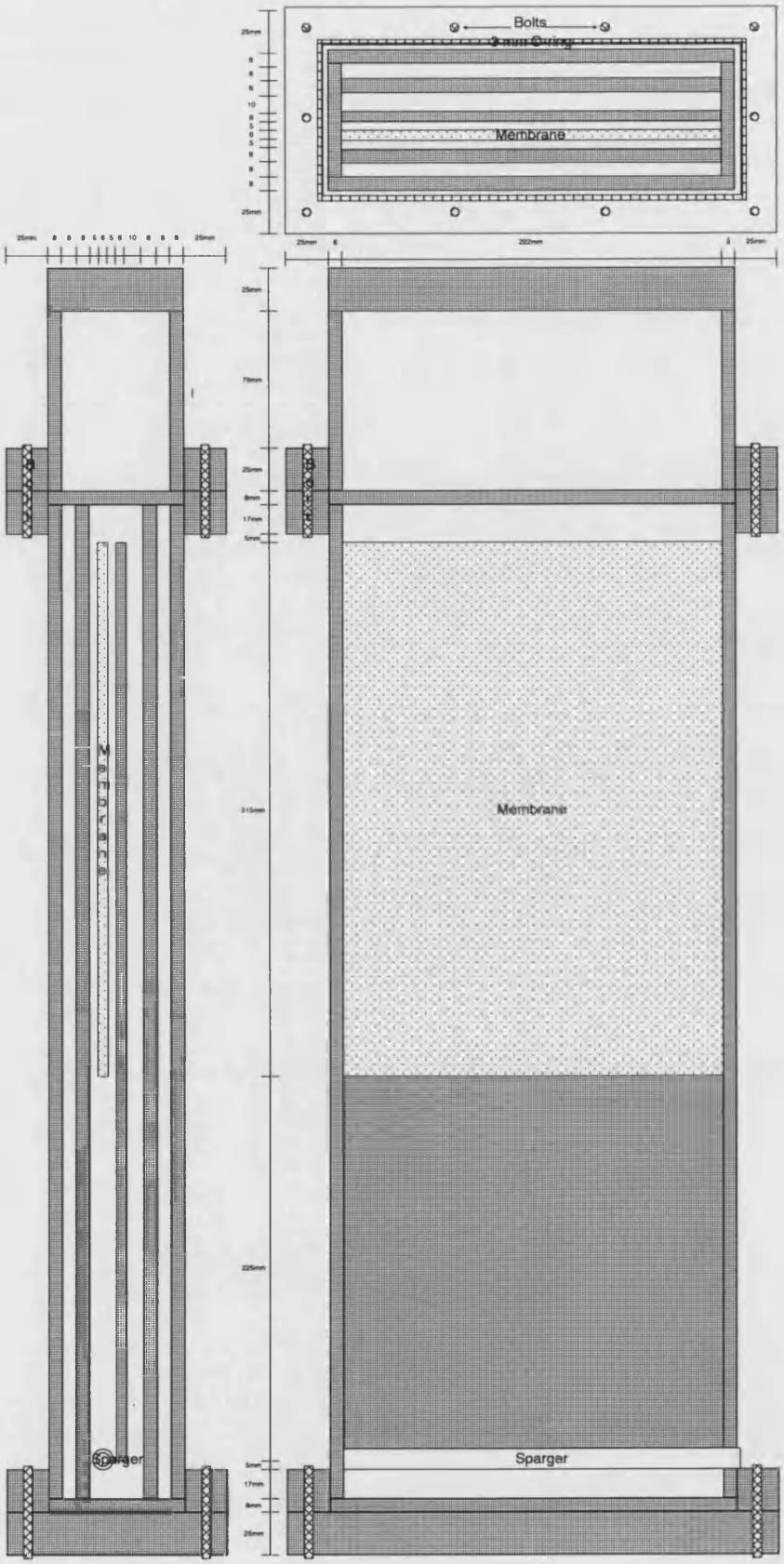

Figure 4-5 Dimensions of MBR

4.2 Setup of Experimental Rig

The setup of the experimental rig is illustrated in Figure 4-6. The influent was made up by diluting a concentrated feed solution with water in a ratio of 1:9. This was to avoid having to prepare large volumes of actual feed concentration frequently. An automatic refilling syringe pump was used to maintain an average concentrated feed flow of 0.97 $ml.min^{-1}$. The water flow of 8.75 $ml.min^{-1}$ was pumped with a peristaltic pump (Watson Marlow). The permeate flow was controlled by a PID control loop using the VisiDAQ Professional Edition software by Advantech, with a gear pump (Flowgen), turbine flowmeter (Cole-Parmer) and PC to maintain a constant flux. The gear pump created a differential pressure across the membrane by suction, hence drawing out the permeate. A pressure transducer (Druck, PMP 4070, range of -1 to 1 bar with corresponding output of –5 to 5 VDC) was used to measure the suction pressure. The dissolved oxygen probe (Uniprobe), pH probe (Fisher), temperature sensor (Farnell Electronic), pressure transducer and turbine flowmeter were interfaced to a PC via the PCI-1710 interface card (available from BEDE Technology) for data logging, using the VisiDAQ software.

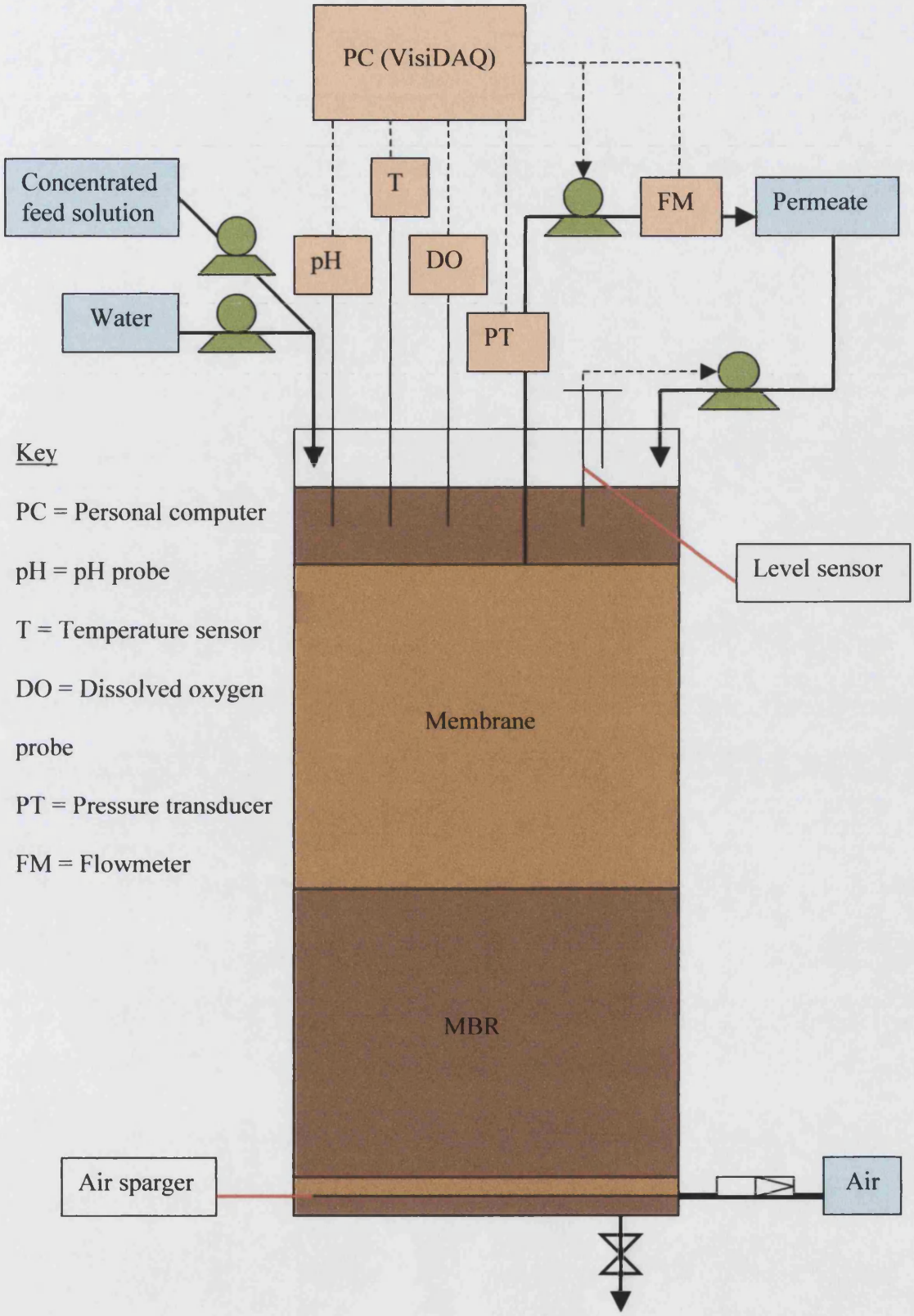

Figure 4-6 Schematic diagram of experimental setup

4.3 Start Up and Operating Conditions

The activated sludge was obtained from the Cam Valley wastewater treatment plant, near the towns of Midsomer Norton and Radstock, Somerset, and acclimatised to the simulated sewage in the MBR. The composition of the simulated sewage is shown in Table 4-1.

Table 4-1 Composition of simulated sewage

Component	Concentration ($g.l^{-1}$)
Peptone	0.2
Meat Extract	0.14
Urea	0.01
$CaCl_2.2H_2O$	0.004
$MgSO_4.7H_2O$	0.002
K_2HPO_4	0.011
NaCl	0.007

The operating conditions were chosen based on that published by workers using the Kubota system. The HRT was set at 6 hours. No sludge was wasted to build up the biomass to the level that MBRs are operated (approximately 12–16 $g.l^{-1}$ MLVSS). The temperature was maintained at 20 °C.

4.4 Analytical Methods

The analytical methods used were from the Standard Methods for the Examination of Water and Wastewater by the American Public Health Association. The total residue (MLSS) and total volatile (MLVSS) and fixed residue were dried at 103 and 550 °C respectively.

5 Results – Intermittent Permeation and Dynamic Critical Flux

5.1 Operating MBRs with Intermittent Permeation

5.1.1 Effect of Increasing and Decreasing Aeration Rate on Membrane Fouling

This series of experiments showed the effect of increasing and then decreasing (d) aeration rate on fouling rate at different fluxes. The aeration rate was characterised by the superficial gas velocity u_g, the volume of air at NTP, delivered per unit cross section of the upflow sector of the aerator, per unit time. It is a calculated empty space velocity not the actual bubble velocity. Figure 5-1 showed that with a low permeate flux of 10 $l.m^{-2}.h^{-1}$ little fouling was observed at the higher superficial gas velocities (u_g = 50 and 83 $mm.s^{-1}$). Fouling was observed at the lowest u_g of 17 $mm.s^{-1}$, and especially when this was achieved by decreasing the aeration rate from a higher value.

A similar trend was observed with a higher permeate flux of 20 $l.m^{-2}.h^{-1}$ although here fouling was observed at u_g = 50 $mm.s^{-1}$ but not at 83 $mm.s^{-1}$ (Figure 5-2).

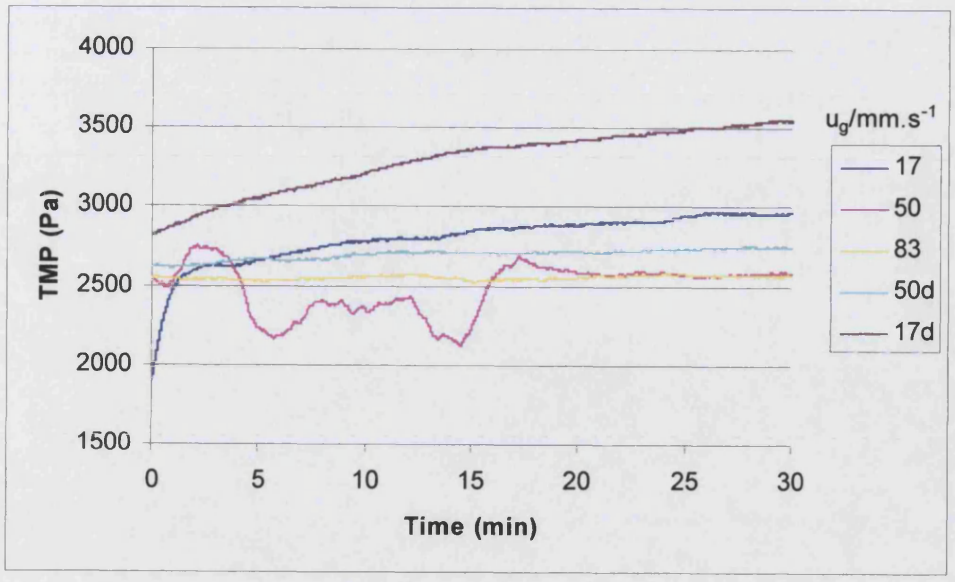

Figure 5-1 TMP at a permeate flux of 10 l.m^{-2}.h^{-1} for increasing and then decreasing (d) u_g (mm.s^{-1}), MLVSS = 3.7 g.l^{-1}

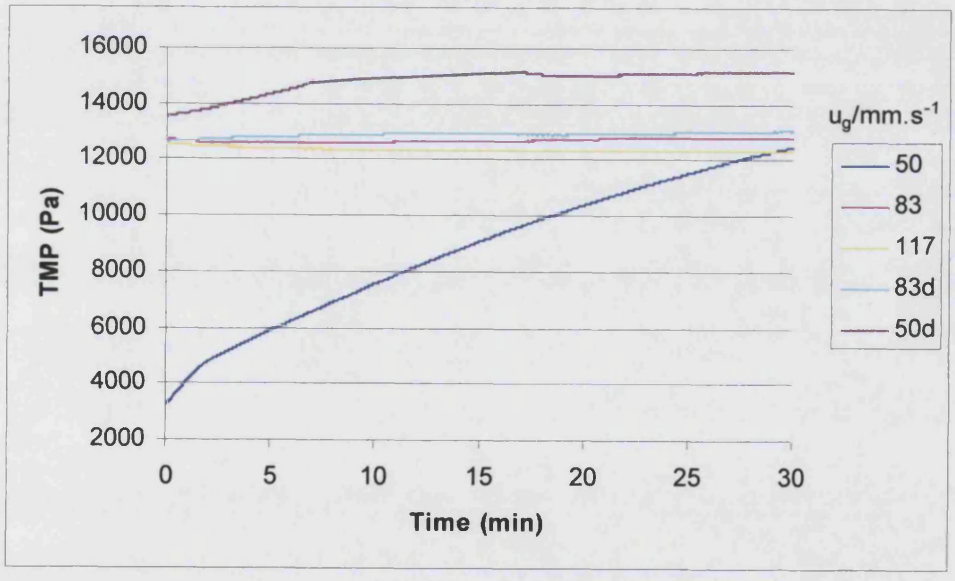

Figure 5-2 TMP at a permeate flux of 20 l.m^{-2}.h^{-1} for increasing and then decreasing (d) u_g (mm.s^{-1}), MLVSS = 3.7 g.l^{-1}

5.1.2 Continuous Vs Intermittent Permeation

Figure 5-3 allowed a comparison between continuous (Figure 5-2) and intermittent permeation (Figure 5-3) at a permeate flux of 20 $l.m^{-2}.h^{-1}$. Permeation was on for 8 minutes and off for 2 minutes. A similar trend was observed again, with little increase in fouling. However, the minimum u_g to prevent fouling was lower compared to continuous permeation. No fouling was apparent at u_g of 83 $mm.s^{-1}$ for continuous permeation, and 50 $mm.s^{-1}$ for intermittent permeation. This suggests that intermittent permeation allows stable operation at a fixed flux with a lower aeration rate. This is important, as aeration is the major energy cost in MBRs. Note that the permeate flux always refer to the instantaneous flux in this work. Intermittent permeation will not be so much better if the average flux was considered instead.

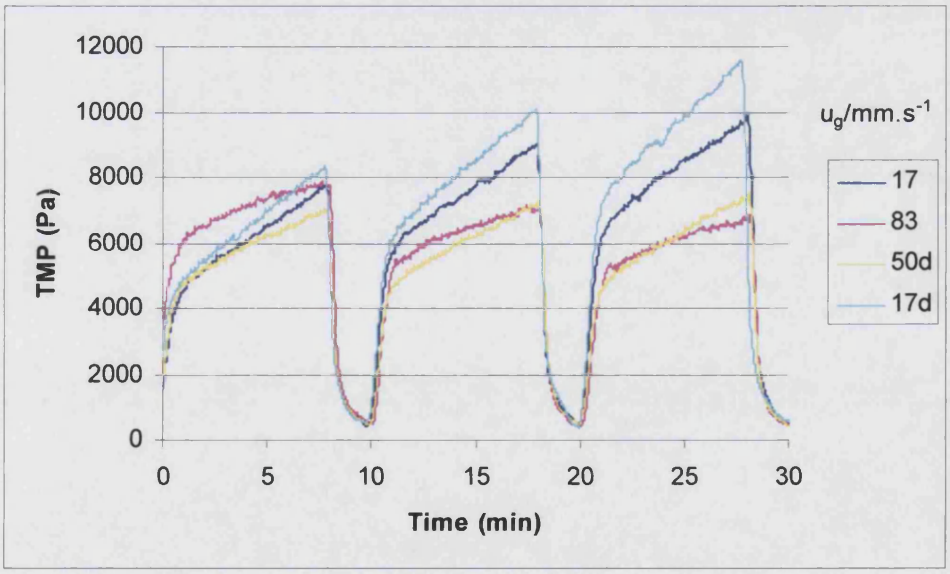

Figure 5-3 TMP at a permeate flux of 20 $l.m^{-2}.h^{-1}$ for increasing and decreasing (d) u_g ($mm.s^{-1}$), with intermittent permeation of 8 min on and 2 min off, MLVSS = 3.7 $g.l^{-1}$

5.1.3 Optimising Intermittent Permeation

Intermittent permeation is an in-situ membrane cleaning technique which involves the stopping of the permeate flux periodically while continuing the aeration. Since there will be no transmembrane pressure during this stoppage, the accumulated particles on the surface of the membrane will be swept away by the crossflow. The duration of the permeation and stoppage period was varied to study the cake deposition and removal respectively. One of the objectives was to also investigate the reversibility of the fouling, that is, whether the cake that was deposited during the period of permeation could be completely removed. The membrane was chemically cleaned with sodium hypochlorite as detailed in Section 6.5 before the start of this series of experiments.

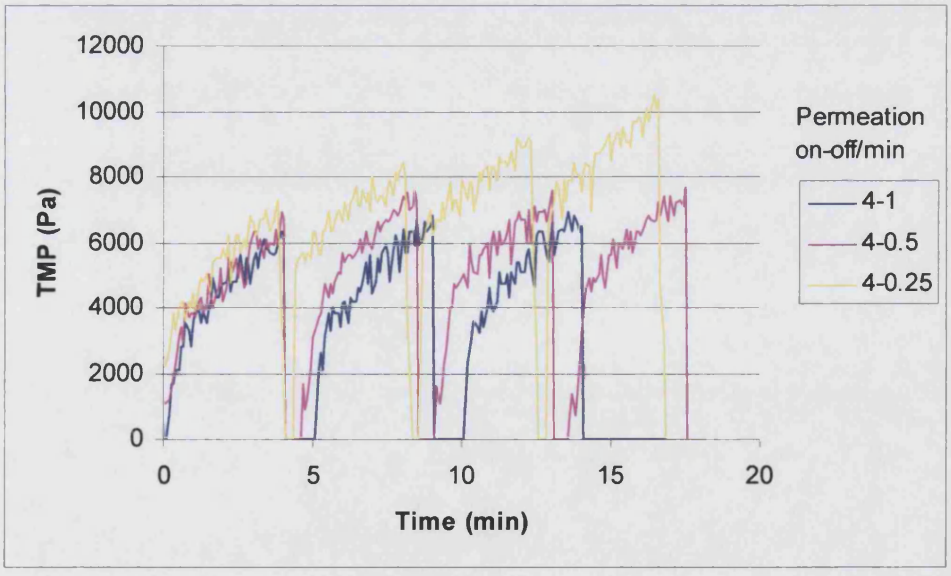

Figure 5-4 TMP at an intermittent permeation cycle of 4 min on followed by 0.25, 0.5 and 1 min off, permeate flux = 25 $l.m^{-2}.h^{-1}$, u_g = 229 $mm.s^{-1}$, MLVSS = 9.76 $g.l^{-1}$

Figure 5-4 showed the TMP for 4 min permeation followed by 0.25, 0.5 and 1 minute stoppage. It was clearly observed that the short cleaning duration of 0.25 minute was insufficient to remove all the particles deposited during the 4 minutes permeation period. The rise in TMP during the 4 minutes permeation was due to cake deposition. The TMP decreased after the stoppage, indicating the removal of some deposit during the stoppage, but the TMP continued to rise for subsequent cycles, indicating cake built up. When the cleaning duration was increased to 0.5 minute, the TMP increased slowly for each cycle. The TMP did not increase for each cycle when the cleaning duration was increased to 1 minute. This implies that the fouling during the 4 minutes permeation can be completely removed. The experimental runs were repeated and found to be reproducible.

The aim of the next series of experiments was to see the effect of a longer permeation period. In Figure 5-5, the permeation duration was increased to 8 minutes. Similar results to the 4 minutes permeation duration were observed. Progressive particle deposition was clearly observed for the stoppage duration of 0.5 minute but the TMP was stable from cycle to cycle when the cleaning interval was increased to 2 minutes. Figure 5-6 showed a further increase in the permeation duration to 16 minutes. The TMP was stable when the cleaning duration was 4 minutes. Intermittent permeation can be used to remove fouling for a stable TMP to be maintained. The duration of permeation up to 16 minutes is not important, as long as the ratio of permeation and stoppage duration is kept at 4:1.

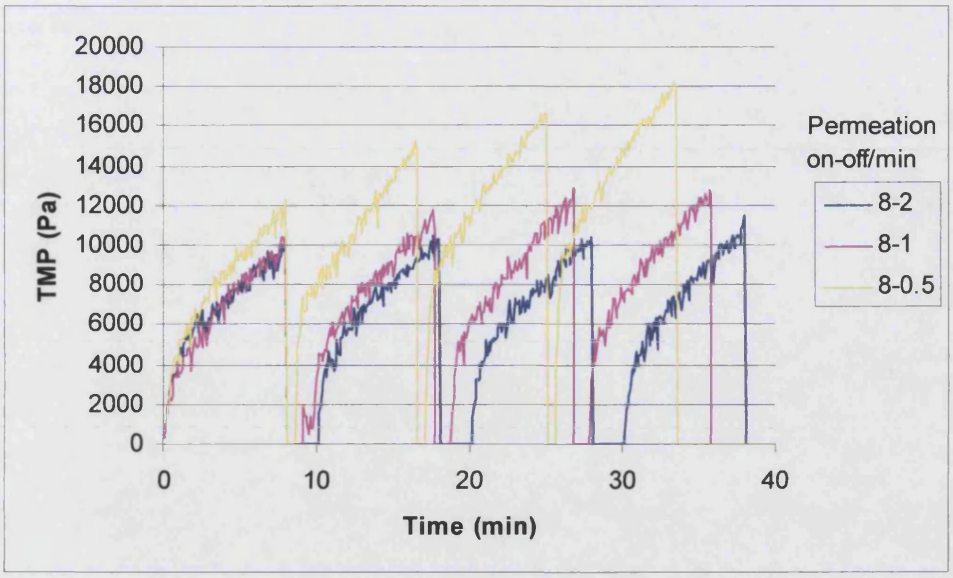

Figure 5-5 TMP at an intermittent permeation cycle of 8 min on followed by 0.5, 1 and 2 min off, permeate flux = 25 $l.m^{-2}.h^{-1}$, u_g = 229 $mm.s^{-1}$, MLVSS = 9.76 $g.l^{-1}$

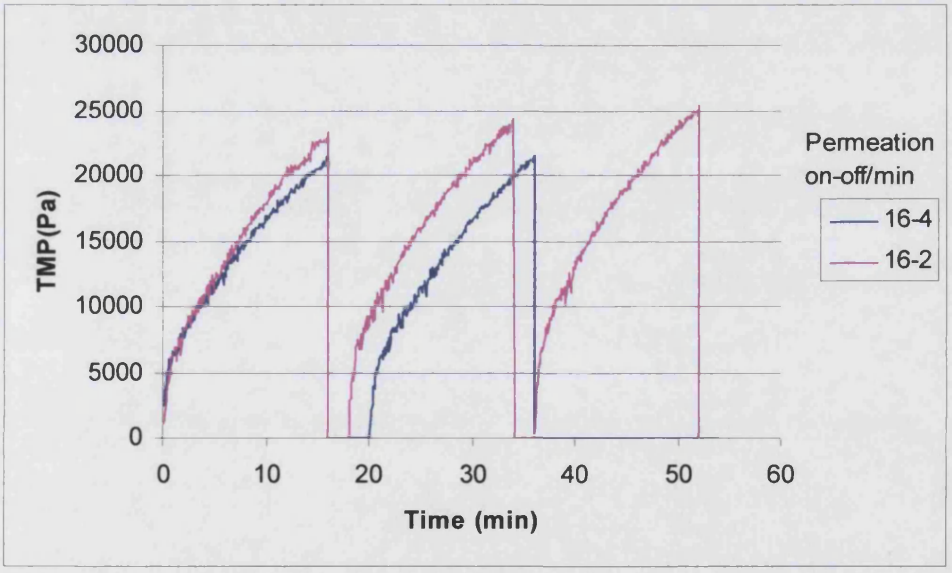

Figure 5-6 TMP at an intermittent permeation cycle of 16 min on followed by 2 and 4 min off, permeate flux = 25 $l.m^{-2}.h^{-1}$, u_g = 229 $mm.s^{-1}$, MLVSS = 9.76 $g.l^{-1}$

5.1.4 Effect of Intermittent Permeation on Membrane Fouling

The effect of intermittent permeation with different stoppage times after 8 minutes permeation is shown in Figure 5-7. 2 types of fouling shall be defined. Within each permeation period, the rate of cake built up, as observed by the TMP increase, is the cake fouling rate. The TMP increase from cycle to cycle after the suspension of permeation is the residual fouling rate. It could be observed that the suspension of permeation of 2 minutes was unable to cope with the operating hydrodynamic conditions. It could be observed that the residual fouling increased gradually at a rate of 12 $Pa.min^{-1}$, and the cake fouling rate was constant from cycle to cycle.

The stoppage time was increased to 4 minutes to investigate the reversibility of fouling. No residual fouling was observed from cycle to cycle, indicating the complete removal of fouling during the 4 minutes suspension of permeation.

When the stoppage time was decreased to 0.5 minute, the residual fouling increased at a higher rate of 95 $Pa.min^{-1}$. Interestingly, the cake fouling rate increased from cycle to cycle. An explanation for this observation is that as the cake built up rapidly on the membrane surface, fouling via pore blocking occurred. This resulted in an increase in the local permeation flux, causing the cake fouling rate to increase from cycle to cycle.

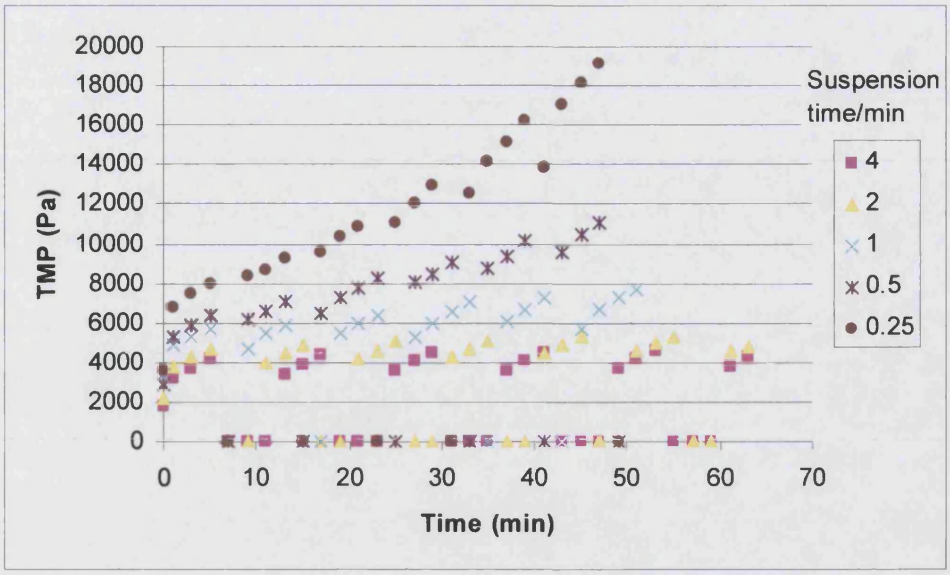

Figure 5-7 Intermittent permeation with various suspension time after 8 minutes permeation, permeate flux = 22 $l.m^{-2}.h^{-1}$, u_g = 37 $mm.s^{-1}$, MLVSS = 14.71 $g.l^{-1}$

Figure 5-8 showed the effect of the stoppage time on the fouling rate. The cake fouling rate increased from cycle to cycle when the suspension of permeation was decreased to 0.5 minute, and was more pronounced at 0.25 minute. Figure 5-9 showed a log plot of the residual fouling rate against linear suspension time. Using an exponential fit and extrapolating, a very low residual fouling of 1 $Pa.min^{-1}$ is expected when the stoppage time is increased to approximately 3.5 minutes. Intermittent permeation is an effective technique to control fouling. When the suspension of permeation is long enough, fouling can be removed completely. Conversely, when the suspension of permeation is too short, increased membrane fouling will occur.

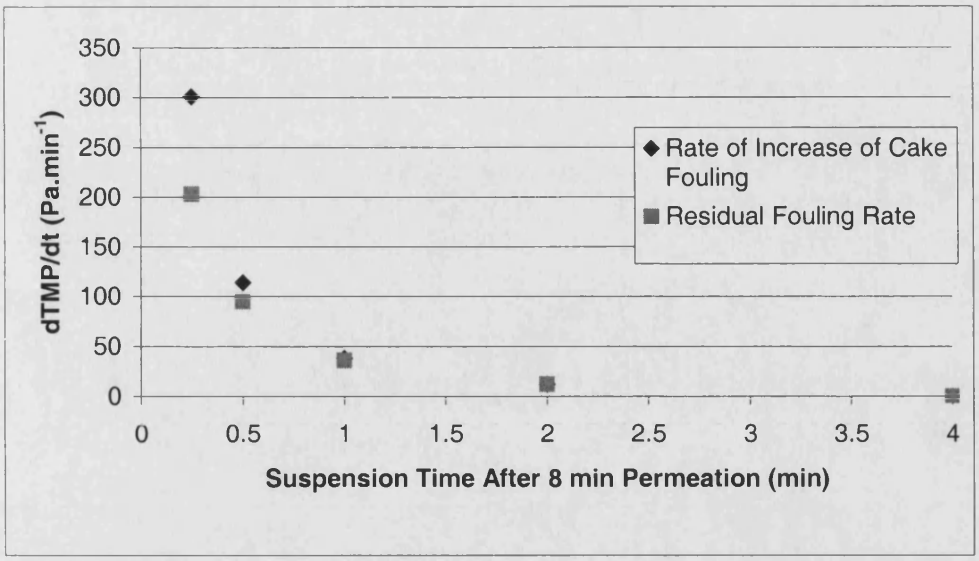

Figure 5-8 Fouling rate for various suspension time after 8 minutes permeation, permeate flux = 22 $l.m^{-2}.h^{-1}$, u_g = 37 $m.s^{-1}$, MLVSS = 14.71 $g.l^{-1}$

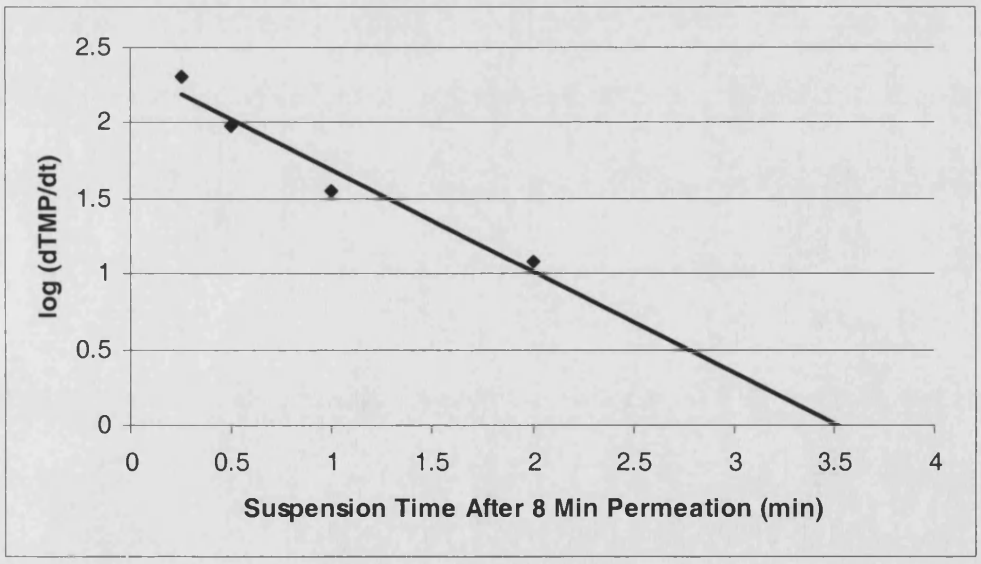

Figure 5-9 Log plot of residual fouling rate against linear suspension time

5.2 Critical Flux Concept in Microfiltration of Activated Sludge

5.2.1 Determination of Dynamic Critical Flux

This series of experiments aim to study the concept of critical flux in the microfiltration of activated sludge. The membrane was chemically cleaned before the start of this series of experiments. Figure 5-10 showed the TMP at increasing and then decreasing permeate fluxes. Each permeate flux was held for 8 minutes followed by 2 minutes suspension. It could be observed that the TMP stabilised quickly for permeate fluxes below 18 $l.m^{-2}.h^{-1}$. At the permeate flux of 20 $l.m^{-2}.h^{-1}$, the TMP increased initially before stabilising. When the permeate flux was further increased to 22 $l.m^{-2}.h^{-1}$, it could clearly be seen that the TMP did not stabilise and increase with time.

The pure water pressure (PWP) is the TMP measured for clean water permeation. Figure 5-11 showed the hysteresis plot for the data in Figure 5-10. The TMPs after 8 minutes permeation were plotted against the respective permeate fluxes. The weak form of critical flux was observed below 12 $l.m^{-2}.h^{-1}$, as the TMP was higher than the PWP, but increased linearly with the permeate flux. The TMP then increased gradually from 12 to 18 $l.m^{-2}.h^{-1}$, beyond which a sharp increase in TMP was observed for further increase of the permeate flux. The critical flux is 12 $l.m^{-2}.h^{-1}$ according to the classical definition of critical flux under continuous permeation. This is very

low and unrealistic in the actual operation of MBRs. The dynamic critical flux shall be defined here as the instantaneous flux at which the TMP stabilises quickly and does not increase with time, which is 18 $l.m^{-2}.h^{-1}$. The dynamic critical flux will be determined in the same manner throughout this work.

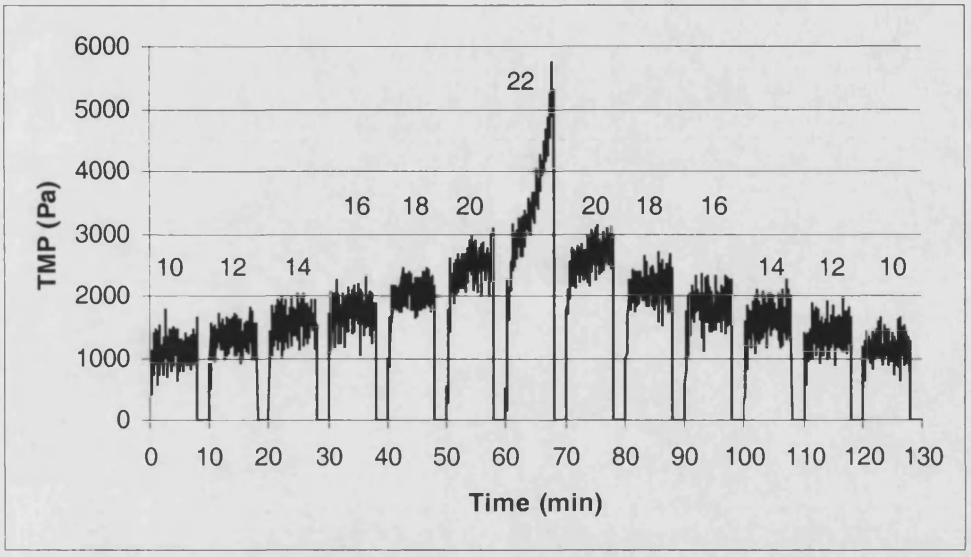

Figure 5-10 TMP at increasing and then decreasing permeate fluxes (numbers indicate fluxes in $l.m^{-2}.h^{-1}$), u_g = 83 $mm.s^{-1}$, MLVSS = 17.69 $g.l^{-1}$

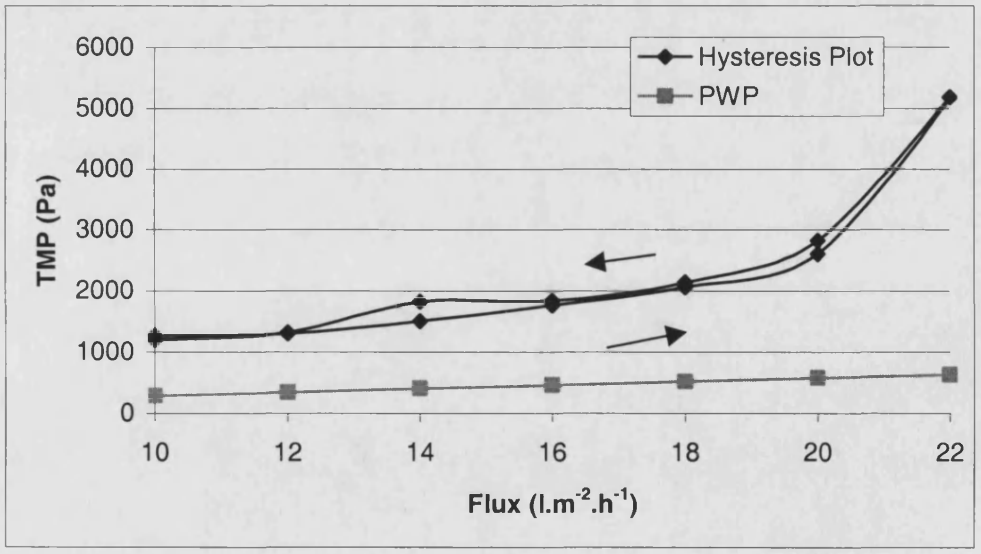

Figure 5-11 Hysteresis plot for a highest permeate flux of 22 $l.m^{-2}.h^{-1}$, u_g = 83 $mm.s^{-1}$, MLVSS = 17.69 $g.l^{-1}$

Figure 5-12 showed the fouling resistance R_f against the permeate flux. This is to differentiate the effect of increased TMP simply as a result of the higher flux through the same cake layer from the increased TMP as a result of an increased cake layer. This shows whether the cake layer is increasing. The fouling resistance did not increase below the dynamic critical flux of 18 $l.m^{-2}.h^{-1}$. Above it, the fouling resistance increased, and was clearly higher at the permeate flux of 22 $l.m^{-2}.h^{-1}$. This suggests an increasing cake layer.

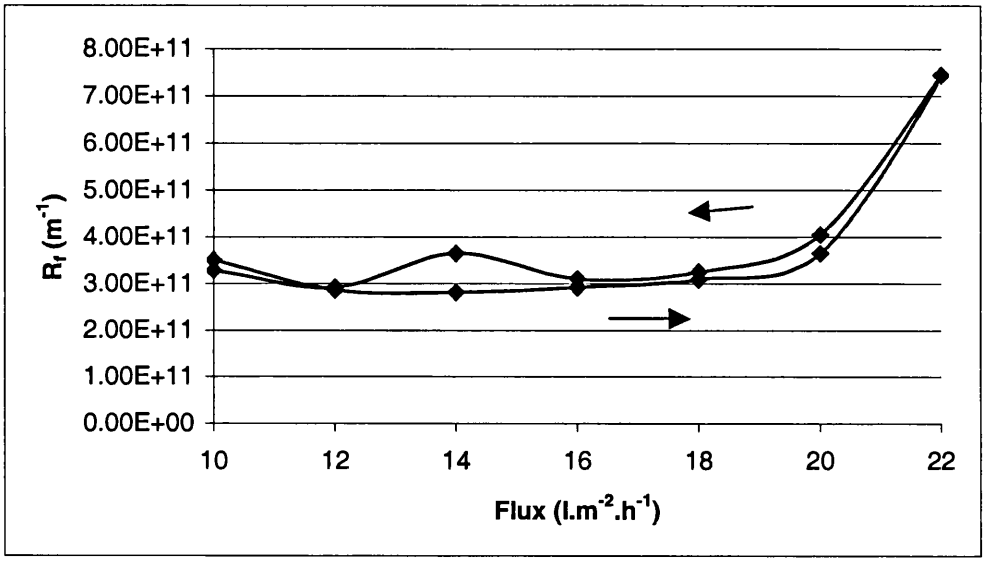

Figure 5-12 Fouling resistance against permeate flux, u_g = 83 $mm.s^{-1}$, MLVSS = 17.69 $g.l^{-1}$

5.2.2 Effect of Stepsize on Dynamic Critical Flux

The effect of stepsize on the dynamic critical flux was studied. The permeate flux was increased from 10 to 24 $l.m^{-2}.h^{-1}$ and then decreased back to 10

$l.m^{-2}.h^{-1}$ with 4 different stepsizes of 14, 7, 3.5 and 2 $l.m^{-2}.h^{-1}$. The hysteresis plots are shown in Figure 5-13.

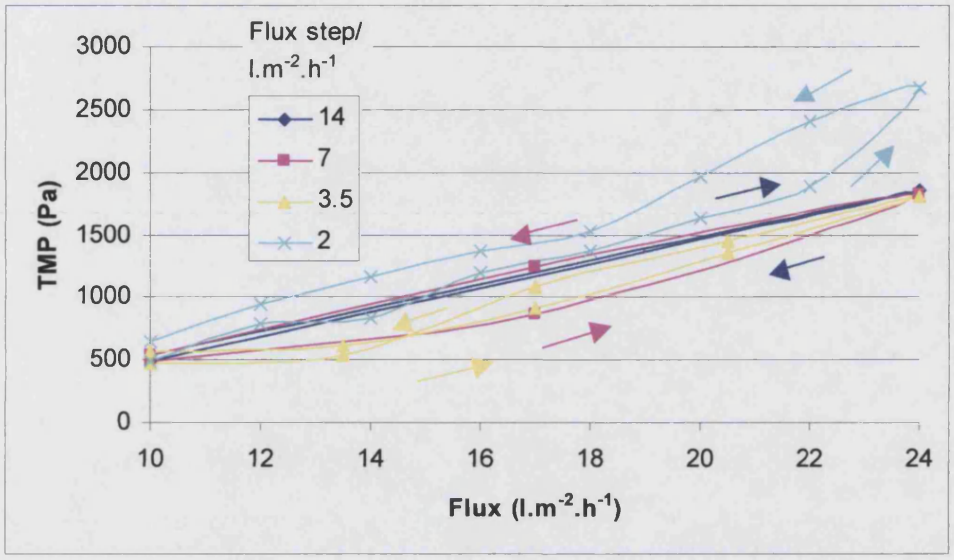

Figure 5-13 Hysteresis plots for 4 different stepsizes of 14, 7, 3.5 and 2 $l.m^{-2}.h^{-1}$, u_g = 83 $mm.s^{-1}$, MLVSS = 16.35 $g.l^{-1}$

In Figure 5-13, it could be observed that the dynamic critical flux was exceeded as the permeate flux was increased to 24 $l.m^{-2}.h^{-1}$, as the TMP did not increase linearly with the permeate flux. The TMPs at the permeate flux of 24 $l.m^{-2}.h^{-1}$ for the 3 different stepsizes of 14, 7 and 3.5 $l.m^{-2}.h^{-1}$ were similar. Decreasing the permeate flux back to 10 $l.m^{-2}.h^{-1}$ showed little increase in the TMP compared to the starting TMP, suggesting little residual fouling. However, when the stepsize was decreased to 2 $l.m^{-2}.h^{-1}$, the slope for the increase in TMP with permeate flux was higher. This suggested that some residual fouling occurred at the larger stepsizes, but was not shown in the TMP. This point will be discussed further for Figure 5-23.

Figure 5-14 showed the fouling resistance against the permeate flux. The fouling resistance increased with increasing permeate flux, showing an increased cake layer. The cake layer was removed when the permeate flux was decreased, as the fouling resistance returned to the original value when the permeate flux was decreased to 10 $l.m^{-2}.h^{-1}$, except for the stepsize of 2 $l.m^{-2}.h^{-1}$ where the final fouling resistance was observed to be higher.

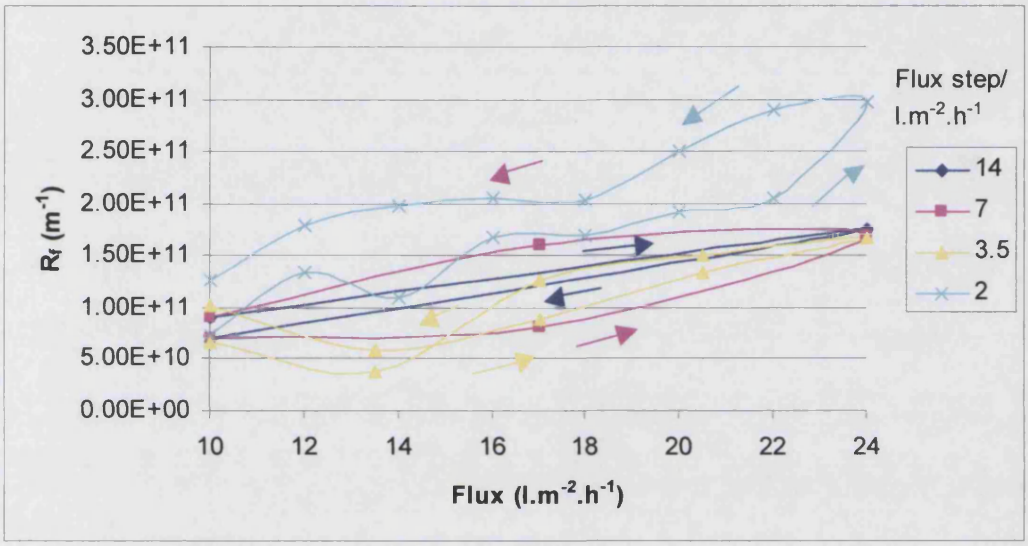

Figure 5-14 Fouling resistance against permeate flux, u_g = 83 $mm.s^{-1}$, MLVSS = 16.35 $g.l^{-1}$

5.2.3 Reversibility of Fouling

The reversibility of fouling was investigated using the protocol for the determination of dynamic critical flux described for Figure 5-10. The permeate flux was increased from 10 to 18 $l.m^{-2}.h^{-1}$ and then decreased back to

10 $l.m^{-2}.h^{-1}$. This cycle was then repeated (2^{nd} cycle) to check for any residual fouling during the 1^{st} cycle. This is shown in Figure 5-15.

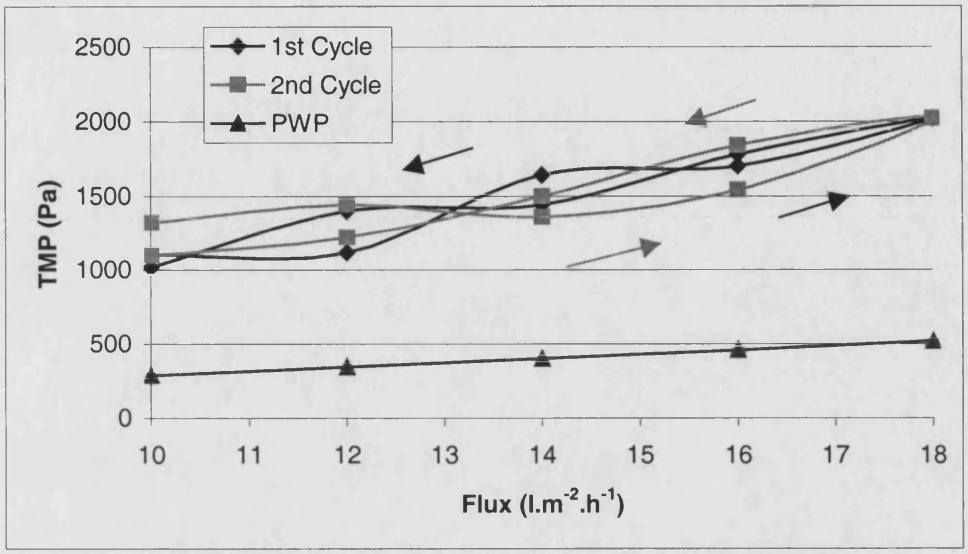

Figure 5-15 Hysteresis plots for a highest permeate flux of 18 $l.m^{-2}.h^{-1}$, u_g = 83 $mm.s^{-1}$, MLVSS = 17.69 $g.l^{-1}$

In Figure 5-15, the TMP was observed to increase linearly with the permeate flux. The variation of the TMP was due to the difficulty in measuring the very low TMPs. The TMP was similar for both increasing and decreasing permeate fluxes. The TMP observed for the 2^{nd} cycle was also similar to the 1^{st} cycle, suggesting no residual fouling. This is expected if the permeate flux is below the dynamic critical flux. Figure 5-16 showed the fouling resistance against the permeate flux. The fouling resistance did not increase at higher permeate fluxes, showing no cake layer increase.

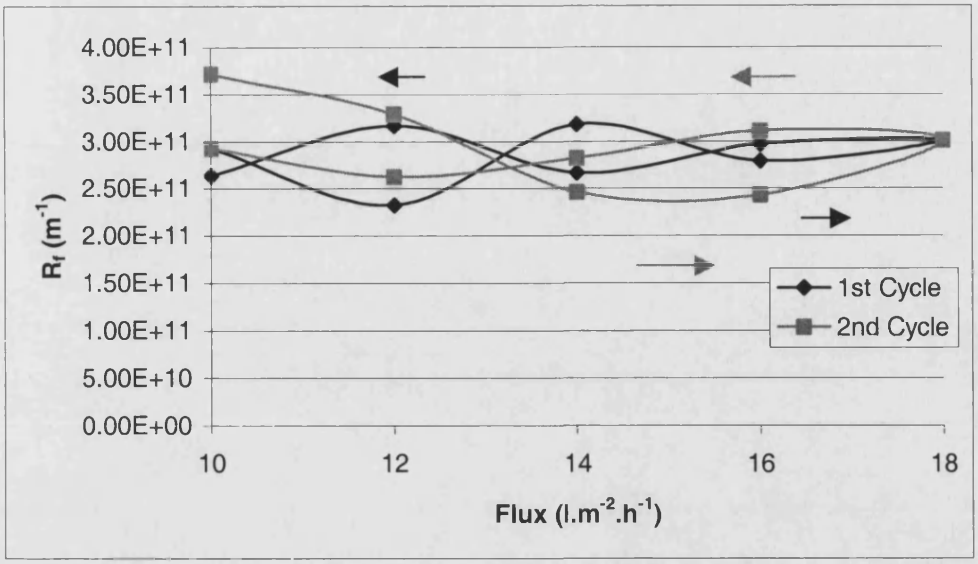

Figure 5-16 Fouling resistance against permeate flux, u_g = 83 mm.s^{-1}, MLVSS = 17.69 g.l^{-1}

The permeate flux was then increased further to 20 l.m^{-2}.h^{-1} and this is shown in Figure 5-17. The observations were similar to that in Figure 5-15. No hysteresis was observed. The fouling resistance against permeate flux plot in Figure 5-18 showed no cake layer increase.

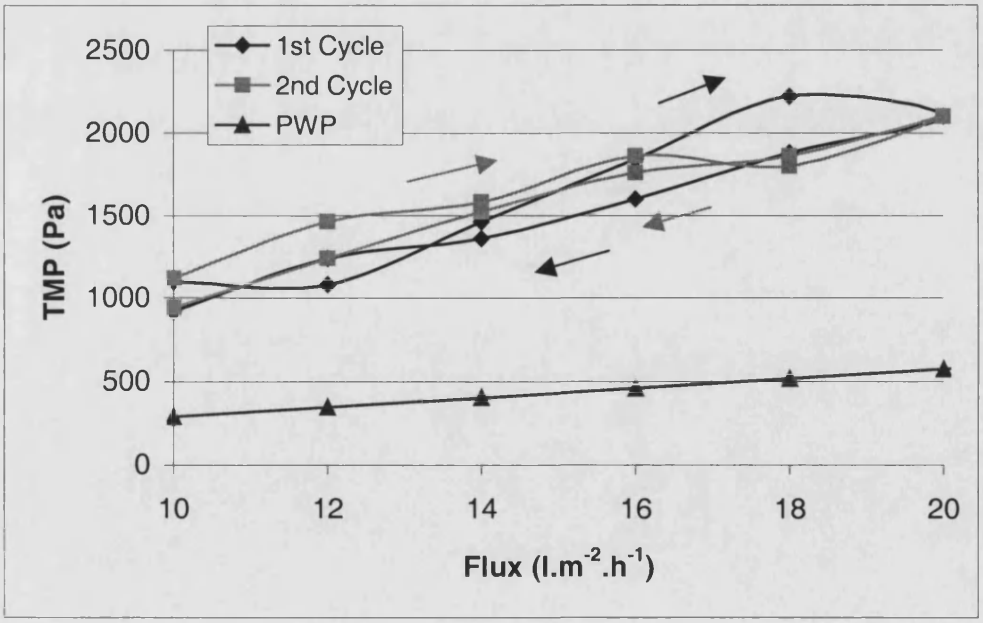

Figure 5-17 Hysteresis plots for a highest permeate flux of 20 l.m^{-2}.h^{-1}, u_g = 83 mm.s^{-1}, MLVSS = 17.69 g.l^{-1}

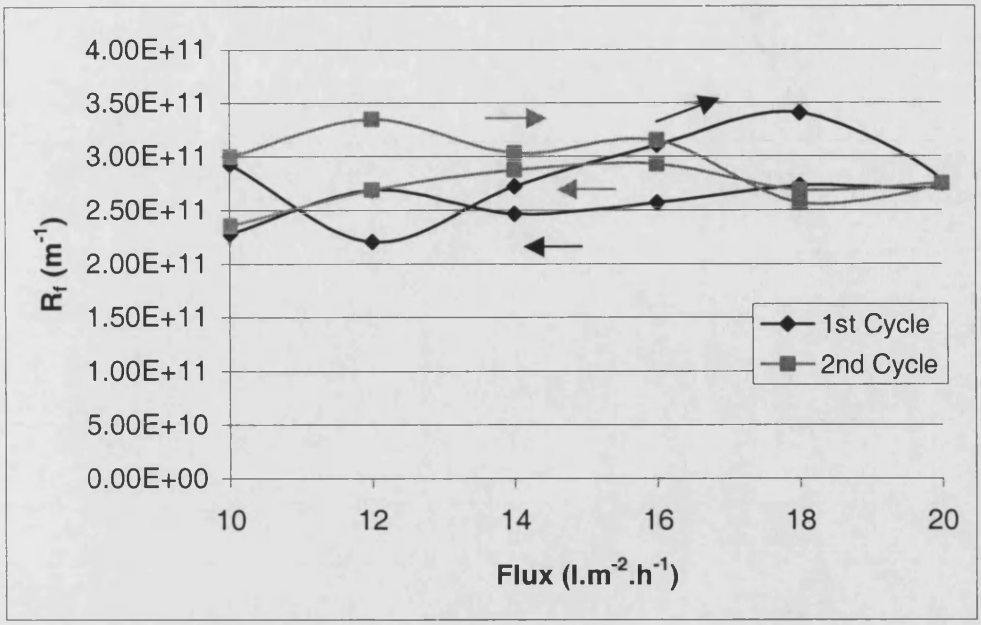

Figure 5-18 Fouling resistance against permeate flux, u_g = 83 mm.s^{-1}, MLVSS = 17.69 g.l^{-1}

Figure 5-19 showed a further increase in the permeate flux to 22 l.m^{-2}.h^{-1}. The dynamic critical flux has now been exceeded, as the linearity between the TMP and the permeate flux was clearly not observed when the permeate flux was increased to 22 l.m^{-2}.h^{-1}. The 2nd cycle showed a lower TMP at the permeate flux of 22 l.m^{-2}.h^{-1} compared to the 1st cycle, hence a 3rd cycle was repeated. The TMPs at the permeate flux of 22 l.m^{-2}.h^{-1} were similar for the 2nd and 3rd cycle. Although the dynamic critical flux was exceeded, decreasing the permeate flux showed similar TMPs as that observed when the permeate flux was increased, suggesting no residual fouling. Figure 5-20 showed that the fouling resistance was clearly higher at the permeate flux of 22 l.m^{-2}.h^{-1}, suggesting an increasing cake layer. The cake layer was removed

when the permeate flux was decreased, as the fouling resistance returned to the original value.

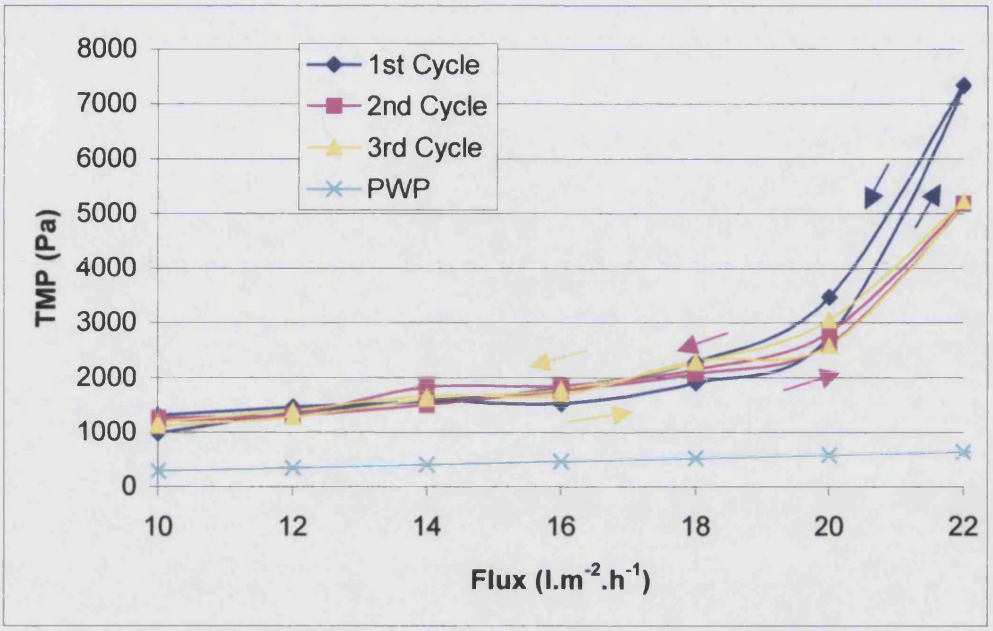

Figure 5-19 Hysteresis plots for a highest permeate flux of 22 $l.m^{-2}.h^{-1}$, $u_g = 83\ mm.s^{-1}$, MLVSS = 17.69 $g.l^{-1}$

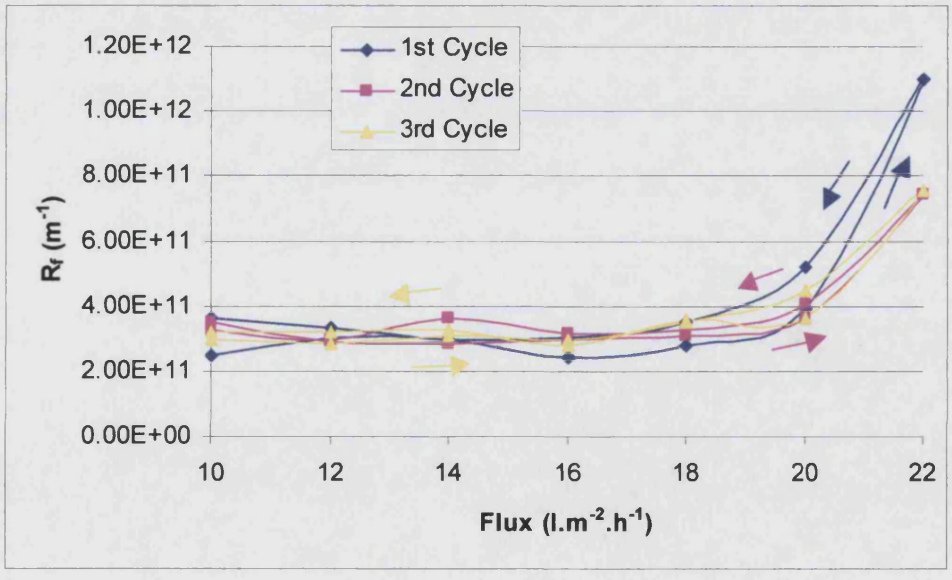

Figure 5-20 Fouling resistance against permeate flux, $u_g = 83\ mm.s^{-1}$, MLVSS = 17.69 $g.l^{-1}$

In Figure 5-21, the permeate flux was increased to 24 $l.m^{-2}.h^{-1}$. A sharp and rapid increase in the TMP was observed when the permeate flux was increased above 20 $l.m^{-2}.h^{-1}$. When the permeate flux was decreased, the TMP below the permeate flux of 18 $l.m^{-2}.h^{-1}$ was similar to that when the permeate flux was increased. This suggested that cake fouling was removed when the permeate flux was decreased below the dynamic critical flux. Figure 5-22 showed that the fouling resistance increased sharply above a permeate flux of 20 $l.m^{-2}.h^{-1}$. The fouling resistance returned to the original value when the permeate flux was decreased back to 18 $l.m^{-2}.h^{-1}$, suggesting the removal of the cake layer.

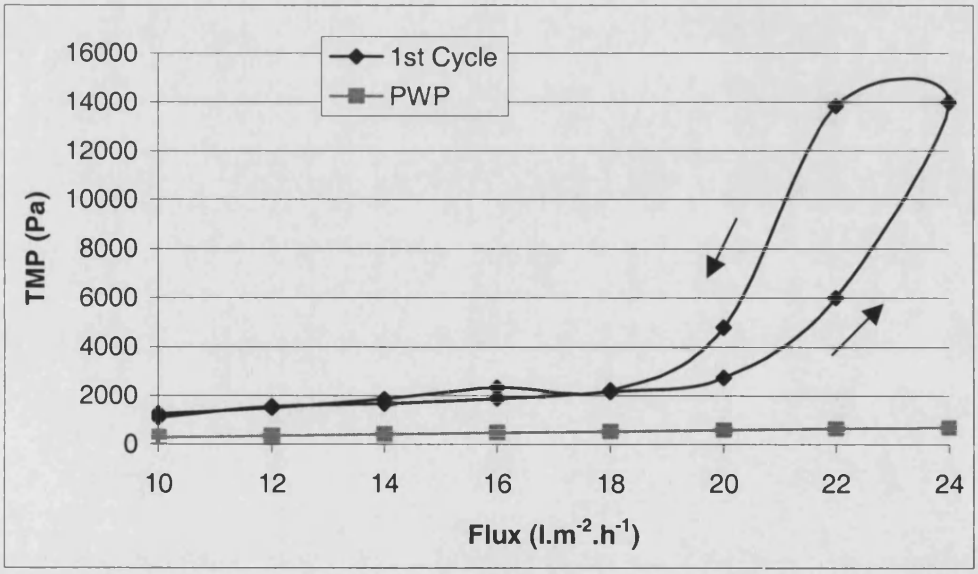

Figure 5-21 Hysteresis plots for a highest permeate flux of 24 $l.m^{-2}.h^{-1}$, u_g = 83 $mm.s^{-1}$, MLVSS = 17.69 $g.l^{-1}$

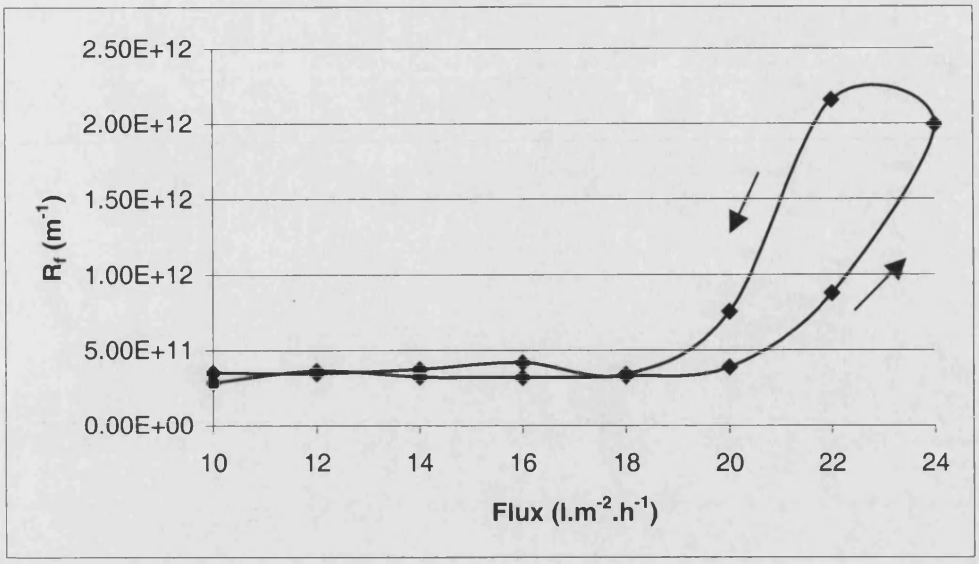

Figure 5-22 Fouling resistance against permeate flux, u_g = 83 mm.s^{-1}, MLVSS = 17.69 g.l^{-1}

The cycle was repeated (2nd and 3rd cycle) and shown in Figure 5-23. It was observed that the 2nd cycle had a higher TMP than that of the 1st cycle when the permeate flux was increased above 18 $l.m^{-2}.h^{-1}$. In fact, the TMP was similar to that of the 1st cycle when the permeate flux was decreased. This suggested that residual fouling occurred during the 1st cycle, but could not be detected at low permeate fluxes. The TMP was limited to a maximum value of 15000 Pa to prevent excessive fouling. This resulted in no further hysteresis as observed in the 3rd cycle. In Figure 5-24, the fouling resistance returned to approximately the original value at low permeate fluxes. At high permeate fluxes, the fouling resistance was higher for the 2nd cycle than the 1st cycle. This suggested residual fouling that was not shown in the TMP at low permeate fluxes. The residual fouling resulted in a sharp increase in the fouling resistance at a lower permeate flux (22 $l.m^{-2}.h^{-1}$ and 20 $l.m^{-2}.h^{-1}$ for the

1st and 2nd cycle respectively). The dynamic critical flux decreased as the membrane fouled. Cho and Fane [116] also reported that critical flux decreased as the TMP increased gradually in an anaerobic MBR.

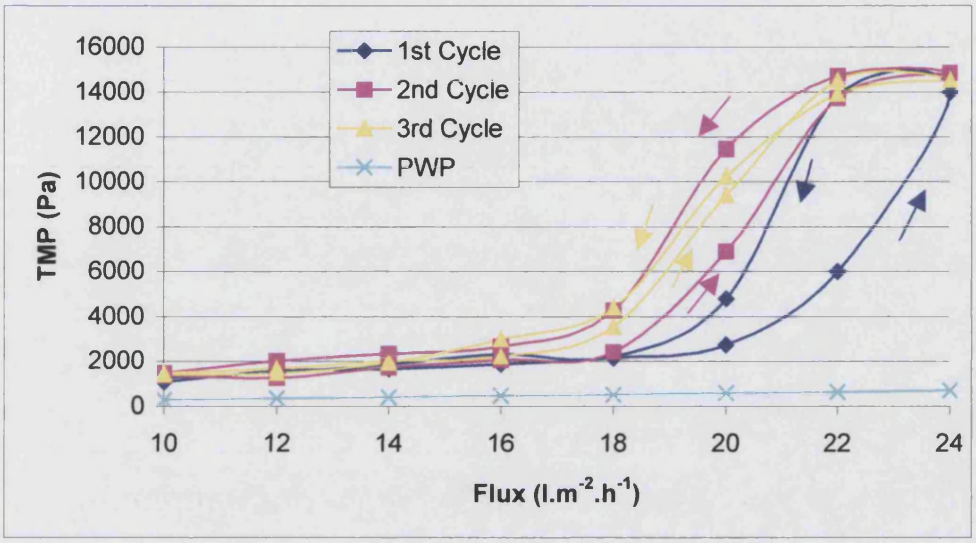

Figure 5-23 Hysteresis plots for a highest permeate flux of 24 $l.m^{-2}.h^{-1}$, $u_g = 83\ mm.s^{-1}$, MLVSS = 17.69 $g.l^{-1}$

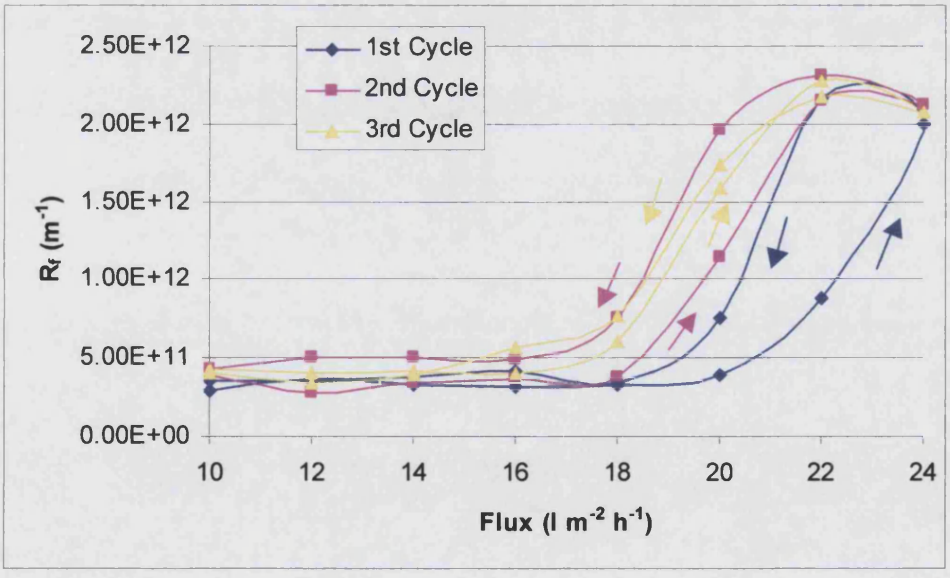

Figure 5-24 Fouling resistance against permeate flux, $u_g = 83\ mm.s^{-1}$, MLVSS = 17.69 $g.l^{-1}$

5.3 Data Analysis

The very low TMP measurements (< 2500 Pa) at low fluxes were difficult to reproduce exactly as seen in Figure 5-14 and Figure 5-16. Using a one-sided t test, the TMP at 12 $l.m^{-2}.h^{-1}$ was significantly higher than the TMP at 10 $l.m^{-2}.h^{-1}$ at a 90 % confidence level. The TMP increase for the subsequent flux increment from 12-14, 14-16 and 16-18 $l.m^{-2}.h^{-1}$ were significant at confidence levels of 75 %, 99 % and 95 % respectively. The difference between 2 means, corresponding standard deviation and significance level for the various flux increment are shown in Table 5-1. At high permeate fluxes, fouling occurred and the different TMP measured for the various cycles in Figure 5-22 is due to residual membrane fouling.

Table 5-1 Statistical analysis of the TMP measurements for the various flux increment

Flux Increment ($l.m^{-2}.h^{-1}$)	Difference Between Means (Pa)	Standard Deviation of Difference Between Means	Significance Level Using One-Sided t-test
10-12	205	110	90
12-14	115	100	75
14-16	295	87	99
16-18	260	113	95

5.4 Summary

Intermittent permeation and dynamic critical flux were studied. It was observed that fouling was reversible and could be removed by the suspension of permeation while maintaining the aeration for a submerged MBR. For a short period of continuous permeation up to 16 minutes, the duration of permeation was not important as long as the permeation on-off ratio was approximately 4:1. Membrane fouling increased exponentially if the suspension of permeation was not long enough.

Fouling was observed to be reversible near the dynamic critical flux. Above the dynamic critical flux, residual fouling occurred, but was not manifested in the TMP at low permeate fluxes. The residual fouling resulted in a lower dynamic critical flux.

6 Results – Membrane Fouling

6.1 Effects of Biomass Concentration and F/M Ratio on Membrane Fouling

The effect of biomass concentration and F/M ratio on membrane fouling was studied. During the experiments the MLVSS concentration was allowed to increase naturally. The F/M ratio therefore changed simultaneously as the hydraulic residence time and feed concentrations remained constant. Any effects noted could have been a result of either the F/M ratio change or the increased MLVSS concentration or a combination. The results do not differentiate these effects.

This series of experiment started with the highest MLVSS of 21.46 $g.l^{-1}$ (F/M ratio of 0.05 $gBOD.gMLVSS^{-1}.d^{-1}$). The MLVSS was subsequently diluted with permeate for the lower MLVSS concentrations. Each experimental run was repeated to ensure data reproducibility. The membrane was chemically cleaned for each MLVSS concentration. Flux was increased and then decreased in a step size of 2 $l.m^{-2}.h^{-1}$ to study the hysteresis. The flux was increased until the TMP reached close to 10000 Pa before decreasing. The TMP was never allowed to exceed 10000 Pa to prevent excessive membrane fouling. The hysteresis for the different biomass concentrations can then be compared. The hysteresis plots for 2 superficial gas velocities of 83 and 208 $mm.s^{-1}$ are shown in Figure 6-1 and Figure 6-3 respectively. The respective

plots of fouling resistance against permeate flux are shown in Figure 6-2 and Figure 6-4.

It could be seen in Figure 6-1 that the biomass concentration of 12.46 $g.l^{-1}$ (F/M ratio of 0.08 $gBOD.gMLVSS^{-1}.d^{-1}$) was the least fouling. The most fouling biomass concentration was the lowest concentration of 5.38 $g.l^{-1}$ (F/M ratio of 0.19 $gBOD.gMLVSS^{-1}.d^{-1}$). Figure 6-2 showed the highest fouling resistance for the lowest MLVSS of 5.38 $g.l^{-1}$ (F/M ratio of 0.19 $gBOD.gMLVSS^{-1}.d^{-1}$) when the permeate flux was decreased back to 10 $l.m^{-2}.h^{-1}$, suggesting high residual fouling.

For the higher u_g of 208 $mm.s^{-1}$, as shown in Figure 6-3, it could be observed that membrane fouling was less pronounced for all the 4 biomass concentrations that were tested, as compared to the lower u_g of 83 $mm.s^{-1}$ in Figure 6-1. The biomass concentrations of 12.46 and 5.38 $g.l^{-1}$ (F/M ratios of 0.08 and 0.19 $gBOD.gMLVSS^{-1}.d^{-1}$ respectively) were again the lowest and highest fouling respectively. The high hysteresis for the biomass concentration of 5.38 $g.l^{-1}$ (F/M ratio of 0.19 $gBOD.gMLVSS^{-1}.d^{-1}$) suggested high residual fouling. It was observed that the highest biomass concentration of 21.46 $g.l^{-1}$ (F/M ratio of 0.05 $gBOD.gMLVSS^{-1}.d^{-1}$) was less fouling than the 9.14 $g.l^{-1}$ (F/M ratio of 0.11 $gBOD.gMLVSS^{-1}.d^{-1}$), which was not the case for the lower u_g. This could be due to the high u_g limiting the cake layer formation, which then resulted in a higher fouling by small particles for the biomass concentration of 9.14 $g.l^{-1}$ (F/M ratio of 0.11 $gBOD.gMLVSS^{-1}.d^{-1}$). A sufficient cake layer was formed to limit fouling by small particles for the

lower u_g. The fouling resistance for the lowest MLVSS of 5.38 $g.l^{-1}$ (F/M ratio of 0.19 $gBOD.gMLVSS^{-1}.d^{-1}$) when the permeate flux was decreased back to 10 $l.m^{-2}.h^{-1}$ for the lower u_g of 83 $mm.s^{-1}$ was 7.88 x 10^{11} m^{-1} in Figure 6-2. Figure 6-4 showed a higher fouling resistance of 1.15 x 10^{12} m^{-1} for the higher u_g of 208 $mm.s^{-1}$, suggesting higher residual fouling at a higher u_g.

It can be concluded that membrane fouling in multi-component systems such as activated sludge involves several factors and a single factor such as MLVSS cannot explain the fouling phenomenon. The results suggest the importance of the interactions between the different species and the hydrodynamic conditions.

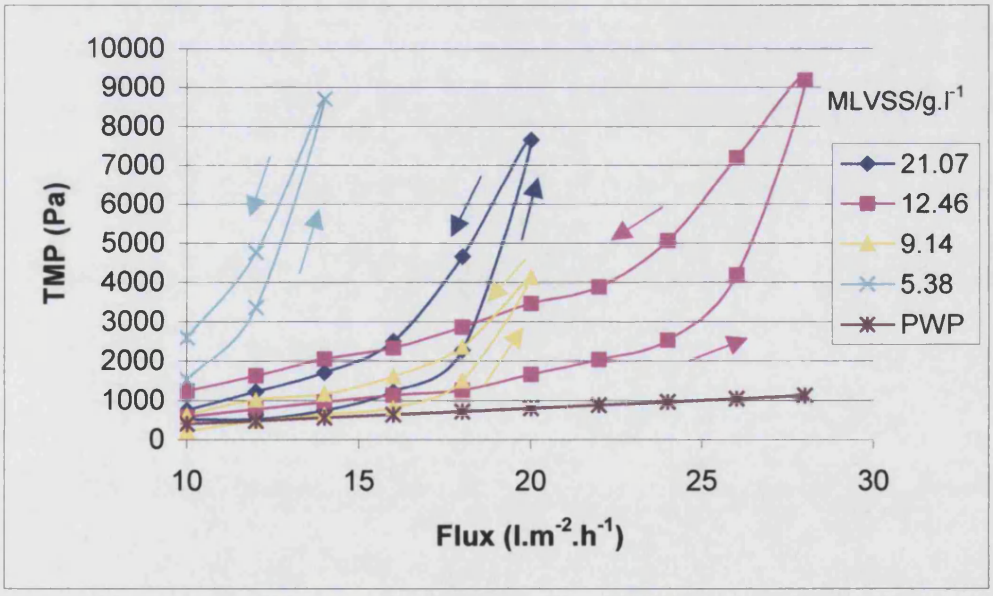

Figure 6-1 Hysteresis plots for various biomass concentrations ($g.l^{-1}$), $u_g = 83\ mm.s^{-1}$

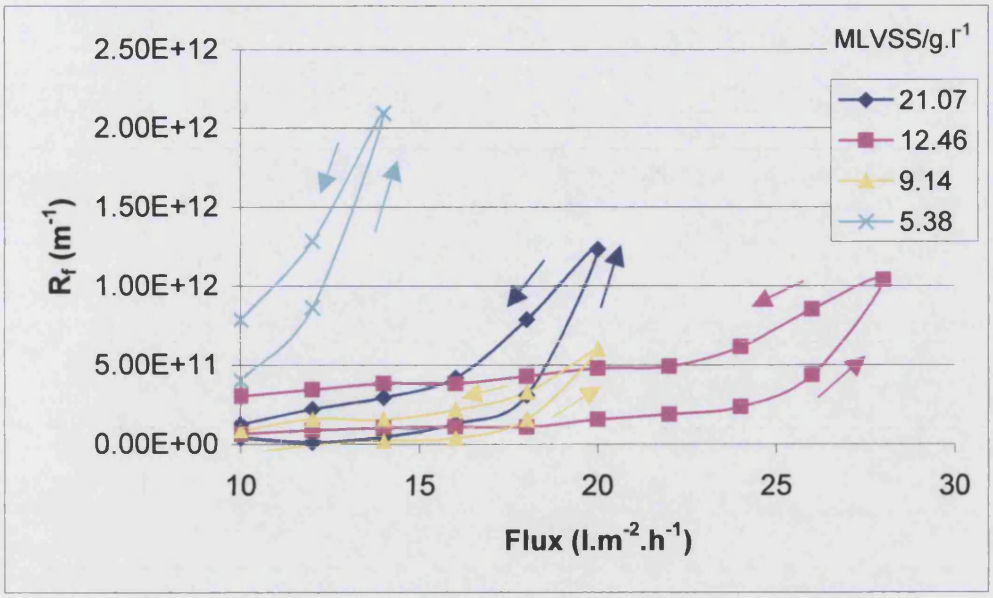

Figure 6-2 Fouling resistance against permeate flux for various biomass concentrations (g.l^{-1}), u_g = 83 mm.s^{-1}

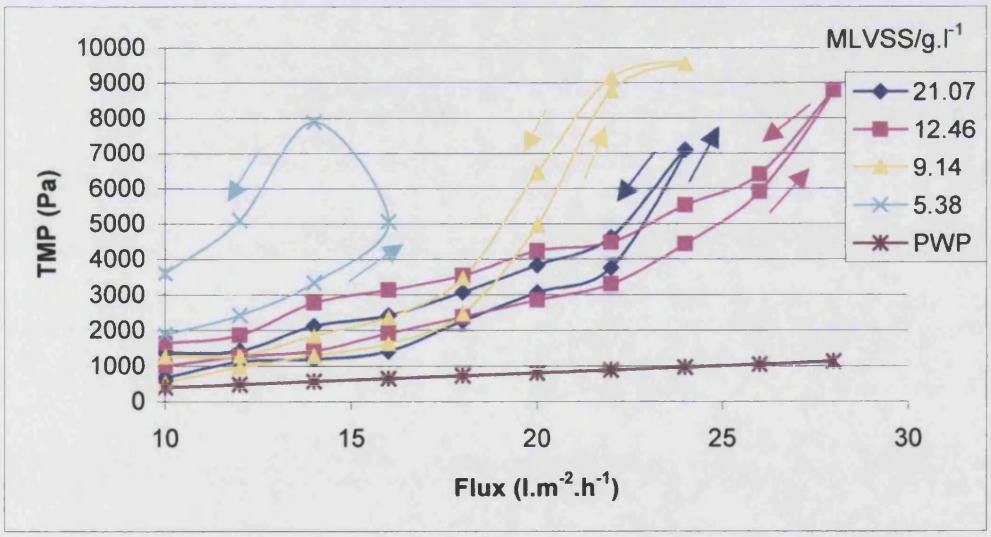

Figure 6-3 Hysteresis plots for various biomass concentrations (g.l^{-1}), u_g = 208 mm.s^{-1}

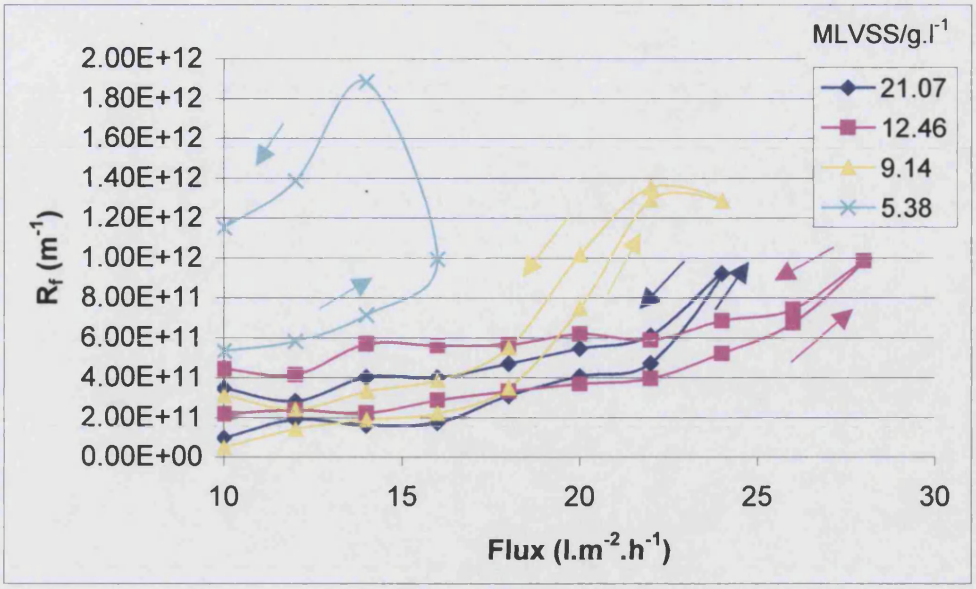

Figure 6-4 Fouling resistance against permeate flux for various biomass concentrations ($g.l^{-1}$), u_g = 208 $mm.s^{-1}$

Figure 6-5 showed how the dynamic critical flux changed as the biomass concentration built up in the MBR. The dynamic critical flux determination was done in duplicate. It could be observed that the dynamic critical flux increased with biomass concentration up to 14.53 $g.l^{-1}$ (F/M ratio of 0.07 $gBOD.gMLVSS^{-1}.d^{-1}$). Further increase in biomass concentration led to a lower dynamic critical flux. Ishida et al. [18] reported an operational range of 12 to 18 $g.l^{-1}$ MLSS and a BOD-MLSS loading of 0.025-0.042 $gBOD.gMLSS^{-1}.d^{-1}$ for the Kubota system. Figure 6-6 plots the dynamic critical flux against F/M ratio. The highest dynamic critical flux occurred at a F/M ratio of 0.07 $gBOD.gMLVSS^{-1}.d^{-1}$.

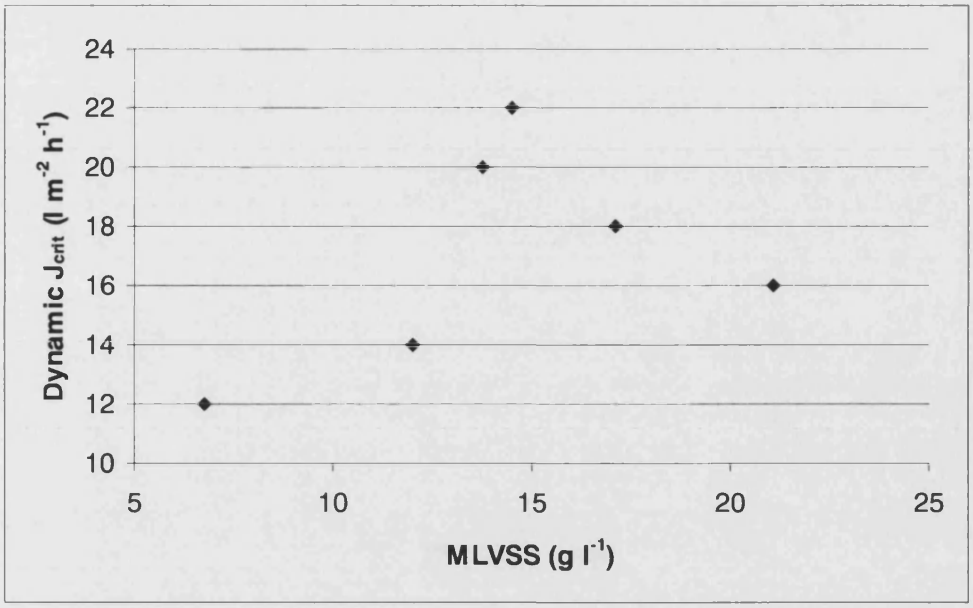

Figure 6-5 Dynamic critical fluxes for various biomass concentrations ($g.l^{-1}$), u_g = 83 $mm.s^{-1}$

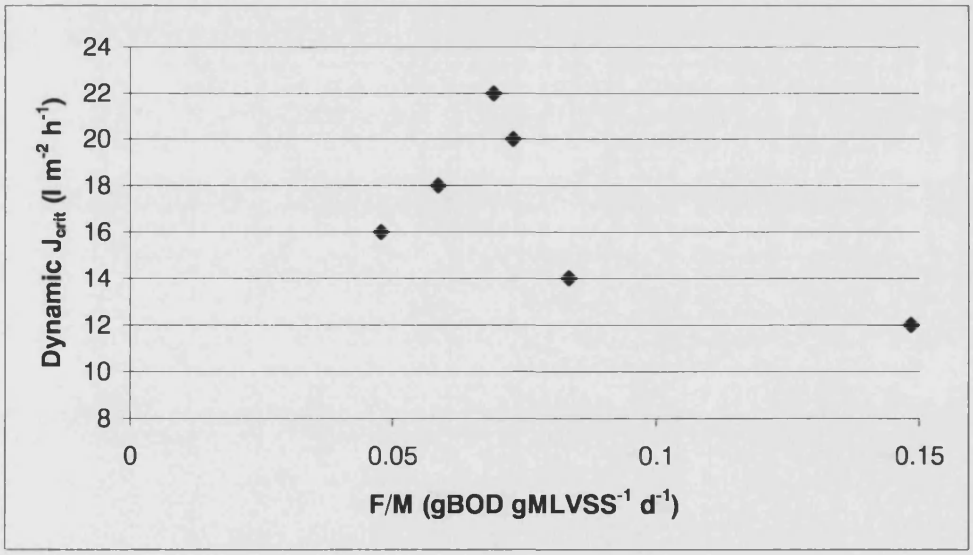

Figure 6-6 Dynamic critical fluxes for various F/M ratios ($gBOD.gMLVSS^{-1}.d^{-1}$), u_g = 83 $mm.s^{-1}$

The results show an optimum MLVSS or F/M ratio that gives the highest permeate flux under a fixed hydrodynamic condition. The highest dynamic critical flux for the system is 22 $l.m^{-2}.h^{-1}$ at a u_g of 83 $mm.s^{-1}$. This occurred at a MLVSS of 14.53 $g.l^{-1}$ or F/M ratio of 0.07 $gBOD.gMLVSS^{-1}.d^{-1}$. Although the experiments were not done under steady-state conditions, both sets of results suggest an optimum MLVSS or F/M ratio of approximately 12-15 $g.l^{-1}$ or 0.05-0.07 $gBOD.gMLVSS^{-1}.d^{-1}$ respectively that gives the highest permeate flux. Comparing with results in the literature, Le Clech et al. [121] reported similar critical flux from 4-8 $g.l^{-1}$ MLSS and a significant increase of critical flux for further MLSS increase to 12 $g.l^{-1}$. Brookes et al. [38] reported a critical MLSS of 10-15 $g.l^{-1}$ beyond which dewaterability was much reduced for 5 pilot plants and 4 full scale plants. It is likely that such an optimum does exist in MBRs, the initial flux increase with increasing MLSS being due to lower EPS and SMP concentrations. The lower flux at very high MLSS concentration is due to viscosity as suggested by Churchouse [11].

6.2 Effect of Aeration Rate on Membrane Fouling

The effect of aeration rate on membrane fouling was investigated in this series of experiments. Figure 6-7, Figure 6-8 and Figure 6-9 showed the results using intermittent permeation of 8 minutes on and 2 minutes off at different fluxes. At a low flux of 10 $l.m^{-2}.h^{-1}$, little fouling was observed as seen in Figure 6-7. In Figure 6-8, when flux was maintained at 20 $l.m^{-2}.h^{-1}$, there was little increase in fouling, except at the lowest u_g of 17 $mm.s^{-1}$. At a high flux

of 30 $l.m^{-2}.h^{-1}$, there was more severe fouling and the TMP was much higher as seen in Figure 6-9. However, the break in permeation resulted in little increase in fouling, except at the lowest u_g of 33 $mm.s^{-1}$, where the TMP increased from cycle to cycle. Permeation at that flux and u_g was unsustainable. Hence, a higher aeration results in a lower stable TMP and can be used to limit residual cake deposition under intermittent permeation conditions.

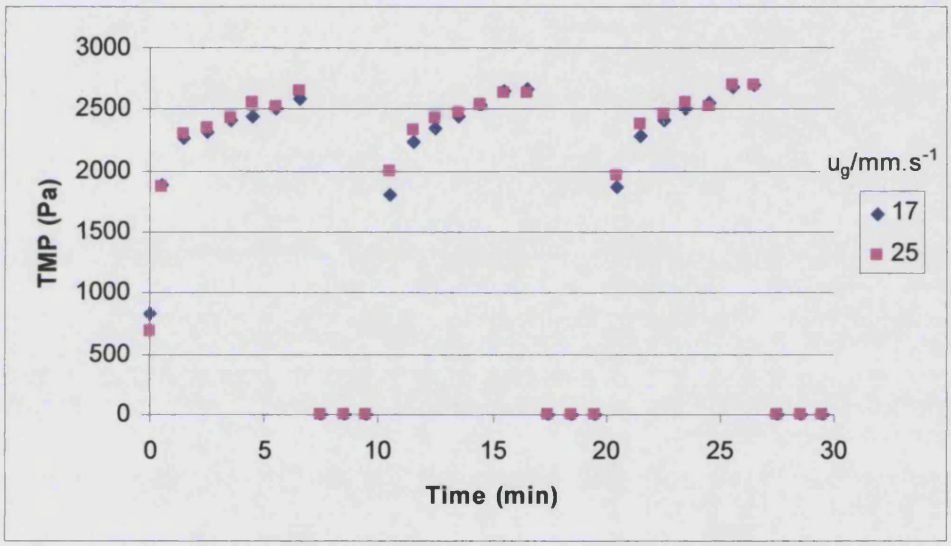

Figure 6-7 TMP at flux of 10 $l.m^{-2}.h^{-1}$ for various u_g ($mm.s^{-1}$), with permeation on for 8 min and off for 2 min, MLVSS = 3.7 $g.l^{-1}$

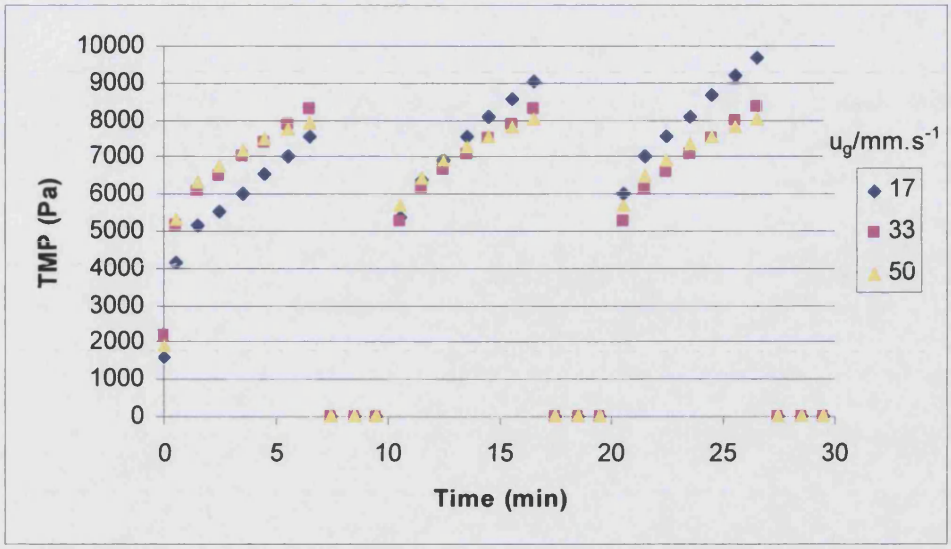

Figure 6-8 TMP at flux of 20 l.m^{-2}.h^{-1} for various u_g (mm.s^{-1}), with permeation on for 8 min and off for 2 min, MLVSS = 3.7 g.l^{-1}

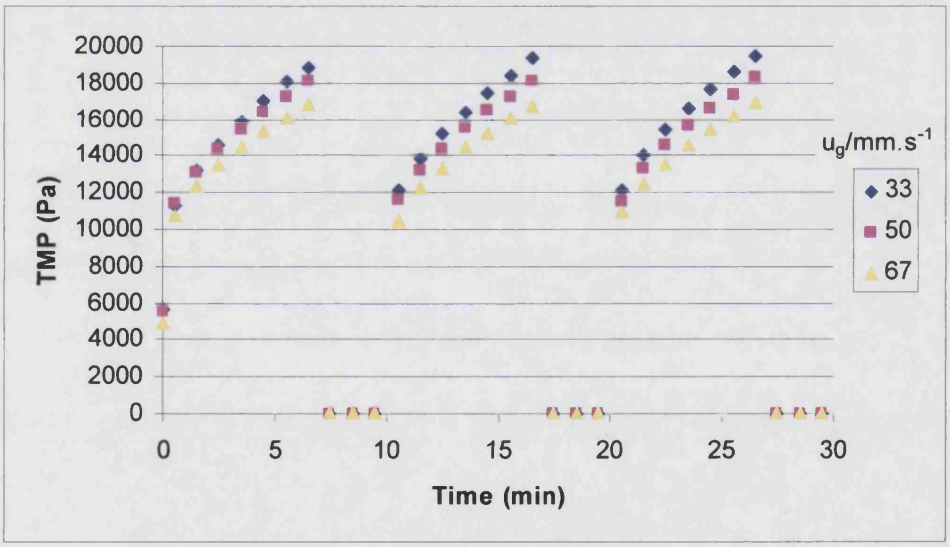

Figure 6-9 TMP at flux of 30 l.m^{-2}.h^{-1} for various u_g (mm.s^{-1}), with permeation on for 8 min and off for 2 min, MLVSS = 3.7 g.l^{-1}

6.2.1 Effects of Aeration Rate and Decreasing Flux on Residual Fouling

Figure 6-10 and Figure 6-11 showed the hysteresis plots at different u_g. The TMP was obtained after 10 minutes of continuous permeation before increasing or decreasing the permeate flux. At the lower u_g of 17 and 33 $mm.s^{-1}$ as shown in Figure 6-10, increasing the flux initially increased the TMP linearly. The critical flux was found to be approximately 8 $l.m^{-2}.h^{-1}$. When the critical flux was exceeded, the slope increased progressively due to increasing fouling. The TMP did not return to the original value when the flux was decreased, implying hysteresis and irreversible fouling. No hysteresis was observed in Figure 6-11 at the higher u_g of 50 and 67 $mm.s^{-1}$, as the TMP returned to the original value. Hysteresis is reduced and fouling is reversible at high u_g.

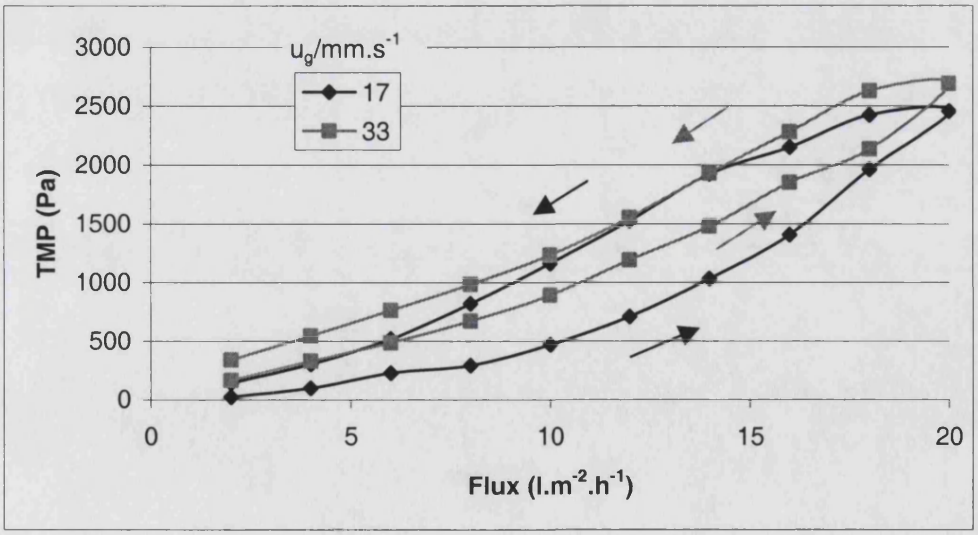

Figure 6-10 Hysteresis plots at low u_g ($mm.s^{-1}$), MLVSS = 0.9 $g.l^{-1}$

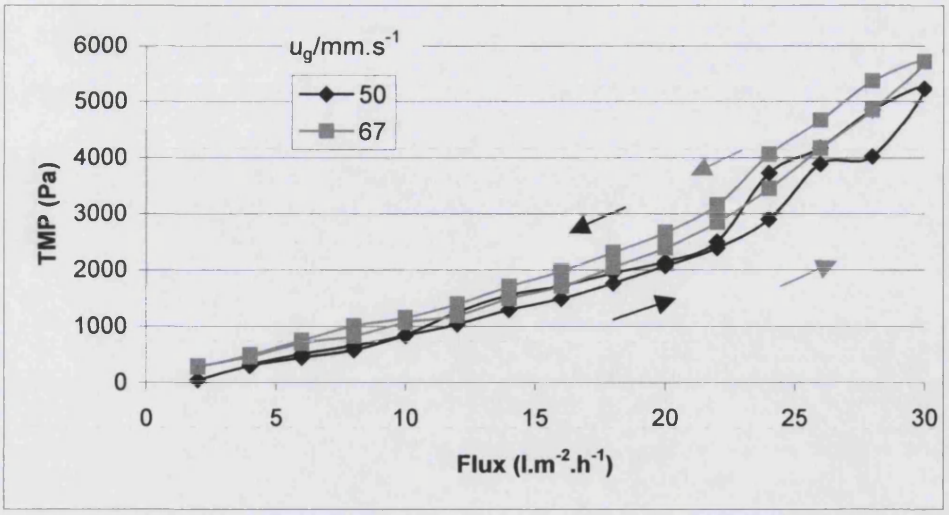

Figure 6-11 Hysteresis plots at high u_g (mm.s^{-1}), MLVSS = 0.9 g.l^{-1}

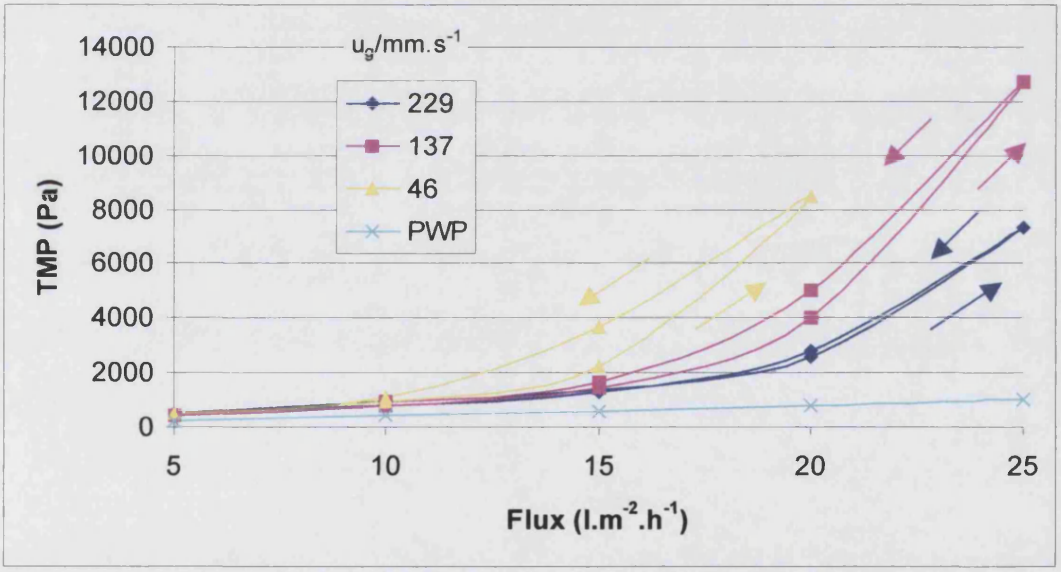

Figure 6-12 Hysteresis plot at various u_g (mm.s^{-1}), MLVSS = 6.78 g.l^{-1}

Figure 6-12 showed the hysteresis plot at different u_g under constant flux operation. At the u_g of 229 and 137 mm.s^{-1}, the TMP increased linearly with

flux up to 15 $l.m^{-2}.h^{-1}$. At the lowest u_g of 46 $mm.s^{-1}$, the dynamic critical flux was 10 $l.m^{-2}.h^{-1}$. The TMP was always higher than that of the PWP. When the dynamic critical flux was exceeded, the TMP increased progressively due to increasing fouling. A hysteresis was observed when the flux was decreased at the u_g of 46 and 137 $mm.s^{-1}$. No hysteresis was observed at the highest u_g of 229 $mm.s^{-1}$. Fouling was reversible in all instances.

6.2.2 Effect of Aeration Rate on Dynamic Critical Flux

Figure 6-13 showed the effect of u_g on dynamic critical flux. The membrane was chemically cleaned for each u_g and dynamic critical flux determination done in duplicate. It could be observed that the dynamic critical flux increased with u_g. Below a u_g of 42 $mm.s^{-1}$, the dynamic critical flux increased rapidly with u_g. This rate of increase then slowed down and no further increase was observed above a u_g of 167 $mm.s^{-1}$. For this system, the maximum dynamic critical flux limit is 22 $l.m^{-2}.h^{-1}$, beyond which further flux increase becomes very difficult.

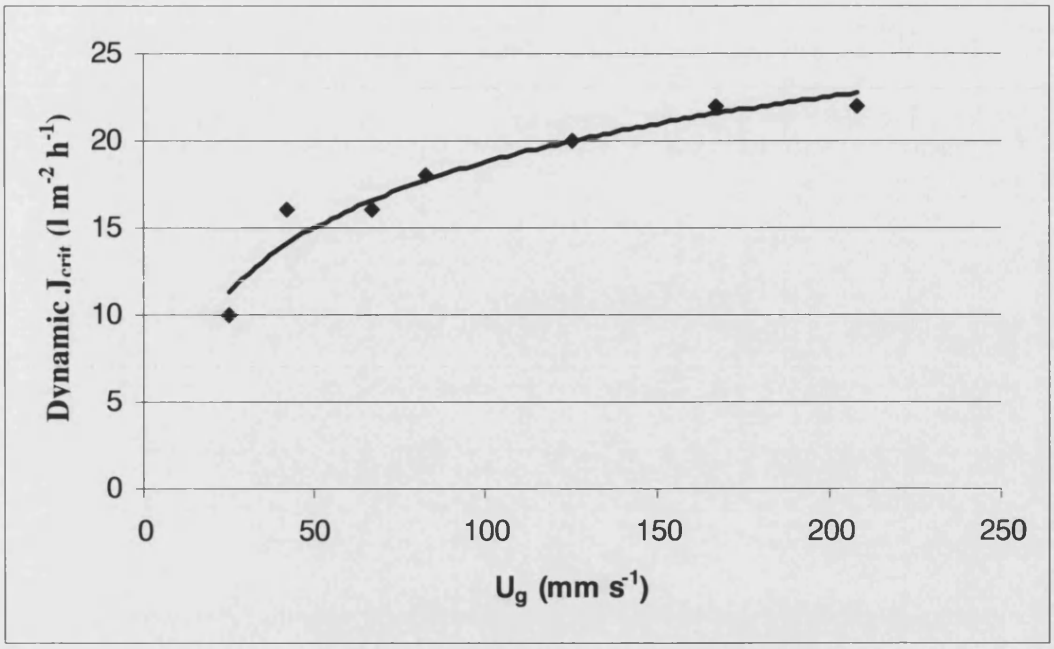

Figure 6-13 Dynamic critical flux at various u_g, MLVSS = 17.15 g.l^{-1}

6.2.3 Effect of Aeration Rate on Residual Fouling

In Figure 6-14, the permeate flux was increased from 15-30 l.m^{-2}.h^{-1} at intervals of 5 l.m^{-2}.h^{-1} for 3 different u_g. Each permeate flux was held for 2 hours and the residual fouling rate determined. The membrane was chemically cleaned for each u_g. The residual fouling rate can be clearly observed to increase rapidly as the permeate flux increased for all the 3 u_g. Low residual fouling rate of less than 6 Pa.min^{-1} was observed at 20 l.m^{-2}.h^{-1} or below for all the 3 u_g, suggesting little effect of u_g on residual fouling rate. At 25 l.m^{-2}.h^{-1} or above, a rapid transition from a low to high residual fouling rate was observed for all the 3 u_g. In this region, the effect of u_g on residual

fouling rate can clearly be observed. A higher u_g resulted in a lower residual fouling rate and the rapid transition from a low to high residual fouling rate occurring at a higher permeate flux. For the lowest u_g of 46 $mm.s^{-1}$, the experimental run could not be completed for the permeate flux of 30 $l.m^{-2}.h^{-1}$ as the TMP increased to 80000 Pa in 30 minutes. The results suggested that little residual fouling below 20 $l.m^{-2}.h^{-1}$ and severe residual fouling above 30 $l.m^{-2}.h^{-1}$, hence this region was further studied in Figure 6-15.

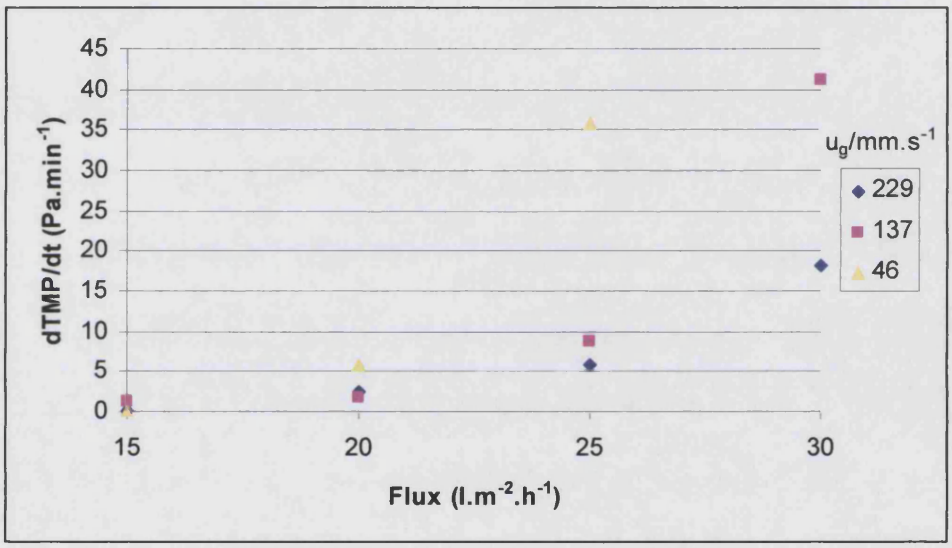

Figure 6-14 Residual fouling rate at various permeate fluxes for different u_g ($mm.s^{-1}$). The MLVSS were 11.99, 12.31 and 12.07 $g.l^{-1}$ for the u_g of 229, 137 and 46 $mm.s^{-1}$ respectively

In Figure 6-15, the u_g was decreased gradually and maintained for 2 hours at each permeate flux level. The membrane was chemically cleaned for each flux level. Figure 6-16 showed a log plot of residual fouling rate against u_g for different permeate fluxes. It could be observed that the membrane fouling rate

increased exponentially as the u_g was gradually decreased. At the highest permeate flux of 28 $l.m^{-2}.h^{-1}$, the membrane fouling rate was relatively high even at high u_g. The exponential relationship between the u_g and the membrane fouling rate indicates the importance of operating with a sufficient u_g. Operating at too low a u_g will result in a much higher rate of membrane fouling.

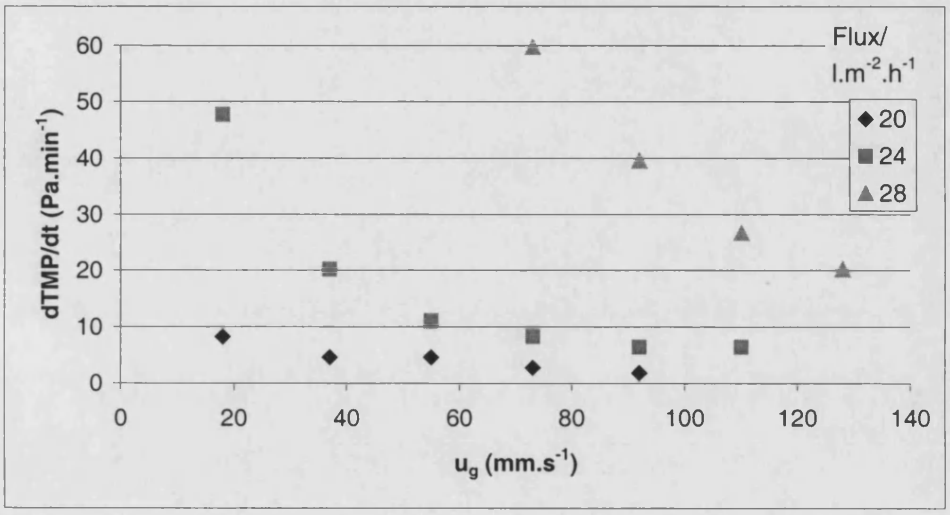

Figure 6-15 Residual fouling rate at various u_g for different permeate fluxes. The MLVSS were 15.2, 15.41 and 14.71 $g.l^{-1}$ for the permeate fluxes of 20, 24 and 28 $l.m^{-2}.h^{-1}$ respectively

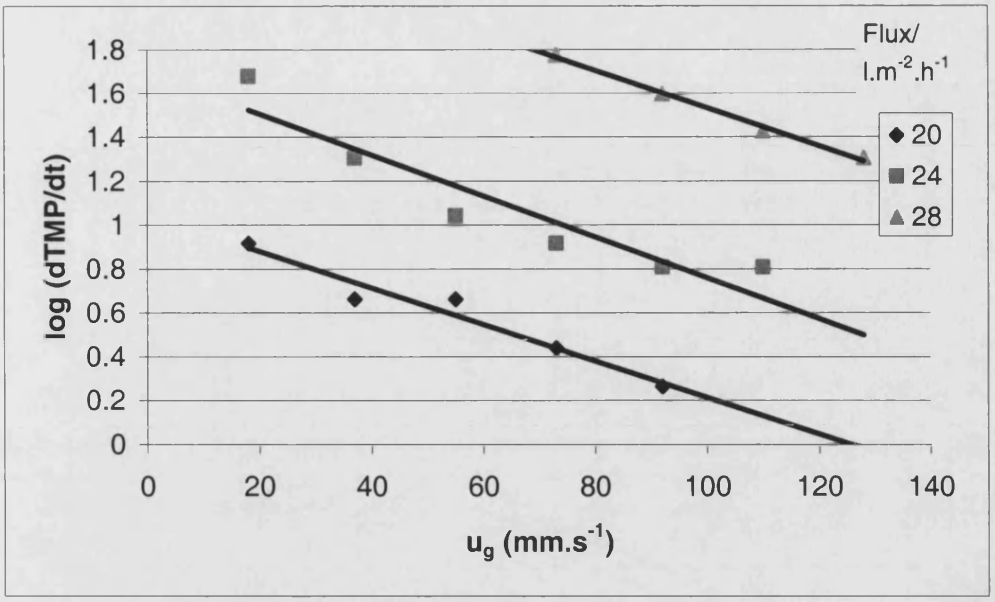

Figure 6-16 Log plot of residual fouling rate against u_g for different permeate fluxes ($l.m^{-2}.h^{-1}$)

Replotting the residual fouling rate against the inverse of the u_g in Figure 6-15 gives Figure 6-17. The straight lines fitted to the data do not pass through the origin. If the line passes through a positive value of u_g then this is the value of u_g for which the appropriate flux is the dynamic critical flux. Extrapolating the lines to the x-axis give u_g of 199, 237 and –117 $mm.s^{-1}$ for decreasing permeate fluxes of 28, 24 and 20 $l.m^{-2}.h^{-1}$. This suggests that the data cannot be used to provide a sensible value of the dynamic critical flux. Forcing the lines through the origin as shown in Figure 6-17 gives the correlation

$$\frac{dTMP}{dt} = \frac{0.684}{u_g} e^{0.3893J}$$

where dTMP/dt, u_g and J are the residual fouling rate ($Pa.min^{-1}$), superficial gas velocity ($mm.s^{-1}$) and permeate flux ($l.m^{-2}.h^{-1}$) respectively.

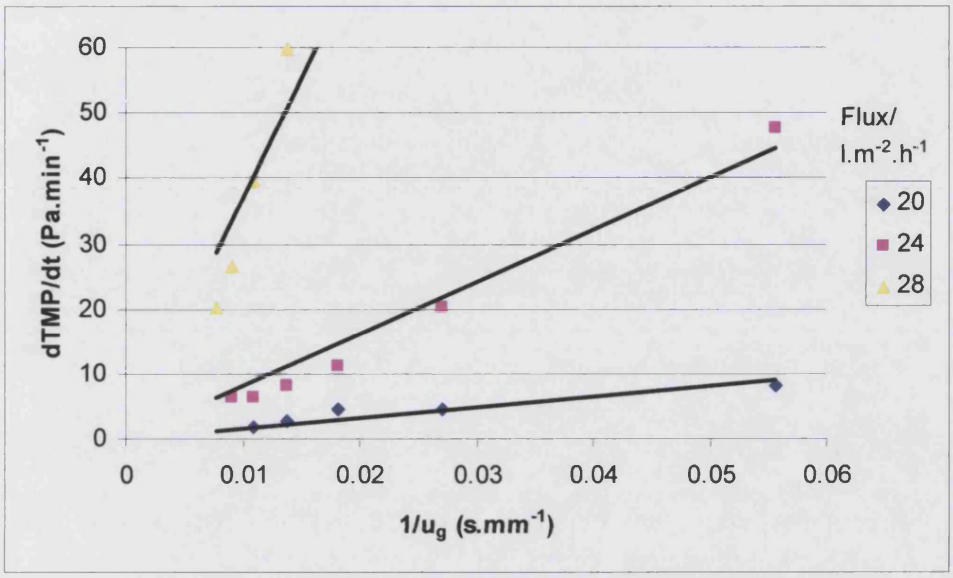

Figure 6-17 Residual fouling rate against 1/ug for different permeate fluxes ($l.m^{-2}.h^{-1}$)

Plotting the slopes in Figure 6-17 against the permeate flux gives Figure 6-18. The graph implies that an increase in the permeate flux results in an exponential increase in the residual fouling rate at the same u_g. Alternatively, the u_g must be increased exponentially to prevent an increase in the residual fouling rate.

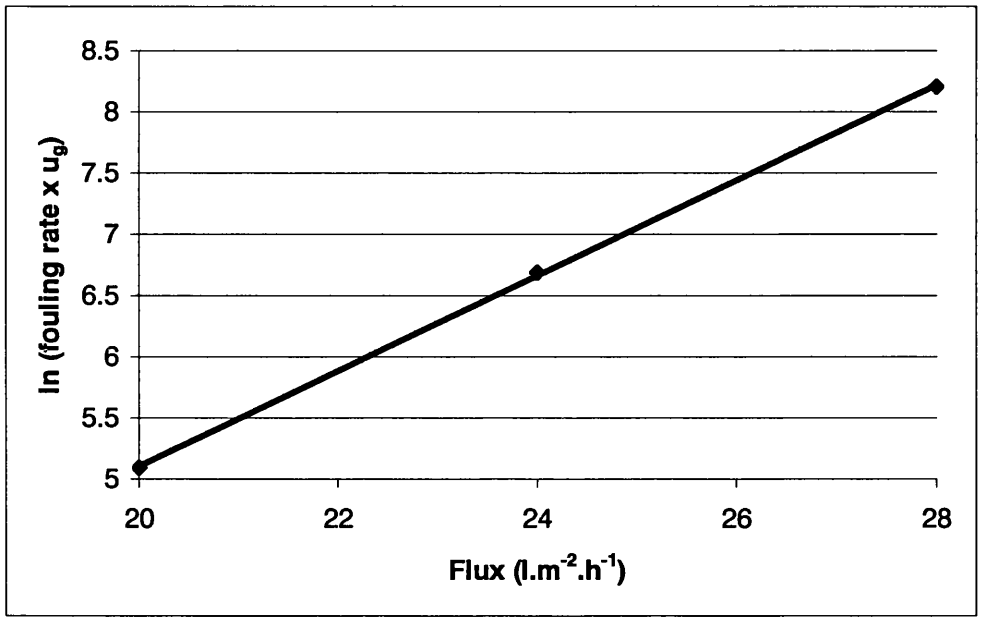

Figure 6-18 Graph of ln (slopes of Figure 6-17) against permeate flux

A higher aeration rate results in a lower stable TMP and hysteresis is reduced. The dynamic critical flux increases with aeration rate up to a maximum, beyond which further flux increase becomes very difficult. For this system, this maximum dynamic critical flux limit is 22 $l.m^{-2}.h^{-1}$ at a u_g of 166 $mm.s^{-1}$ for a MLVSS of 17.15 $g.l^{-1}$. The membrane fouling rate increases exponentially with decreasing aeration rate. A correlation was obtained to describe the relationship between the membrane fouling rate, u_g and permeate flux. The correlation is:

$$\frac{dTMP}{dt} = \frac{0.684}{u_g} e^{0.3893J}$$

where dTMP/dt, u_g and J are the residual fouling rate ($Pa.min^{-1}$), superficial gas velocity ($mm.s^{-1}$) and permeate flux ($l.m^{-2}.h^{-1}$) respectively. The correlation suggests severe membrane fouling at too low a u_g or too high a permeate flux.

6.3 Effect of Permeate Flux on Membrane Fouling

The effect of permeate flux on the membrane fouling rate was further investigated and shown in Figure 6-19. Flux was increased gradually and maintained for 2 hours at each u_g and the residual fouling rate determined at each flux. In this series of experiments, the membrane was chemically cleaned for each u_g. Figure 6-20 showed a log plot of residual fouling rate against permeate flux for different u_g. It could be observed that the membrane fouling rate increased exponentially with the permeate flux, as expected from the discussion above in Section 6.2.3, except for the u_g of 229 $mm.s^{-1}$. Exponential fits to experimental data for membrane fouling rate and permeate flux were also reported in the literature [122] [123]. It was also observed that a higher u_g resulted in a lower membrane fouling rate.

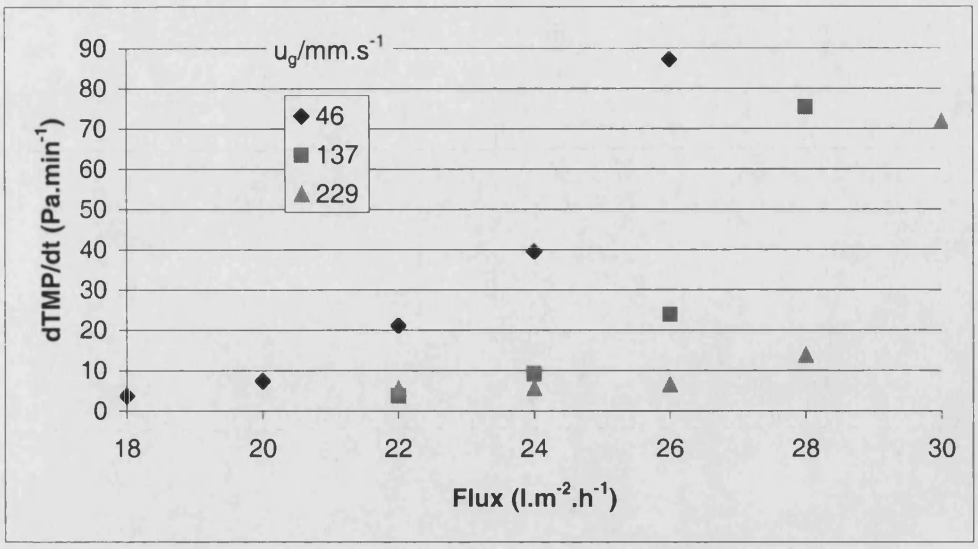

Figure 6-19 Residual fouling rate at various permeate fluxes for different u_g (mm.s^{-1}). The MLVSS was 12.79, 16.48 and 16.06 g.l^{-1} for the u_g of 46, 137 and 229 mm.s^{-1} respectively

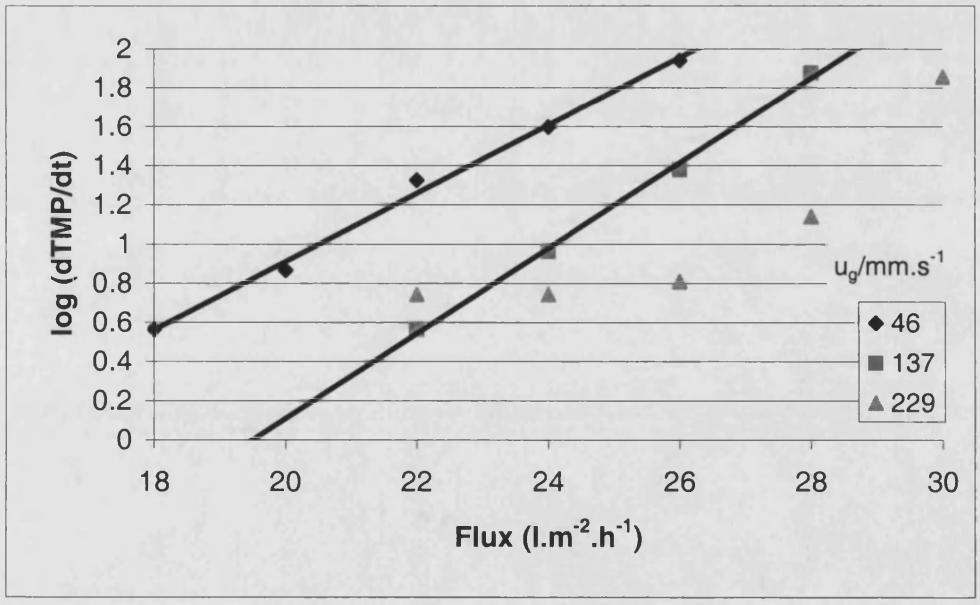

Figure 6-20 Log plot of residual fouling rate against permeate flux for different u_g (mm.s^{-1})

Applying the correlation obtained in Figure 6-17 to Figure 6-19 results in a poor fit. This is illustrated in Figure 6-21. It can be observed that the correlation under predicts the residual fouling rate for the u_g of 46 $mm.s^{-1}$ and 137 $mm.s^{-1}$. The deviation between correlation and data increases as the permeate flux increases. For the u_g of 229 $mm.s^{-1}$, the under prediction of the correlation is only obvious at the permeate flux of 30 $l.m^{-2}.h^{-1}$. Going back to the protocol with which the data was obtained, the permeate flux was held at each level for 2 hours before a stepwise increase. The starting permeate flux level was 14 $l.m^{-2}.h^{-1}$ for the u_g of 46 $mm.s^{-1}$ and 137 $mm.s^{-1}$. The TMP was only observed to increase at the permeate flux of 18 $l.m^{-2}.h^{-1}$ and 22 $l.m^{-2}.h^{-1}$ for the u_g of 46 $mm.s^{-1}$ and 137 $mm.s^{-1}$ respectively. Below these permeate flux levels, the TMP was stable for 2 hours and was not shown in Figure 6-19. The starting permeate flux level was 20 $l.m^{-2}.h^{-1}$ for the u_g of 229 $mm.s^{-1}$ and no TMP increase was observed. This difference in protocol is thought to provide a likely explanation for the under prediction of the correlation.

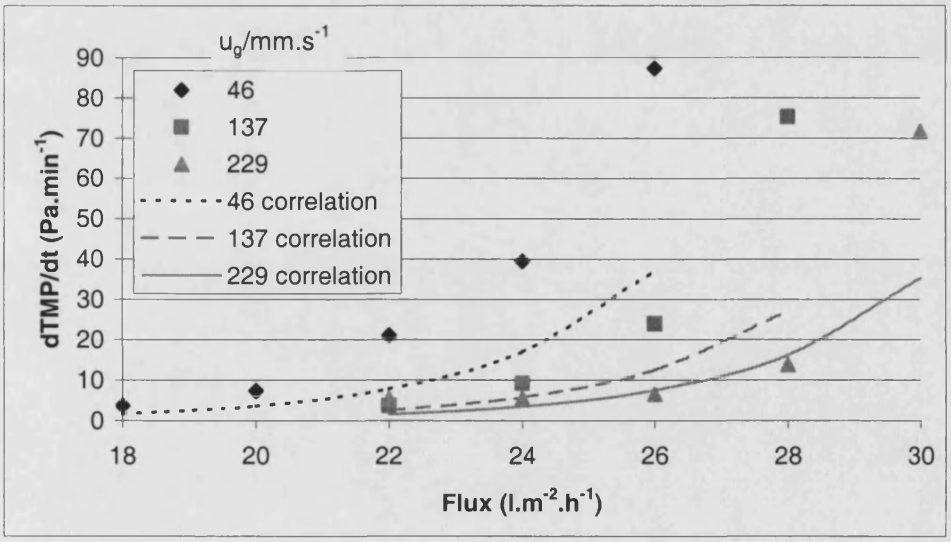

Figure 6-21 Comparison of correlation with Figure 6-19. Numbers of legend indicate u_g in $mm.s^{-1}$.

6.4 Effect of Membrane Fouling

Since particle deposition on the membrane surface depends on the permeate flux, the starting permeate flux should not affect the membrane fouling rate. However, the results suggest a time-dependent factor that increases the fouling rate. This factor is thought to be gradual membrane fouling by small particles, which is not manifested in the TMP.

While the deposition of large particles can be clearly and conveniently shown by an increase in TMP, a stable TMP does not necessary indicate no fouling for a multi-component system. Ognier et al. [122] and Shim et al. [124] operated MBRs with a stable TMP for weeks, before a sharp and abrupt increase in TMP was observed. Clearly, membrane fouling must have occurred which change the properties of the membrane. As discussed in the work of Fane et al. [125], it was suggested that an increase in the TMP is due to the deposition of the dominant cake foulant, which is the biomass floc. Membrane fouling due to other low concentration species is not manifested in the TMP in a short period of time.

As the membrane fouls with time, the characteristic of the membrane changes. The critical flux under the same hydrodynamic condition decreases for a fouled membrane. Cho and Fane [116] showed that critical flux decreased as a membrane gradually fouled with time for an anaerobic MBR. Figure 5-22 gave the same observation. As the membrane fouled at the higher fluxes, the dynamic critical flux was clearly observed to decrease in the 3rd cycle. It is

also interesting to note that the TMP for the 3 cycles (membranes with different degree of fouling) remained similar below a flux of 16 $l.m^{-2}.h^{-1}$. Above a flux of 16 $l.m^{-2}.h^{-1}$, the effect of fouling on TMP was more pronounced at higher permeate fluxes.

The deviation between data and correlation in Figure 6-21 is likely to be due to the effect of membrane fouling. Figure 6-22 compares the correlation with Figure 6-15. A good fit is observed for the experimental runs at the lower fluxes of 20 $l.m^{-2}.h^{-1}$ and 24 $l.m^{-2}.h^{-1}$. The fitting becomes poor for the highest flux of 28 $l.m^{-2}.h^{-1}$. The rate of increase of TMP is faster than an exponential relationship, probably due to membrane fouling which is expected to be more severe at higher permeate fluxes. This suggests that the correlation is only applicable for systems where the membranes are relatively clean. The effects will be different for fouled membranes.

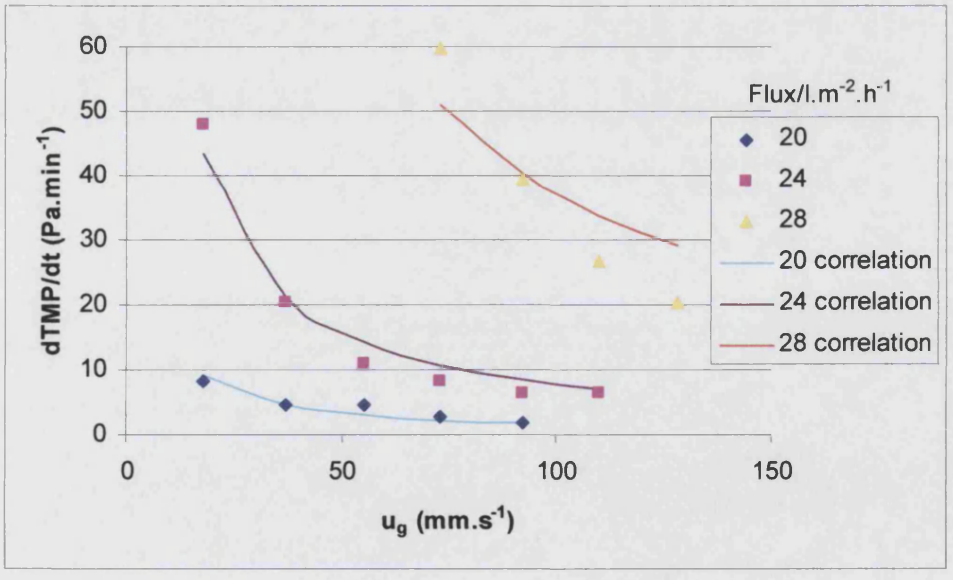

Figure 6-22 Comparison of correlation with Figure 6-15. Numbers of legend indicate permeate flux in $l.m^{-2}.h^{-1}$.

6.5 Effect of Membrane History on Results

The results of this work underline the importance of membrane history in influencing TMP measurements as discussed in Section 6.4. For complex feed solutions such as activated sludge, it is thought that fouling occurs even under sub-critical conditions, that is when a constant TMP is observed. Whilst such sub-critical fouling cannot be observed as a TMP increase, it results in a decrease in the critical flux under the same hydrodynamic conditions. The TMP measurements below this lower critical flux are similar to those before fouling. However, the TMP measurements above this lower critical flux would be higher than those before fouling, as seen in Figure 5-22.

In Figure 6-15, the u_g was gradually decreased at each flux level. At the lowest flux level of 20 $l.m^{-2}.h^{-1}$, the residual fouling rates were low and membrane history is not expected to have a large influence. At the highest flux level of 28 $l.m^{-2}.h^{-1}$ where the residual fouling rates were high, membrane history has an increasing impact with decreasing u_g, since the membrane became more fouled with each experimental run. In Figure 6-19, the permeate flux was gradually increased at each u_g. The importance of membrane history increases at higher permeate fluxes as the membrane fouled, resulting in higher residual fouling rates. Hence, the deviation between results and correlation increased with higher fluxes in Figure 6-21.

Repeat experimental runs showed that the residual fouling rates were difficult to reproduce. For the lowest u_g of 46 $mm.s^{-1}$ in Figure 6-19, a repeat

experimental run showed that a constant TMP could be realized at 16 $l.m^{-2}.h^{-1}$. Hence, the dynamic critical flux was reproducible. Above the dynamic critical flux, the deviation between the 2 experimental runs increased with increasing fluxes, reaching 200 % at the highest TMP of 26 $l.m^{-2}.h^{-1}$. As the MBR was operated without sludge wastage to build up the biomass concentration, a steady state condition cannot be achieved. The changing biomass concentration and foulants such as EPS and SMP are expected to affect membrane fouling. Below the dynamic critical flux, the influence of membrane history on TMP measurements is expected to be limited. Above the dynamic critical flux, membrane history becomes important and sub-critical fouling results in higher TMP measurements. Hence, TMP measurements for long-term experimental runs under high fouling conditions are difficult to reproduce. The experimental approach using dynamic critical flux determination in Figure 6-5, Figure 6-6, Figure 6-13 showed a maximum of 22 $l.m^{-2}.h^{-1}$ for the system, similar to that suggested by the approach using residual fouling rate determination in Figure 6-15 and Figure 6-19. The impact of biological variation and membrane history on TMP measurements under low fouling conditions is low.

The membrane was chemically cleaned with sodium hypochlorite before each series of experiments to provide a standard condition and minimise the effect of membrane history. This was done by soaking the membrane overnight in 0.5 % sodium hypochlorite. The pure water permeability was checked to ensure that it is greater than 2600 $l.m^{-2}.h^{-1}.bar^{-1}$. The TMP-Flux relationship for pure water is shown in Figure 6-23.

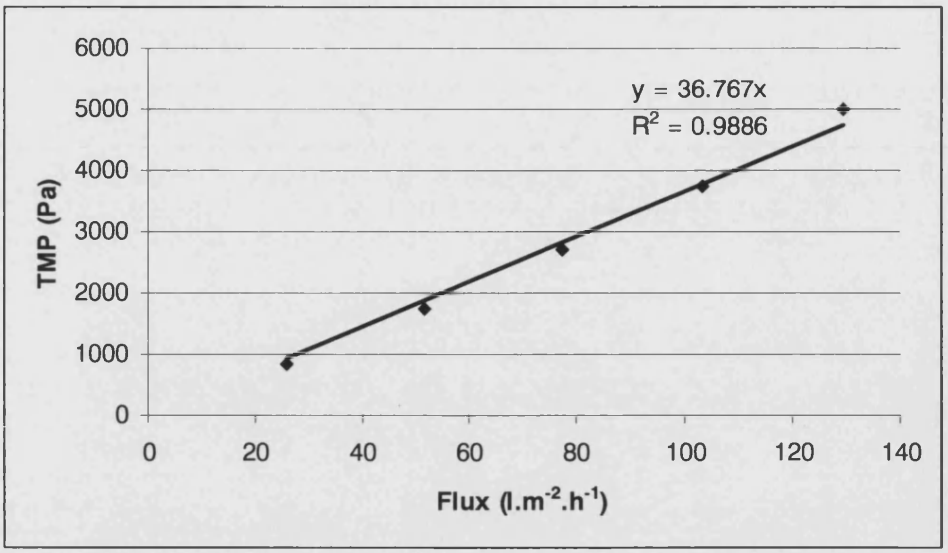

Figure 6-23 TMP-Flux relationship for pure water

6.6 Summary

The effects of MLVSS or F/M ratio, aeration rate and permeate flux on membrane fouling were studied. An optimum MLVSS or F/M ratio that gives the highest permeate flux under a fixed hydrodynamic condition was observed. The highest dynamic critical flux for the system is 22 $l.m^{-2}.h^{-1}$ at a u_g of 83 $mm.s^{-1}$. This occurred at a MLVSS of 14.53 $g.l^{-1}$ or F/M ratio of 0.07 $gBOD.gMLVSS^{-1}.d^{-1}$. The dynamic critical flux increases with aeration rate up to a maximum, beyond which further flux increase becomes very difficult. For this system, this maximum dynamic critical flux limit is 22 $l.m^{-2}.h^{-1}$ at a u_g of 166 $mm.s^{-1}$ for a MLVSS of 17.15 $g.l^{-1}$. A correlation was obtained to describe the relationship between the membrane fouling rate, u_g and permeate flux. Operating at too low a u_g or too high a permeate flux will result in severe membrane fouling.

7 Results – Varying Flux and Long-Term Behaviour of MBR

7.1 Behaviour of MBR Under Varying Flux Operation

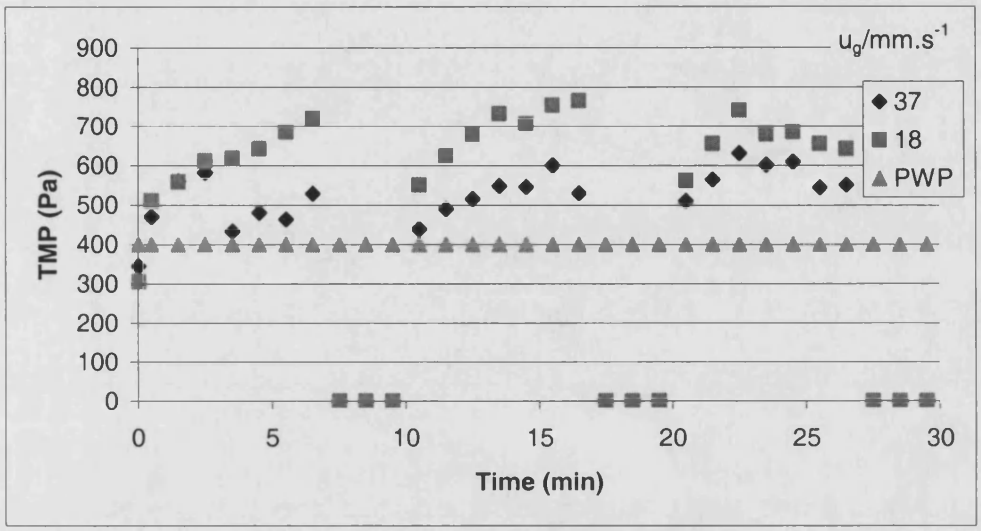

Figure 7-1 TMP at flux of 10 l.m^{-2}.h^{-1} for different u_g (mm.s^{-1}), MLVSS = 8.72 g.l^{-1}

The membrane was chemically cleaned before commencing the experimental runs. No fouling was observed at a low flux level of 10 l.m^{-2}.h^{-1}, even at a low u_g of 18 mm.s^{-1} as shown in Figure 7-1. At a high flux level of 25 l.m^{-2}.h^{-1} shown in Figure 7-2, fouling was clearly observed at the u_g of 201 mm.s^{-1}. Slight fouling was observed even at the higher u_g of 220 mm.s^{-1}, suggesting long-term unsustainability.

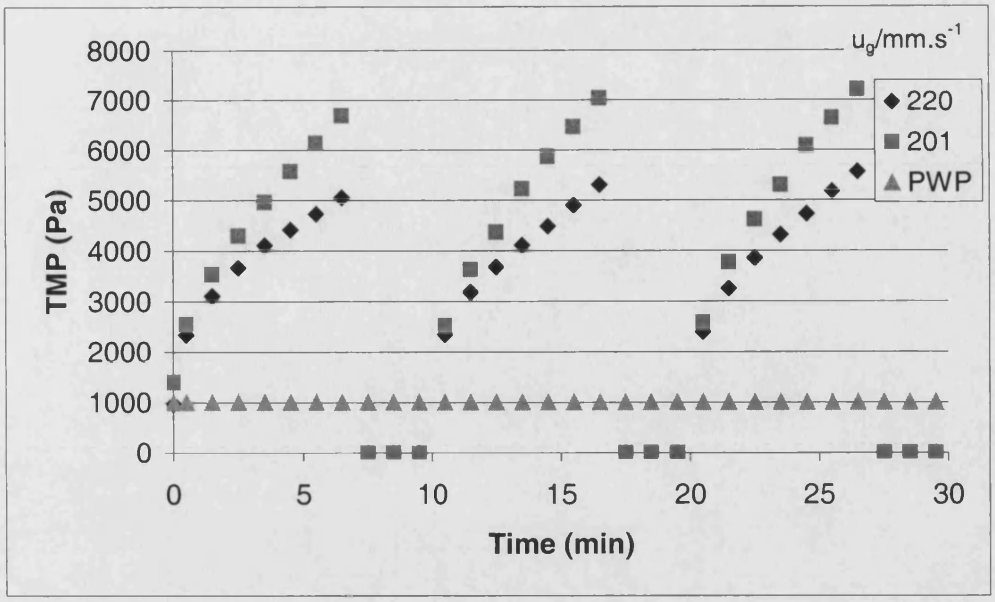

Figure 7-2 TMP at flux of 25 l.m^{-2}.h^{-1} for different u_g (mm.s^{-1}), MLVSS = 8.72 g.l^{-1}

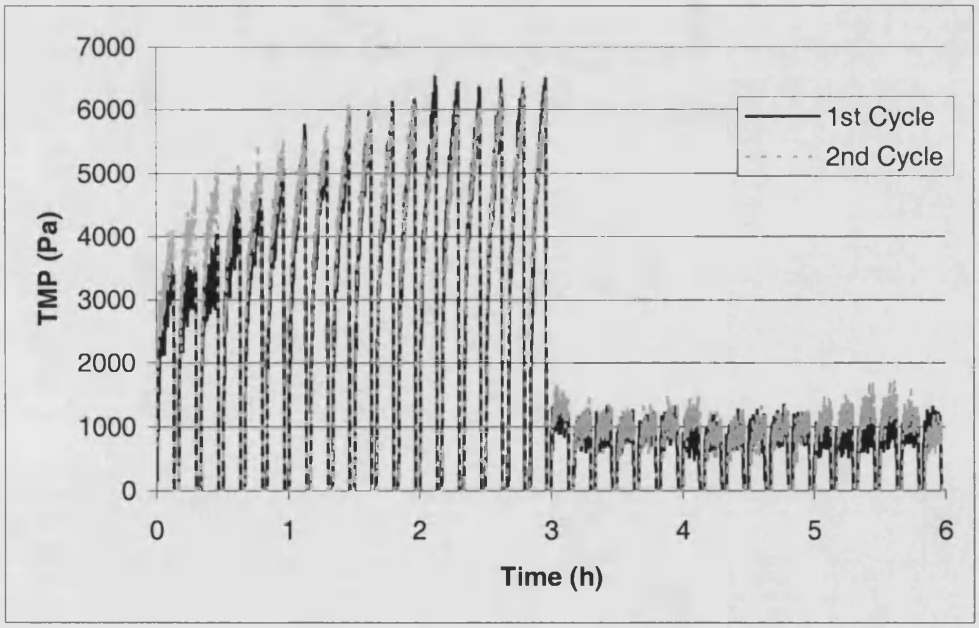

Figure 7-3 TMP at varying flux of 25-10 l.m^{-2}.h^{-1} for varying u_g of 220-18 mm.s^{-1} respectively, MLVSS = 8.72 g.l^{-1}

Figure 7-3 showed the result of varying flux of 25-10 $l.m^{-2}.h^{-1}$ for varying u_g of 220-18 $mm.s^{-1}$ respectively for 3 hours each. Fouling was observed at the high flux level of 25 $l.m^{-2}.h^{-1}$ as expected from Figure 7-2. When the flux level and u_g was decreased to 10 $l.m^{-2}.h^{-1}$ and 18 $mm.s^{-1}$ respectively after 3 hours, the TMP decreased and no fouling was observed as expected from Figure 7-1. Repeating this cycle (2nd cycle) and comparing with the 1st cycle showed similar TMP after 3 hours under each condition. This suggests that turning-up/turning down of throughput in MBRs treating municipal wastewater is sustainable.

While a temporary flux increase is known to be possible in MBRs [18] [14] [12] [22], the results showed that it is possible to vary the aeration rate simultaneously. A high aeration rate is used to prevent excessive membrane fouling only during high throughput to optimize the energy consumption of MBRs. Fouling is removed when the permeate flux is reduced below the dynamic critical flux during low flows, allowing long-term sustainability.

7.2 Long-Term Microfiltration of Activated Sludge

The membrane was chemically cleaned before starting the experimental runs. Figure 7-4 showed the long-term microfiltration of activated sludge at a permeate flux of 10 $l.m^{-2}.h^{-1}$ and a u_g of 83 $mm.s^{-1}$. It could be observed that the TMP increased slightly during the first 20 hours, and then remained relatively constant at a low TMP of approximately 700 Pa for more than 200

hours. From the results shown in Figure 6-13, the dynamic critical flux is 18 $l.m^{-2}.h^{-1}$ for a u_g of 83 mm s^{-1}. The permeate flux of 10 $l.m^{-2}.h^{-1}$ was much lower than the dynamic critical flux. There was little fouling and a stable TMP was observed.

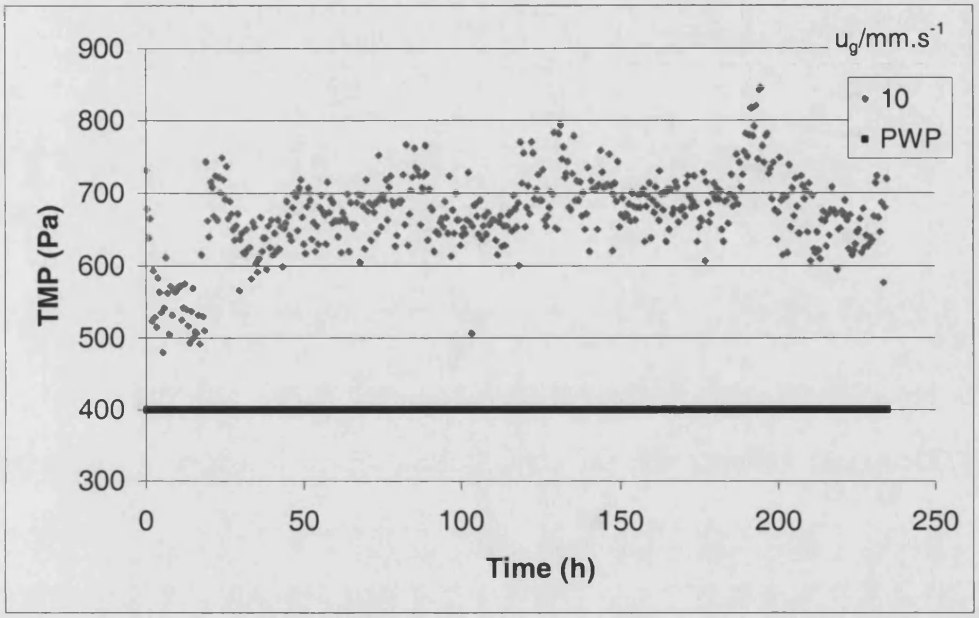

Figure 7-4 TMP at a permeate flux of 10 $l.m^{-2}.h^{-1}$ and a u_g of 83 $mm.s^{-1}$, MLVSS = 18.56 $g.l^{-1}$

Figure 7-5 and Figure 7-6 showed the TMP evolution at a higher permeate flux of 20 $l.m^{-2}.h^{-1}$ and a u_g of 83 $mm.s^{-1}$. It could be observed in Figure 7-5 that the TMP remained constant for approximately 6 hours, and then increased gradually. The data points were recorded at 30 seconds interval. Each data point in Figure 7-6 was obtained by averaging every 30 data points and therefore represented the average TMP for a 900 seconds interval. Figure 7-6 revealed a slightly increasing TMP during the initial 6 hours. This may

explain why critical flux was not observed in long-term operation of MBRs. Critical flux determined by the flux stepping method usually has a filtration time of 30 minutes or less for each flux step and slight TMP increase cannot be observed in the short filtration time. The work of Vigneswaran et al. [112] suggested membrane fouling occurring even at a constant TMP as the critical flux concept based on DOTM and material balance were lower than that based on constant TMP.

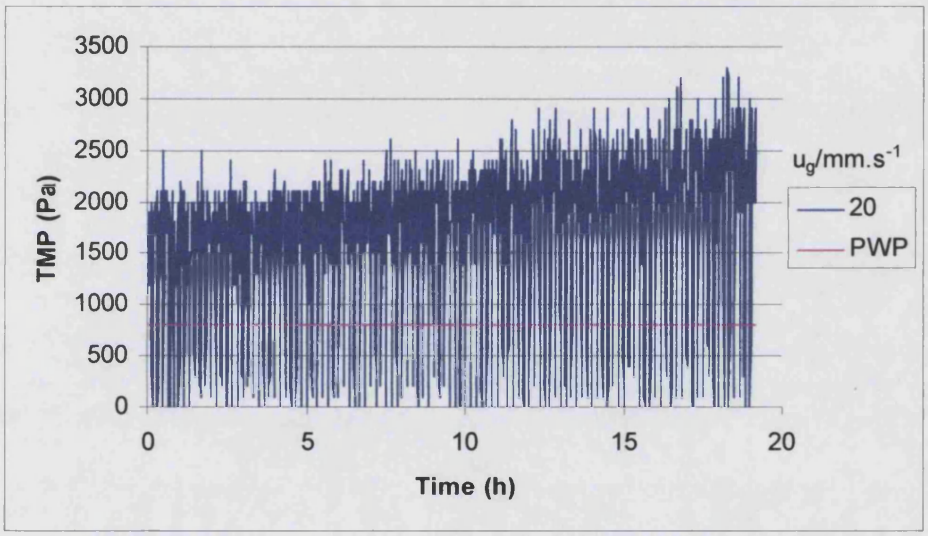

Figure 7-5 TMP at a permeate flux of 20 l.m^{-2}.h^{-1} and a u_g of 83 mm.s^{-1}, MLVSS = 17.69 g.l^{-1}

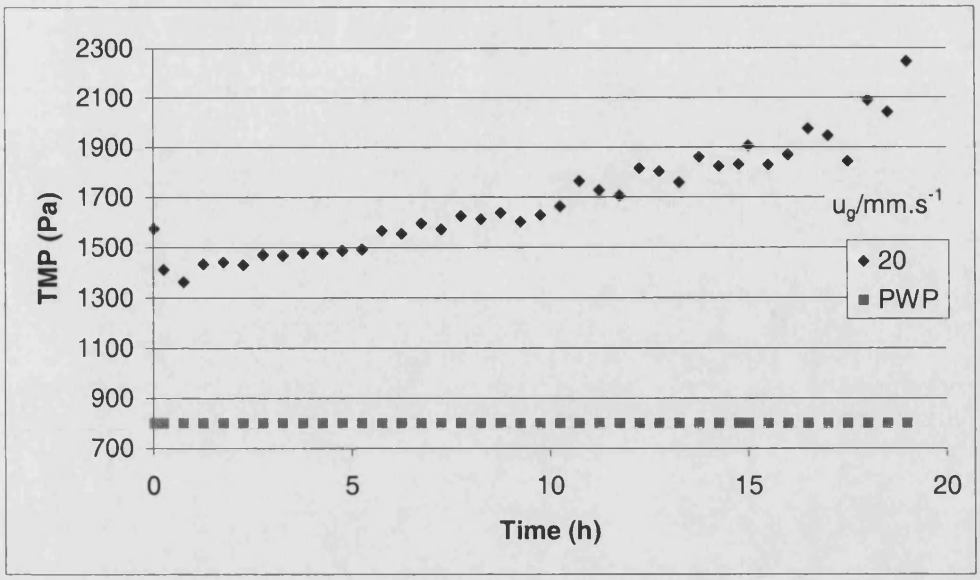

Figure 7-6 TMP at a permeate flux of 20 l.m^{-2}.h^{-1} and a u_g of 83 mm.s^{-1}, MLVSS = 17.69 g.l^{-1}

Near the dynamic critical flux, the TMP increased after some time, possibly due to membrane fouling that could not be observed in the TMP during short filtration times. Operating much lower than the dynamic critical flux allowed long-term operation with a stable TMP. Membrane fouling is likely to occur but at a much reduced rate. Since membranes are the major cost factor in MBR plants, economics dictate that full scale MBR plants are operated at sustainable flux with slight TMP increase and occasional chemical cleaning, rather than much lower than the dynamic critical flux with constant TMP.

7.3 Summary

The behaviour of MBR under varying flux operation and long-term operation was studied. For submerged MBRs treating municipal wastewater, a high aeration rate can be used to prevent excessive membrane fouling at a high permeate flux for a short period of time. Fouling is removed when the permeate flux is reduced below the dynamic critical flux, allowing long-term sustainability. Near the dynamic critical flux, the TMP increase after some time during long-term operation is likely to be due to membrane fouling that is not observed in the TMP during the short filtration time for the determination of dynamic critical flux.

8 Conclusions

8.1 Varying Throughput Operation of MBRs

This work has explored and shown that the turn-up/turn-down design of MBRs is possible using a combination of suitable hydrodynamic conditions and intermittent permeation. The current wastewater treatment plants are designed to treat three times DWF at a fixed aeration rate. The turn-up/turn-down design allows the aeration rate, which is a major cost component in submerged MBRs, to be decreased during periods of low flows. The aeration rate is then increased concurrently with the permeate flux during short periods of high flows to prevent excessive membrane fouling. This allows fouling to be removed with a subsequent reduction in the permeate flux, allowing long-term sustainability.

8.2 Concept of Dynamic Critical Flux

A dynamic critical flux has been defined as the instantaneous flux at which the TMP stabilises quickly and does not increase with time under intermittent permeation. Near the dynamic critical flux, the TMP increase after some time during long-term operation is likely to be due to membrane fouling that is not observed in the TMP during the short filtration time for the determination of dynamic critical flux. A stable TMP can be achieved by operating much lower

than the dynamic critical flux. There appears to be no critical flux or dynamic critical flux for long-term operation of MBR. The determination of the short-term dynamic critical flux does not include the long-term fouling mechanism, which causes gradual TMP increase. However, the determination of the short-term dynamic critical flux is useful as it gives an indication to sustainable operation of real MBR plants where chemical cleaning is only occasionally necessary.

8.3 Effects of Hydrodynamic Parameters on Membrane Fouling

How membrane fouling can be controlled has been studied. Fouling can be removed by the suspension of permeation while maintaining the aeration for a submerged MBR. Membrane fouling increases exponentially if the suspension of permeation is not long enough. Operational parameters such as aeration rate and permeate flux which control the hydrodynamic conditions have been shown to heavily influence membrane fouling. A higher aeration rate results in a lower stable TMP and hysteresis is reduced. The dynamic critical flux increases with aeration rate up to a maximum, beyond which further flux increase becomes very difficult. The maximum dynamic critical flux for the system at a MLVSS of 17.15 $g.l^{-1}$ is 22 $l.m^{-2}.h^{-1}$ at a u_g of 166 $mm.s^{-1}$. The membrane fouling rate increases exponentially with decreasing aeration rate and increasing permeate flux. Severe membrane fouling occurs if the permeate flux is too high or the aeration rate is too low. A correlation was

obtained to describe the relationship between the membrane fouling rate, u_g and permeate flux. The correlation is:

$$\frac{dTMP}{dt} = \frac{0.684}{u_g} e^{0.3893J}$$

where dTMP/dt, u_g and J are the residual fouling rate ($Pa.min^{-1}$), superficial gas velocity ($mm.s^{-1}$) and permeate flux ($l.m^{-2}.h^{-1}$) respectively.

8.4 MLVSS or F/M Ratio

The effect of MLVSS concentration or F/M ratio on permeate flux has been investigated. For a fixed hydrodynamic condition, there is an optimum MLVSS concentration or F/M ratio which gives the highest permeate flux. The highest dynamic critical flux for the system is 22 $l.m^{-2}.h^{-1}$ at a u_g of 83 $mm.s^{-1}$. This occurred at a MLVSS concentration of 14.53 $g.l^{-1}$ or F/M ratio of 0.07 $gBOD.gMLVSS^{-1}.d^{-1}$. The lower permeate flux at high MLVSS concentration or low F/M ratio is likely to be due to increasing viscosity, while that at low MLVSS concentration or high F/M ratio being due to higher EPS and SMP concentrations as suggested in the literature. Membrane fouling in multi-component systems such as activated sludge involves the interactions between the different species and the hydrodynamic conditions.

8.5 Optimal MBR Design?

This work and recent publications have shed some light towards a possible optimal MBR design. It appears that the HRT and MLSS of full scale MBRs are 1.5-5.5 hours and 10-15 $g.l^{-1}$. The most stable performance occurs on plants with low fluxes of less than 15 $l.m^{-2}.h^{-1}$ and long SRT of greater 30 days [25].

- ColtsNeck: Flux 10.7 $l.m^{-2}.h^{-1}$ and SRT greater than 200 days
- Cohasset: Flux 15 $l.m^{-2}.h^{-1}$ and SRT greater than 100 days
- Swanage: Flux 10 $l.m^{-2}.h^{-1}$ and SRT greater than 50 days
- Porlock: Flux 13 $l.m^{-2}.h^{-1}$ and SRT greater than 50 days

While lower membrane fouling is expected at lower fluxes, the reason for greater process stability at longer SRT is less clear. EPS and SMP are thought to be important foulants in MBRs. Contrary to the CASP where SMP increases at high sludge ages due to cell lysis, recent work have shown that EPS and SMP decrease at long SRT in MBRs. Several conclusions have been suggested by the work of Brookes et al. [38], Chang et al. [75] and Lee et al. [61].

- Carbohydrate is the dominant species and no protein was measured in SMP. Protein is the dominant species in EPS except at short SRT (4 days).
- EPS and SMP decreased with longer SRT from 4-30 days and appeared to stabilize thereafter. EPS and SMP concentrations were found to be lowest for an MBR without sludge wastage. The protein

concentration remained relatively stable while the carbohydrate concentration decreased with longer SRT.

- The protein to carbohydrate ratio thus increased with longer SRT, as did filtration resistance.

Hence, greater process stability at longer SRT is likely to be due to lower SMP concentration. It is thought that floc deposition results in a rapid TMP rise. Under sub-critical operation, floc deposition is minimal and the gradual TMP rise observed in long-term operation of MBRs is due to SMP accumulation on the membrane. SMP is mainly carbohydrate, and the work of Cho and Fane [116] showed carbohydrate accumulation on the membrane, although it must be mentioned that theirs was an anaerobic system. While flocs are unlikely to foul the membrane under sub-critical operation, increasing MLSS concentration is expected to result in increase viscosity. An exponential relationship between MLSS and viscosity is usually reported in the literature. Pilot plant data suggested that viscosity increased rapidly above 18 $g.l^{-1}$ MLSS [11]. Hence, lower permeate flux is expected at higher MLSS concentration due to increase viscosity. There should exist an optimal SRT or F/M ratio where flux is the highest. Such an optimum is observed in this work at a MLVSS concentration of 14.53 $g.l^{-1}$ or F/M ratio of 0.07 $gBOD.gMLVSS^{-1}.d^{-1}$. Knowing the variations in influent across MBRs, it is unlikely that the optimal SRT or F/M ratio will be the same across MBRs. This remains to be explored. Currently, it is thought that MBRs should be designed and operated at:

- SRT greater than 30 days to minimize SMP fouling
- MLVSS less than 15 $g.l^{-1}$ to avoid the problem of increase viscosity

9 Future Work

9.1 Membrane Fouling by Polydispersed Feed Solutions

Membrane fouling by polydispersed feed solutions such as activated sludge is currently not well understood. This work has suggested the interactions between the different species and hydrodynamic conditions to be important. The concept of a dynamic cake layer protecting the membrane from fouling by smaller species is quite plausible as discussed in Section 6.1. Future work can be done using more defined feed solutions such as yeast, BSA and latex beads of different sizes to gain a better understanding of the interactions. Direct observation through the membrane (DOTM) will be useful in observing particle deposition on the membrane surface for polydispersed feed solutions.

9.2 Effects of Biomass Concentration and F/M Ratio on Membrane Fouling

This work has suggested an optimum operating region where the permeate flux is the highest. This implies a lower cost of treatment for MBRs. MLVSS and F/M ratio were used as design parameters under non-steady conditions in this work. Given the variability of sewage and the complex interactions of the many factors affecting the permeate flux in MBRs, such an optimum MLVSS or F/M ratio is likely to differ but still exist across MBR plants. It will be

interesting to investigate the effect of F/M ratio or SRT under steady-state conditions in future work to confirm the existence of an optimal region where the permeate flux is the highest. Factors such as EPS and SMP concentrations, MLVSS, particle size, viscosity and microscopic examination of the sludge could be monitored to evaluate their influence on the permeate flux.

9.3 Membrane Bioreactor Design

There is currently a lack of information on the effect of bioreactor design on membrane fouling. Chisti [126] has studied the hydrodynamics of airlift bioreactors. How the hydrodynamics affect a membrane submerged in the riser is not well understood. Recently, Shim et al. [124] showed that the ratio of downcomer to riser area affected membrane fouling. A ratio of downcomer to riser area of 4.5 allowed stable filtration for 5 months. A lower ratio of 1.6 could only be operated for less than a month. Other bioreactor design variables such as the gas-liquid dispersion height are likely to be important in the fouling of submerged membranes. All the published work focused on the effects of operating parameters on membrane fouling. Much improvement to MBRs may yet be achieved in the area of bioreactor design.

9.4 Optimising Bubble Size

Slug flow, characterised by bubbles colliding and coalescing forming large bubbles, has been reported to be favorable for permeate flux enhancement. Small bubbles, having a larger gas-liquid interfacial area, are favorable for gas-liquid mass transfer. For the turn-up/turn-down design, small bubbles can be used to enhance gas-liquid mass transfer during periods of low flows since little fouling is expected. During periods of high flows, gas slugs can then be used to enhance the permeate flux. Another possibility is to alternate between small and large bubbles. Fouling accumulated during bubble flow may be removed by periodic slug flow. Gas-liquid mass transfer is enhanced and energy is saved during bubble flow. This requires information on the effect of bubble size on membrane fouling. Manipulating bubble size will be closely linked to sparger design and bioreactor design, which affects gas holdup.

Acknowledgements

The author is grateful to his supervisor, Professor John Howell, for his guidance, enthusiasm, valuable insights and comments on this work.

This work was supported through the EPSRC WITE Programme (GR/M68565) - £0.75M - with Cranfield University, Imperial College, and 7 UK water utility companies.

The provision of lab-scale membranes by Kubota Corporation is greatly appreciated.

References

[1] P.Cote, H.Buisson, and M.Praderie, Immersed Membranes Activated Sludge Process Applied to the Treatment of Municipal Wastewater *Water Science and Technology*, vol. 38, no. 4–5, pp. 437-442, 1998.

[2] M.Gander, B.Jefferson, and S.Judd, Aerobic MBRs for Domestic Wastewater Treatment: A Review with Cost Considerations *Separation and Purification Technology*, vol. 18, pp. 119-130, 2000.

[3] J.A.Howell, Membrane Processes for the Treatment of Activated Sludge *Euromembrane*, vol. 1, pp. 462-468, 1995.

[4] S.Churchouse, Membrane Bioreactors Going From Lab to Large Scale Application: - Problems to Clear Solutions? Membranes and the Environment: A special post-ICOM workshop in honour of Roger Ben Aim, Tony Fane and John Howell, Oxford, UK, 14-17 July, 2002.

[5] C.W.Smith, D.Di Gregorio, and R.M.Talcott,. The Use of Ultrafiltration Membrane for Activated Sludge Separation Proc., 24th Annual Purdue Industrial Waste Conference, Purdue University, West Lafayette, Indiana, pp. 1300-1310, 1969.

[6] P.Cote, J.-L.Bersillon, and G.Faup, Bubble Free Aeration Using Membranes: Process Analysis *Journal of Water Pollution Control Federation*, vol. 60, no. 11, pp. 1986-1992, 1988.

[7] A.G.Livingston, Extractive Membrane Bioreactors: A New Process Technology for Detoxifying Chemical Industry Wastewaters *Journal of Chemical Technology and Biotechnology*, vol. 60, pp. 117-124, 1994.

[8] K.Yamamoto, M.Hiasa, T.Mahmood, and T.Matsuo, Direct Solid-Liquid Separation Using Hollow Fiber Membrane in an Activated Sludge Aeration Tank *Water Science and Technology*, vol. 21, pp. 43-54, 1989.

[9] Z.Cadi, H.Huyard, J.Manem, and R.Moletta, Anaerobic Digestion of a Synthetic Wastewater Containing Starch by a Membrane Reactor *Environmental Technology*, vol. 15, pp. 1029-1039, 1994.

[10] W.Liu, J.A.Howell, T.C.Arnot, and J.A.Scott, A Novel Extractive Membrane Bioreactor for Treating Biorefractory Organic Pollutants in the Presence of High Concentrations of Inorganics: Application to a Synthetic Acidic Affluent Containing High Concentrations of Chlorophenol and Salt *Journal of Membrane Science*, vol. 181, pp. 127-140, 2001.

[11] S.Churchouse, Membrane Bioreactors for Wastewater Treatment – Operating Experiences with the Kubota Submerged Membrane Activated Sludge Process *Membrane Technology*, vol. 83, pp. 5-9, 1997.

[12] B.Gunder and K.Krauth, Replacement of Secondary Clarification by Membrane Separation – Results with Plate and Hollow Fibre Modules *Water Science and Technology*, vol. 38, no. 4–5, pp. 383-393, 1998.

[13] B.Gunder and K.Krauth, Replacement of Secondary Clarification by Membrane Separation - Results with Tubular, Plate and Hollow Fibre Modules *Water Science and Technology*, vol. 40, no. 4-5, pp. 311-320, 1999.

[14] T.Ueda and K.Hata, Domestic Wastewater Treatment by a Submerged Membrane Bioreactor with Gravitational Filtration *Water Research*, vol. 33, no. 12, pp. 2888-2892, 1999.

[15] H.Kishino, H.Ishida, H.Iwabu, and I.Nakano, Domestic Wastewater Reuse Using a Submerged Membrane Bioreactor *Desalination*, vol. 106, pp. 115-119, 1996.

[16] W.J.Davies, M.S.Le, and C.R.Heath, Intensified Activated Sludge Process with Submerged Membrane Microfiltration *Water Science and Technology*, vol. 38, no. 4–5, pp. 21-27, 1998.

[17] T.Murakami, J.Usui, K.Takamura, and T.Yoshikawa, Application of Immersed-Type Membrane Separation Activated Sludge Process to Municipal Wastewater Treatment *Water Science and Technology*, vol. 41, no. 10-11, pp. 295-301, 2000.

[18] H.Ishida, Y.Yamada, M.Tsuboi, and S.Matsumura, Submerged Membrane Activated Sludge Process (KSMASP) - Its Application into Activated Sludge Process with High Concentration of MLSS *Int 2nd Conf on Advances in Water and Effluent Treatment*, vol. pp. 321-330, 1993.

[19] H.Buisson, P.Cote, M.Praderie, and H.Paillard, The Use of Immersed Membranes for Upgrading Wastewater Treatment Plants *Water Science and Technology*, vol. 37, no. 9, pp. 89-95, 1998.

[20] S.Rosenberger, U.Kruger, R.Witzig, W.Manz, U.Szewzyk, and M.Kraume, Performance of a Bioreactor with Submerged Membranes for Aerobic Treatment of Municipal Waste Water *Water Research*, vol. 36, pp. 413-420, 2002.

[21] R.Ben Aim, Applications and Nutrient Removal, Membrane Bioreactors and Water Reclamation Principles and Practice, Singapore, 18 November, 2003.

[22] P.Cote, H.Buisson, C.Pound, and G.Arakaki, Immersed Membrane Activated Sludge for the Reuse of Municipal Wastewater *Desalination*, vol. 113, pp. 189-196, 1997.

[23] T.Ueda, K.Hata, and Y.Kikuoka, Treatment of Domestic Sewage From Rural Settlements by a Membrane Bioreactor *Water Science and Technology*, vol. 34, no. 9, pp. 189-196, 1996.

[24] C.Chiemchaisri, K.Yamamoto, and S.Vigneswaran, Household Membrane Bioreactor in Domestic Wastewater Treatment *Water Science and Technology*, vol. 27, no. 1, pp. 171-178, 1993.

[25] G.Leslie, Critical Performance Issues in MBR Reclamation Plants, Membrane Bioreactors and Water Reclamation Principles and Practice, Singapore, 18 November, 2003.

[26] S.Holler and W.Trosch, Treatment of Urban Wastewater in a Membrane Bioreactor at High Organic Loading Rates *Journal of Biotechnology*, vol. 92, pp. 95-101, 2001.

[27] C.H.Xing, E.Tardieu, Y.Qian, and X.H.Wen, Ultrafiltration Membrane Bioreactor for Urban Wastewater Reclamation *Journal of Membrane Science*, vol. 177, pp. 73-82, 2000.

[28] S.Chaize and A.Huyard, Membrane Bioreactor on Domestic Wastewater Treatment Sludge Production and Modelling Approach *Water Science and Technology*, vol. 23, pp. 1591-1600, 1991.

[29] X.Huang, R.Liu, and Y.Qian, Behaviour of Soluble Microbial Products in a Membrane Bioreactor *Process Biochemistry*, vol. 36, pp. 401-406, 2000.

[30] N.Cicek, H.Winnen, M.T.Suidan, B.E.Wrenn, V.Urbain, and J.Manem, Effectiveness of the Membrane Bioreactor in the Biodegradation of High Molecular Weight Compounds *Water Research*, vol. 32, no. 5, pp. 1553-1563, 1998.

[31] X.Huang, P.Gui, and Y.Qian, Effect of Sludge Retention Time on Microbial Behaviour in a Submerged Membrane Bioreactor *Process Biochemistry*, vol. 36, pp. 1001-1006, 2001.

[32] D.J.Barker and D.C.Stuckey, A Review of Soluble Microbial Products (SMP) in Wastewater Treatment Systems *Water Research*, vol. 33, no. 14, pp. 3063-3082, 1999.

[33] B.E.Rittmann, W.Bae, E.Namkung, and C.J.Lu, A Critical Evaluation of Microbial Product Formation in Biological Processes *Water Science and Technology*, vol. 19, no. 517–528, 1987.

[34] A.D.Bailey, G.S.Hansford, and P.L.Dold, The Use of Crossflow Microfiltration to Enhance the Performance of an Activated Sludge Reactor *Water Research*, vol. 28, no. 2, pp. 297-301, 1994.

[35] V.Urbain, B.Mobarry, V.de Silva, D.A.Stahl, B.E.Rittmann, and J.Manem, Integration of Performance, Molecular Biology and Modelling to Describe the Activated Sludge Process *Water Science and Technology*, vol. 37, no. 3, pp. 223-229, 1998.

[36] I-T.Yeom, Y-M.Nah, and K-H.Ahn, Treatment of Household Wastewater Using an Intermittently Aerated Membrane Bioreactor *Desalination*, vol. 124, pp. 193-204, 1999.

[37] C.Chiemchaisri, Y.K.Wong, T.Urase, and K.Yamamoto, Organic Stabilization and Nitrogen Removal in Membrane Separation Bioreactor for Domestic Wastewater Treatment *Water Science and Technology*, vol. 25, no. 10, pp. 231-240, 1992.

[38] A.Brookes, S.Judd, E.Reid, E.Germain, S.Smith, H.Alvarez, P.Le Clech, T.Stephenson, E.Turra, and B.Jefferson, Biomass Characterisation in Membrane Bioreactors, IMSTEC'03 5th International Membrane Science and Technology Conference Sydney Australia November 10-14, 2003.

[39] Y.Lee, J.Cho, Y.Seo, J.W.Lee, and K-H.Ahn, Modeling of Submerged Membrane Bioreactor Process for Wastewater Treatment *Desalination*, vol. 146, pp. 451-457, 2002.

[40] C.H.Xing, Y.Qian, X.H.Wen, W.Z.Wu, and D.Sun, Physical and Biological Characteristics of a Tangential-Flow MBR for Municipal Wastewater Treatment *Journal of Membrane Science*, vol. 191, pp. 31-42, 2001.

[41] K.Parameshwaran, C.Visvanathan, and R.Ben Aim, Membrane as Solid/Liquid Separator and Air Diffuser in Bioreactor *Journal of Environmental Engineering*, vol. September, pp. 825-834, 1999.

[42] J.Lee, W-Y.Ahn, and C-H.Lee, Comparison of the Filtration Characteristics Between Attached and Suspended Growth Microorganisms in Submerged Membrane Bioreactor *Water Research*, vol. 35, no. 10, pp. 2435-2445, 2001.

[43] H.Winnen, M.T.Suidan, P.V.Scarpino, B.E.Wrenn, N.Cicek, V.Urbain, and J.Manem, Effectiveness of the Membrane Bioreactor in the Biodegradation of High Molecular-Weight Compounds *Water Science and Technology*, vol. 34, no. 9, pp. 197-203, 1996.

[44] N.Cicek, J.P.Franco, M.T.Suidan, and V.Urbain, Using a Membrane Bioreactor *Journal American Water Works Association*, vol. 90, no. 11, pp. 105-113, 1998.

[45] N.Cicek, J.P.Franco, M.T.Suidan, V.Urbain, and J.Manem, Characterization and Comparison of a Membrane Bioreactor and a Conventional Activated-Sludge System in the Treatment of Wastewater Containing High-Molecular-Weight Compounds *Water Environment Research*, vol. 71, no. 1, pp. 64-70, 1999.

[46] E.B.Muller, A.H.Stouthamer, H.W.van Verseveld, and D.H.Eikelboom, Aerobic Domestic Waste Water Treatment in a Pilot Plant with Complete Sludge Retention by Cross-Flow Filtration *Water Research*, vol. 29, no. 4, pp. 1179-1189, 1995.

[47] J-S.Kim, C-H.Lee, and I-S.Chang, Effect of Pump Shear on the Performance of a Crossflow Membrane Bioreactor *Water Research*, vol. 35, no. 9, pp. 2137-2144, 2001.

[48] T.Ueda, K.Hata, Y.Kikuoka, and O.Seino, Effects of Aeration on Suction Pressure in a Submerged Membrane Bioreactor *Water Research*, vol. 31, no. 3, pp. 489-494, 1997.

[49] Xiao-Jun Fan, V.Urbain, Y.Qian, and J.Manem, Nitrification and Mass Balance With a Membrane Bioreactor for Municipal Wastewater Treatment *Water Science and Technology*, vol. 34, no. 1–2, pp. 129-136, 1996.

[50] K-H.Ahn and K-G.Song, Application of Microfiltration with a Novel Fouling Control Method for Reuse of Wastewater from a Large-Scale Resort Complex *Desalination*, vol. 129, pp. 207-216, 2000.

[51] K-H.Ahn, H-Y.Cha, and K-G.Song, Retrofitting Municipal Sewage Treatment Plants Using and Innovative Membrane Bioreactor System *Desalination*, vol. 124, pp. 279-286, 1999.

[52] L.van Dijk and G.C.G.Roncken, Membrane Bioreactors for Wastewater Treatment: The State of the Art and New Developments *Water Science and Technology*, vol. 35, no. 10, pp. 35-41, 1997.

[53] H.Thomas, S.Judd, and J.Murrer, Fouling Characteristics of Membrane Filtration in Membrane Bioreactors *Membrane Technology*, vol. 122, pp. 10-13, 2000.

[54] G.Owen, M.Bandi, J.A.Howell, and S.J.Churchouse, Economic Assessment of Membrane Processes for Water and Waste Water Treatment *Journal of Membrane Science*, vol. 102, pp. 77-91, 1995.

[55] J.Hermia, Constant Pressure Blocking Filtration Laws: Application to Power Law Non-Newtonian Fluids *Trans.I.Chem.E.*, vol. 60, pp. 183-187, 1982.

[56] R.W.Field. Mass Transport and the Design of Membrane Systems. In: *Industrial Membrane Separation Technology*, eds. K.Scott and R.Hughes. London: Blackie, 1996, pp. 67-113.

[57] L.Defrance, M.Y.Jaffrin, B.B.Gupta, P.Paullier, and V.Geaugey, Contribution of Various Constituents of Activated Sludge to Membrane Bioreactor Fouling *Bioresource Technology*, vol. 73, pp. 105-112, 2000.

[58] C.Wisniewski and A.Grasmick, Floc Size Distribution in a Membrane Bioreactor and Consequences for Membrane Fouling *Colloids and Surfaces A: Physicochemical and Engineering Aspects*, vol. 138, pp. 403-411, 1998.

[59] E.H.Bouhabila, R.Ben Aim, and H.Buisson, Fouling Characterisation in Membrane Bioreactors *Separation and Purification Technology*, vol. 22-23, pp. 123-132, 2001.

[60] I-S.Chang and C-H.Lee, Membrane Filtration Characteristics in Membrane-Coupled Activated Sludge System - The Effect of Physiological States of Activated Sludge on Membrane Fouling *Desalination*, vol. 120, pp. 221-233, 1998.

[61] W.Lee, S.Kang, and H.Shin, Sludge Characteristics and their Contribution to Microfiltration in Submerged Membrane Bioreactors *Journal of Membrane Science*, vol. 216, pp. 217-227, 2003.

[62] S.Rosenberger and M.Kraume, Filterability of Activated Sludge in Membrane Bioreactors *Desalination*, vol. 151, no. 2, pp. 195-200, 2002.

[63] E.Tardieu, A.Grasmick, V.Geaugey, and J.Manem, Hydrodynamic Control of Bioparticle Deposition in a MBR Applied to Wastewater Treatment *Journal of Membrane Science*, vol. 147, pp. 1-12, 1998.

[64] Y.Shimizu, K.Uryu, Y.Okuno, and A.Watanabe, Cross-Flow Microfiltration of Activated Sludge Using Submerged Membrane with Air Bubbling *Journal of Fermentation and Bioengineering*, vol. 81, no. 1, pp. 55-60, 1996.

[65] Y.Shimizu, Y.Okuno, K.Uryu, S.Ohtsubo, and A.Watanabe, Filtration Characteristics of Hollow Fiber Microfiltration Membranes Used in Membrane Bioreactor for Domestic Wastewater Treatment *Water Research*, vol. 30, no. 10, pp. 2385-2392, 1996.

[66] S.S.Madaeni, A.G.Fane, and D.E.Wiley, Factors Influencing Critical Flux in Membrane Filtration of Activated Sludge *Journal of Chemical Technology and Biotechnology*, vol. 74, pp. 539-543, 1999.

[67] A.Beaubien, M.Baty, F.Jeannot, E.Francoeur, and J.Manem, Design and Operation of Anaerobic Membrane Bioreactors: Development of a Filtration Testing Strategy *Journal of Membrane Science*, vol. 109, pp. 173-184, 1996.

[68] L.Defrance and M.Y.Jaffrin, Reversibility of Fouling Formed in Activated Sludge Filtration *Journal of Membrane Science*, vol. 157, pp. 73-84, 1999.

[69] C.Wisniewski and A.Grasmick, Influence of Shear Stresses on Biokinetics and Suspension Filterability in a Membrane Bioreactor (MBR), 1997.

[70] K-H.Choo and C-H.Lee, Hydrodynamic Behaviour of Anaerobic Biosolids During Crossflow Filtration in the Membrane Anaerobic Bioreactor *Water Research*, vol. 32, no. 11, pp. 3387-3397, 1998.

[71] J-G.Choi, T-H.Bae, J-H.Kim, T-M.Tak, and A.A.Randall, The Behaviour of Membrane Fouling Initiation on the Crossflow Membrane Bioreactor System *Journal of Membrane Science*, vol. 203, pp. 103-113, 2002.

[72] H.Nagaoka, S.Ueda, and A.Miya, Influence of Bacterial Extracellular Polymers on the Membrane Separation Activated Sludge Process *Water Science and Technology*, vol. 34, no. 9, pp. 165-172, 1996.

[73] R.Liu, X.Huang, Y.F.Sun, and Y.Qian, Hydrodynamic Effect on Sludge Accumulation Over Membrane Surfaces in a Submerged Membrane Bioreactor *Process Biochemistry*, vol. 39, no. 2, pp. 157-163, 2003.

[74] H-S.Shin and S-T.Kang, Characteristics and Fates of Soluble Microbial Products in Ceramic Membrane Bioreactor at Various Sludge Retention Times *Water Research*, vol. 37, pp. 121-127, 2003.

[75] I-S.Chang, S-O.Bag, and C-H.Lee, Effects of Membrane Fouling on Solute Rejection During Membrane Filtration of Activated Sludge *Process Biochemistry*, vol. 36, pp. 855-860, 2001.

[76] H.Nagaoka, S.Yamanishi, and A.Miya, Modeling of Biofouling by Extracellular Polymers in a Membrane Separation Activated Sludge System *Water Science and Technology*, vol. 38, no. 4–5, pp. 497-504, 1998.

[77] H.Nagaoka, S.Kono, S.Yamanishi, and A.Miya, Influence of Organic Loading Rate on Membrane Fouling in Membrane Separation Activated Sludge Process *Water Science and Technology*, vol. 41, no. 10-11, pp. 355-362, 2000.

[78] J.A.Howell, Sub-Critical Flux Operation of Microfiltration *Journal of Membrane Science*, vol. 107, pp. 165-171, 1995.

[79] Z.F.Cui and K.I.T.Wright, Flux Enhancements with Gas Sparging in Downwards Crossflow Ultrafiltration: Performance and Mechanism *Journal of Membrane Science*, vol. 117, pp. 109-116, 1996.

[80] S.Chang and A.G.Fane, Characteristics of Microfiltration of Suspensions with Inter-fibre Two-Phase Flow *Journal of Chemical Technology and Biotechnology*, vol. 75, pp. 533-540, 2000.

[81] S.Laborie, C.Cabassud, L.Durand-Bourlier, and J.M.Laine, Flux Enhancement by a Continuous Tangential Gas Flow in Ultrafiltration Hollow Fibres for Drinking Water Production: Effects of Slug Flow on Cake Structure *7th World Filtration Congress in Budapest, Hungary*, 1996.

[82] C.Cabassud, S.Laborie, L.Durand-Bourlier, and J.M.Laine, Air Sparging in Ultrafiltration Hollow Fibres: Relationship Between Flux Enhancement, Cake Characteristics and Hydrodynamic Parameters *Journal of Membrane Science*, vol. 181, pp. 57-69, 2001.

[83] M.Mercier, C.Maranges, C.Fonade, and C.Lafforgue-Delorme, Yeast Suspension Filtration: Flux Enhancement Using an Upward Gas/Liquid Slug Flow - Application to Continuous Alcoholic Fermentation with Cell Recycle *Biotechnology and Bioengineering*, vol. 58, no. 1, pp. 47-57, 1998.

[84] S.Chang and A.G.Fane, Filtration of Biomass with Axial Inter-fibre Upward Slug Flow: Performance and Mechanisms *Journal of Membrane Science*, vol. 180, pp. 57-68, 2000.

[85] Z.F.Cui and K.I.T.Wright, Gas-Liquid Two-Phase Cross-flow Ultrafiltration of BSA and Dextran Solutions *Journal of Membrane Science*, vol. 90, pp. 193-189, 1994.

[86] Z.F.Cui, S.R.Bellara, and P.Homewood, Airlift Crossflow Membrane Filtration - A Feasibility Study with Dextran Ultrafiltration *Journal of Membrane Science*, vol. 128, pp. 83-91, 1997.

[87] S.R.Bellara, Z.F.Cui, and D.S.Pepper, Gas Sparging to Enhance Permeate Flux in Ultrafiltration Using Hollow Fibre Membranes *Journal of Membrane Science*, vol. 121, pp. 175-184, 1996.

[88] L.Vera, R.Villarroel, S.Delgado, and S.Elmaleh, Enhancing Microfiltration Through an Inorganic Tubular Membrane by Gas Sparging *Journal of Membrane Science*, vol. 165, pp. 47-57, 2000.

[89] C-K.Lee, W-G.Chang, and Y-H.Ju, Air Slugs Entrapped Cross-flow Filtration of Bacterial Suspensions *Biotechnology and Bioengineering*, vol. 41, pp. 525-530, 1993.

[90] M.Mercier-Bonin, C.Lagane, and C.Fonade, Influence of a Gas/Liquid Two-Phase Flow on the Ultrafiltration and Microfiltration Performances: Case of a Ceramic Flat Sheet Membrane *Journal of Membrane Science*, vol. 180, pp. 93-102, 2000.

[91] R.Ghosh and Z.F.Cui, Mass Transfer in Gas-Sparged Ultrafiltration: Upward Slug Flow in Tubular Membranes *Journal of Membrane Science*, vol. 162, pp. 91-102, 1999.

[92] Q.Y.Li, Z.F.Cui, and D.S.Pepper, Fractionation of HSA and IgG by Gas Sparged Ultrafiltration *Journal of Membrane Science*, vol. 136, pp. 181-190, 1997.

[93] Q.Y.Li, R.Ghosh, S.R.Bellara, Z.F.Cui, and D.S.Pepper, Enhancement of Ultrafiltration by Gas Sparging with Flat Sheet Membrane Modules *Separation and Purification Technology*, vol. 14, pp. 79-83, 1998.

[94] R.Ghosh, Q.Y.Li, and Z.F.Cui, Fractionation of BSA and Lysozyme Using Ultrafiltration: Effect of Gas Sparging *AIChE Journal*, vol. 44, no. 1, pp. 61-67, 1998.

[95] C.Cabassud, S.Laborie, and J.M.Laine, How Slug Flow Can Improve Ultrafiltration Flux in Organic Hollow Fibres *Journal of Membrane Science*, vol. 128, pp. 93-101, 1997.

[96] I-S.Chang and S.J.Judd, Air Sparging of a Submerged MBR for Municipal Wastewater Treatment *Process Biochemistry*, vol. 37, pp. 915-920, 2002.

[97] R.W.Field, D.Wu, J.A.Howell, and B.B.Gupta, Critical Flux Concept for Microfiltration Fouling *Journal of Membrane Science*, vol. 100, pp. 259-272, 1995.

[98] V.Chen, A.G.Fane, S.Madaeni, and I.G.Wenten, Particle Deposition During Membrane Filtration of Colloids: Transition Between Concentration Polarization and Cake Formation *Journal of Membrane Science*, vol. 125, pp. 109-122, 1997.

[99] D.Y.Kwon, S.Vigneswaran, H.H.Ngo, and H.S.Shin, An Enhancement of Critical Flux in Crossflow Microfiltration With a Pretreatment of Floating Medium Flocculator/Prefilter *Water Science and Technology*, vol. 36, no. 12, pp. 267-274, 1997.

[100] S.S.Madaeni, The Effect of Operating Conditions on Critical Flux in Membrane Filtration of Latexes *Trans IchemE*, vol. 75, Part B, 1997.

[101] S.S.Madaeni, An Investigation of the Mechanism of Critical Flux in Membrane Filtration Using Electron Microscopy *Journal of Porous Materials*, vol. 4, pp. 239-244, 1997.

[102] D.Y.Kwon and S.Vigneswaran, Influence of Particle Size and Surface Charge on Critical Flux of Crossflow Microfiltration *Water Science and Technology*, vol. 38, no. 4-5, pp. 481-488, 1998.

[103] D.Wu, J.A.Howell, and R.W.Field, Critical Flux Measurement for Model Colloids *Journal of Membrane Science*, vol. 152, pp. 89-98, 1999.

[104] B.Fradin and R.W.Field, Crossflow Microfiltration of Magnesium Hydroxide Suspensions: Determination of Critical Fluxes, Measurement and Modelling of Fouling *Separation and Purification Technology*, vol. 16, pp. 25-45, 1999.

[105] M.Manttari and M.Nystrom, Critical Flux in NF of High Molar Mass Polysaccharides and Effluents From the Paper Industry *Journal of Membrane Science*, vol. 170, pp. 257-273, 2000.

[106] S.Metsamuuronen, J.A.Howell, and M.Nystrom, Critical Flux in Ultrafiltration of Myoglobin and Baker's Yeast *Journal of Membrane Science*, vol. 196, pp. 13-25, 2002.

[107] H.K.Vyas, R.J.Bennet, and A.D.Marshall, Performance of Crossflow Microfiltration During Constant Transmembrane Pressure and Constant Flux Operations *International Dairy Journal*, vol. 12, no. 5, pp. 473-479, 2002.

[108] D.Y.Kwon, S.Vigneswaran, A.G.Fane, and R.Ben Aim, Experimental Determination of Critical Flux in Crossflow Microfiltration *Separation and Purification Technology*, vol. 19, pp. 169-181, 2000.

[109] V.Chen, Performance of Partially Permeable Microfiltration Membranes Under Low Fouling Conditions *Journal of Membrane Science*, vol. 147, pp. 265-278, 1998.

[110] H.Li, A.G.Fane, H.G.L.Coster, and S.Vigneswaran, Direct Observation of Particle Deposition on the Membrane Surface During Crossflow Microfiltration *Journal of Membrane Science*, vol. 149, pp. 83-97, 1998.

[111] H.Li, A.G.Fane, H.G.L.Coster, and S.Vigneswaran, An Assessment of Depolarisation Models of Crossflow Microfiltration by Direct Observation Through the Membrane *Journal of Membrane Science*, vol. 172, pp. 135-147, 2000.

[112] S.Vigneswaran, D.Y.Kwon, H.H.Hgo, and J.Y.Hu, Improvement of Microfiltration Performance in Water Treatment: Is Critical Flux a Viable Solution? *Water Science and Technology*, vol. 41, no. 10-11, pp. 309-315, 2000.

[113] L.Defrance and M.Y.Jaffrin, Comparison Between Filtrations at Fixed Transmembrane Pressure and Fixed Permeate Flux: Application to a Membrane Bioreactor Used for Wastewater Treatment *Journal of Membrane Science*, vol. 152, pp. 203-210, 1999.

[114] L.Vera, R.Villarroel-Lopez, S.Delgado, and S.Elmaleh, Cross-Flow Microfiltration of Biologically Treated Wastewater *Desalination*, vol. 114, pp. 65-75, 1997.

[115] S.Elmaleh, L.Vera, R.Villarroel-Lopez, L.Abdelmoumni, N.Ghaffor, and S.Delgado, Dimensional Analysis of Steady State Flux for Microfiltration and Ultrafiltration Membranes *Journal of Membrane Science*, vol. 139, pp. 37-45, 1998.

[116] B.D.Cho and A.G.Fane, Fouling Transients in Nominally Sub-critical Flux Operation of a Membrane Bioreactor *Journal of Membrane Science*, vol. 209, pp. 391-403, 2002.

[117] D.Si-Hassan, A.Ould-Dris, M.Y.Jaffrin, and Y.K.Benkahla, Optimisation of an Intermittent Cross-Flow Filtration Process of Mineral Suspensions *Journal of Membrane Science*, vol. 118, pp. 185-198, 1996.

[118] T.Tanaka, H.Itoh, K.Itoh, and K.Nakanishi, Crossflow Filtration of Baker's Yeast with Periodical Stopping of Permeation Flow and Bubbling *Biotechnology and Bioengineering*, vol. 47, pp. 401-404, 1995.

[119] J.N.Kuruzovich and P.R.Piergiovanni, Yeast Cell Microfiltration: Optimization of Backwashing for Delicate Membranes *Journal of Membrane Science*, vol. 112, pp. 241-247, 1996.

[120] V.T.Kuberkar and R.H.Davis, Microfiltration of Protein-Cell Mixtures with Crossflushing or Backflushing *Journal of Membrane Science*, vol. 183, pp. 1-14, 2001.

[121] P.Le Clech, B.Jefferson, and S.J.Judd, Impact of Aeration, Solids Concentration and Membrane Characteristics on the Hydraulic Performance of a Membrane Bioreactor *Journal of Membrane Science*, vol. 218, no. 1-2, pp. 117-129, 2003.

[122] S.Ognier, C.Wisniewski, and A.Grasmick, Biofouling in Membrane Bioreactors: Phenomenon Analysis and Modelling *MBR 3 Cranfield University Wednesday 16th May 2001*, vol. pp. 29-43, 2001.

[123] X-j.Fan, V.Urbain, Y.Qian, and J.Manem, Ultrafiltration of Activated Sludge with Ceramic Membranes in a Cross-flow Membrane Bioreactor Process *Water Science and Technology*, vol. 41, no. 10-11, pp. 243-250, 2000.

[124] J.K.Shim, I-K.Yoo, and Y.M.Lee, Design and Operation Considerations for Wastewater Treatment Using a Flat Submerged Membrane Bioreactor *Process Biochemistry*, vol. 38, pp. 279-285, 2002.

[125] A.G.Fane, P.Beatson, and H.Li, Membrane Fouling and its Control in Environmental Applications *Water Science and Technology*, vol. 41, no. 10-11, pp. 303-308, 2000.

[126] M.Y.Chisti. *Airlift Bioreactors*, London: Elsevier, 1989.

Publications

Journal Publications:

Howell, J.A; Chua, H.C.; Arnot, T.C. (2003) "Effects of membrane history and environment on the fouling of a submerged membrane bioreactor treating simulated primary effluent", Submitted to the Journal of Membrane Science.

Howell, J.A.; Arnot, T.C.; Chua, H.C. (2003) "Turn-up turn-down of membrane operation in membrane bioreactors ", Annals of the New York Academy of Sciences, 984, 492-501.

Chua, H.C.; Arnot, T.C.; Howell, J.A.; (2002), "Controlling fouling in membrane bioreactors operated with a variable throughput", Desalination, 149, 225-229.

Howell, J.A.; Arnot, T.C.; Chua, H.C.; Field, R.W.; Godino, P.; Hatziantoniou, D.; Metsamuuronen, S.; (2002) "Controlled flux behaviour of Membrane Processes", Macromolecular Symposia, Wiley-VCH, 188, 23-36.

Conferences:

Chua, H.C.; Arnot, T.C.; Howell, J.A.; (2002) "Controlling fouling in membrane bioreactors operated with a variable throughput" International Conference on Membranes and Membrane Processes (ICOM'02), Toulouse, France, 7-12 July.

Chua, H.C.; Howell, J.A.; Arnot, T.C.; Sim, M.C. (2001) "Operating Membrane Bioreactors under Varying Flux Conditions." NAMS 2001, 15-20 May, Kentucky, USA.

Chua, H.C.; Howell, J.A.; Arnot, T.C.; Sim, M.C. (2001) "Near Critical Flux Operation of Membrane Bioreactors under Dynamic Load." United Engineering Foundation Conference on Advanced Membrane Technology, 14-19 October, Barga, Italy.

Howell, J.A.; Arnot, T.C.; Chua, H.C.; Field, R.W.; Godino, P.; Hatziantoniou, D.; Metsamuuronen, S.; (2001) "Controlled flux behaviour of membrane processes." Microsymposium on Polymer Membranes, 16-21 July, Prague, Czech Republic.

Chua, H.C.; Arnot, T.C.; Howell, J.A.; (2001) "Turn-Up/Turn-Down of Throughput in Membrane Bioreactors." European Membrane Society (EMS) XVIII Summer School '2001 "Using Membranes to Assist in Cleaner Processes", 9-14 September 2001, Ladek Zdroj, Poland. Poster presentation.